PHEROMONAL SIGNALING AND TRANS-SYNAPTIC TRACING IN DROSOPHILA

by
Chun-Chieh Lin

A dissertation submitted to Johns Hopkins University in conformity with the requirements for the degree of Doctor of Philosophy

Baltimore, Maryland
June, 2015

ABSTRACT

Pheromonal Signaling and Trans-synaptic Tracing in *Drosophila*

Chun-Chieh Lin

Animals use olfactory cues for navigating complex environments. Food odors in particular provide crucial information regarding potential foraging sites. Many social behaviors are known to occur at such food sites, such as aggregation, courtship, and egg-laying. Yet how food odors might regulate such behaviors at these sites is unclear. Pheromones are specialized animal-derived odorants used to communicate critical social information between members of the same species. If connections exist between food odors and pheromone signaling remains largely unexplored. Using *Drosophila melanogaster* as an animal model, we found that *Drosophila* males actively deposit the pheromone 9-tricosene upon food-odor stimulation. This male specific pheromone acts as a potent aggregation pheromone for both genders, as an aphrodisiac to increase successful courtship, and as a cue to guide female oviposition decisions. We use genetic, molecular, electrophysiological, and behavioral approaches to show that 9-tricosene activates antennal basiconic Or7a receptors. We also demonstrate that loss of Or7a+ neurons or the Or7a receptor abolishes aggregation behavior and oviposition site-selection. Bioinformatic analysis of olfactory receptors indicates that Or7a is one of the most rapidly evolving odorant receptors. All together, our results indicate that 9-tricosene is a close range olfactory signal in *Drosophila,* deposited in response to food-odors, which influences social behaviors via the Or7a odorant receptor. Males utilize 9-tricosene to influence egg-laying site preferences in females. These studies link food-odor

perception to male pheromone deposition, aggregation behavior and subsequent female decision-making.

We demonstrated that Or7a+ neurons are responsible for 9-tricosene guided oviposition decisions. Recently, Or19a+ neurons were found to detect citrus fruit as oviposition substrates. Interestingly, the Or7a DL5 and Or19a DC1 projection neurons (PNs) share highly similar axonal projection patterns in the higher olfactory brain region that are distinct from previously described food and pheromone regions. Characterizing the olfactory circuits in higher olfactory centers that are activated by Or7a+ and Or19a+ neurons would reveal how chemosensory cues are processed in the oviposition decision-making process. We therefore sought to decipher the connectivity and functions of higher olfactory brain regions.

To this end, my other research goal has been to develop a novel and unbiased genetically encoded method (CLAMP, Cell Labeling Across Membrane Partners) that enables the identification and functional manipulation of downstream neurons based solely on neuronal connectivity- a task not previously possible in *Drosophila*. This technique allows me to identify candidate second and tertiary olfactory neurons that mediate pheromone signaling and perform functional manipulation with optogenetic and thermogenetic tools. In combination with behavior assays, I will be able to decipher the full circuit basis for oviposition decision-making. Furthermore, CLAMP can also be applied to the mapping and manipulating of any uncharacterized *Drosophila* circuit and might be applicable in other model systems.

Thesis advisor: Christopher Potter

Reader: Alex Kolodkin

ACKNOWLEDGEMENTS

Getting a Ph.D. at Hopkins has been an amazing journey. Along the journey, I am so grateful to have met so many incredible people that helped and supported me in exploring the beauty of science. Without them, science would not be as exciting and fun.

First and foremost I wish to express my deepest gratitude to my mentor, Christopher Potter for being so supportive and positively guiding me through all the difficulties. Chris is not only a scientist I look up to but also a friend I trust. Talking science with Chris is always fun because he sincerely cares about your ideas and would polish them into mature and doable projects. It has been a great honor to work with you!

I would like to thank my thesis committee: King-Wai Yau, Alex Kolodkin, Dwight Bergles and Mark Wu, for their continuous encouragements and insightful comments. In particular, I would like to thank King-Wai Yau for introducing me to the Hopkins Neuroscience department and being my moral support through my Ph.D. Also, I would like to thank Mark Wu for sharing his career advices as a successful physician scientist.

I would also like to thank Randy Reed for his amazing thoughts and hard questions. His door is always open for young and naïve minds like mine. Instead of providing direct and simple answers, he always proposes more difficult questions in a very constructive way.

I am also thankful to my labmates, Lena Riabinina, Sonia Chin, Darya Task and Liz Marr for making the Potter lab such a great environment to do science. Each success is a little bit sweeter and each failure is less harsh because of your friendship and companion.

I would like to thank my parents for trusting me, no matter what. They are always supporting me with their unconditional love.

Finally, I would like to thank my wife, Yu-Chun Huang for making my life more beautiful. Without you, I wouldn't have made it here today!

DEDICATION

To my family

Who nourishes my courage to explore the unknown

TABLE OF CONTENTS

LIST OF FIGURES

Chapter 1: General Introduction:

1.1 The olfactory system

The anatomical and functional organization of the olfactory system is surprisingly similar between flies and mammals. The conservation of neural circuitry in insect olfactory system provides a great opportunity to decipher the questions as to how olfactory information is received, processed and interpreted by the brain. The discovery of odorant receptors in rodents (Buck and Axel, 1991), *Caenorhabditis elegans* (Sengupta et al., 1996) and *Drosophila melanogaster* (Clyne et al., 1999; Gao and Chess, 1999; Vosshall et al., 1999) has significantly changed our understanding of how chemosensory information is organized in the periphery and projected to the higher brain regions.

Olfactory receptor neurons (ORNs) in *Drosophila melanogaster* are housed in a porous cuticular structure called sensilla in the third antennal segments and maxillary palps. Each sensillum can contain 1-4 ORNs. There are ~1200 ORNs in each antenna, housed in three distinct sensillum categories: basiconic (ab1-ab10), trichoid (at1-at4) and coeloconic sensilla (ac1-ac4) (Couto et al., 2005; Larsson et al., 2004). Basiconic ORNs are generally tuned to fruit odors, trichoid to pheromones and coeloconic ORNs to volatile products of microbial degradations and humidity (Goldman et al., 2005; Ha and Smith, 2006; Hallem and Carlson, 2006; Yao et al., 2005) (Figure 1.1 A). Even simpler than antenna are the maxillary palps, which contains an order of magnitude fewer ORNs (~120) and all of the ORNs are housed in the basiconic sensilla (pb1-pb3) (de Bruyne et al., 1999) (Figure 1.1 A). Furthermore, ORNs are grouped in an invariant manner in each sensillum. A recent study describes a non-synaptic inhibition (ephaptic effect) of the

ORNs in the same sensillum: transient activation of one neuron in the sensillum could inhibit the spontaneous activity of neighboring neuron through exchange of ions (Su et al., 2012). This suggests the stereotypical grouping exhibits functional significance and might be important for odor interpretation in the higher olfactory processing regions.

Odorants bind to olfactory receptors (ORs) on ORNs, which project their axons to discrete foci (called glomeruli) in the antennal lobe (AL) (Figure 1.1 B). ORNs that express the same olfactory receptors send their axons and converge onto the same glomerulus (Couto et al., 2005; Fishilevich and Vosshall, 2005). Projection neurons (PNs) then relay the odor information from particular glomeruli to higher centers of the brain, the mushroom bodies and the lateral horn (Jefferis et al., 2007). The AL is the site where olfactory information processing begins. In the AL, stereotypic synaptic connections are made between the axonal termini of ORNs and dendritic arborizations of PNs. The one-to-one connectivity between ORNs and cognate PNs suggests a simple and reliable information flow between primary ORNs and secondary PNs. However, the diversity and wiring variability of local interneurons further enriches the information processing in the AL by sending interglomerular connections between different odor channels (Chou et al., 2010) (Figure 1.1 B). The next effect of this information processing is odor tuning of PNs can be broader than their cognate ORNs by excitatory interneurons.

The mushroom body is involved in olfactory learning and memory (Davis, 2005; de Belle and Heisenberg, 1994) whereas the lateral horn is implicated in innate behaviors, such as attraction, repulsion and response to pheromones (Jefferis et al., 2007; Kido and Ito, 2002) (Figure 1.1 B). Innate is not equal to invariant. It is a common observation that

the same stimuli can generate different behavior outputs according to context, time, hormonal state and many other factors. Despite the wealth of knowledge about olfactory organization and information processing of ORNs, PNs and local interneurons at the AL, little is known about what the cognate synaptic partners of PNs at the mushroom body and lateral horn are or how they represent odor information and elicit olfactory behaviors.

1.2 *Drosophila* exhibit a range of olfactory-mediated behaviors

The chemosensory inputs from the periphery are integrated in the central brain regions and translated into behavior outputs. *Drosophila* exhibits a variety of simple and complex behaviors. Advances in the understanding of chemosensory receptors and neural circuitry of innate behaviors such as attraction, repulsion and feeding provide insight into sensory mechanisms utilized throughout evolution (Pool et al., 2014; Stensmyr et al., 2012; Suh et al., 2004). Apple cider vinegar (ACV) triggers robust attraction behavior at low concentrations. By using calcium imaging, the olfactory channels responsible for this attraction response were identified as Or42b and Or92a ORNs (Semmelhack and Wang, 2009). Labeled-line coding could thus explain ACV attraction in *Drosophila*. Activation of a single or very few classes of ORNs is able to generate attraction behavior. Interestingly, flies are repelled by ACV at high concentration and it was found that high concentration of ACV activates other classes of ORNs beside Or42b and Or92a ORNs. There is a concentration-dependent behavioral switch as increasing concentration recruits activation of other low-affinity receptors (Semmelhack and Wang, 2009).

Two other examples of labeled-line coding for avoidance behaviors are ORN and PN representations of CO_2 and strong acid sensations (Ai et al., 2010; de Bruyne et al.,

2001; Suh et al., 2004). Each of the compounds activates only one or two classes of ORN/PN and generates repulsion behavior. CO_2 activates Gr21a/Gr63a receptors in the ab1c ORNs, whereas strong acid activates Ir64a ORNs in the sacculus (Ai et al., 2010; Suh et al., 2004). Interestingly, the PNs of the two repulsive channels send axonal projections to the lateral horn, forming a cup-shape pattern distinct from previous described food and pheromone region (Sonia Chin, Graduate Thesis Project in C. Potter laboratory).

Chemosensory systems are also critical in complex behaviors such as courtship, aggression and oviposition. Male courtship behavior is a widely accepted model to study complex, genetically specified and innate behavior and consists of a well-defined sequence of behaviors: Orientation, tapping, singing, licking and copulation (Sokolowski, 2001). Multiple sensory modalities are incorporated in this process. Females would feel male taps and licks, hear the male song, smell male odor and see the male shape to decide whether to copulate with him. On the other hand, males also use chemosensory cues to evaluate if the female is virgin and only mate with virgin females (through male-specific pheromone cVA, see below).

Drosophila female flies utilize a complex decision making process to determine appropriate locations for egg laying (Yang et al., 2008). Females preferentially lay their eggs in food sources so as to increase survival of their progeny, as larval diet is largely determined by the oviposition location. It is interesting that oviposition site selection is different from general place preference (attraction behavior). Female flies prefer to lay eggs in substrates containing acetic acid while they avoids residing in location with acetic acid (Joseph et al., 2009). Similarly, longer chain acids elicit positive oviposition

preference but elicit negative location preferences (Harada et al., 2008). Thus, general place preference behavior (attraction and repulsion) appears to utilize distinct circuits from oviposition site selection. Although peripheral activation might be the same, the output behaviors can be varied depending on the internal states and activated circuitry.

1.3 Pheromone Signaling

Pheromones are specialized molecules that have evolved as social signals between members of the same species. *Drosophila* pheromones consist of long-chain cuticular hydrocarbons (CHCs) that are produced by specialized cells (oenocytes) in the fly abdominal wall and form a waxy layer on the body surface (Billeter et al., 2009). Given the nature of its production, the CHCs are present on the cuticle of > 2 day-old mature flies. There is strong sexual dimorphism between male and female CHCs compositions: Only female flies produce dienes (which contain two double bonds, 7,11 Heptocosadiene for instance) where monoenes are much more prominent in males (7-tricosene, 9-tricosene for instance) (Everaerts et al., 2010). Most CHCs are not volatile and are detected through the gustatory system (e.g., by taste receptors on the tarsi (feet) that are stimulated when an animal taps and licks other animal's cuticle) (Ferveur et al., 1997). For instance, 7-tricosene, an abundant male CHC is sensed via the gustatory system to modulate courtship behaviors (Lu et al., 2012; Thistle et al., 2012). However, some of the shorter CHCs have been hypothesized to function as a close range olfactory cue to guide animal behaviors (Ferveur and Sureau, 1996). Indeed, recent solid-phase micro-extraction gas chromatography experiments verified the presence of volatile CHC pheromones in

the headspace of flask containing flies, suggesting pheromone detection might be medicated through the olfactory system (Everaerts et al., 2010).

Cis-vaccenyl acetate (cVA) is a male specific volatile pheromone. Instead of being manufactured by oenocytes on the abdominal wall, cVA is produced and stored in the male internal organ (ejaculatory bulb) and transferred to females only during copulation (Billeter et al., 2009), where it plays a role in modification of female receptivity. cVA is known to evoke different behaviors in different sexes. In males, it suppresses courtship behavior at high concentration and provokes aggression at low concentration (Wang and Anderson, 2010), whereas in females, it enhances courtship behavior (Ejima et al., 2007; Kurtovic et al., 2007). cVA can also promote aggregation behaviors in both sexes (Bartelt et al., 1985). cVA activates at1 sensillum which only houses one neuron- Or67d+ ORN (Couto et al., 2005; Ha and Smith, 2006). This male specific compound can activate Or67d receptor directly or indirectly. In the indirect pathway, detection of cVA is facilitated by Lush (a secreted odorant binding protein) and SNMP (sensory neuron membrane protein): cVA binds to Lush and induces a conformational change of the Or67d receptor and the process is facilitated by SNMP (Benton et al., 2007; Gomez-Diaz et al., 2013; Laughlin et al., 2008). Remarkably, circuitry of cVA-Or67d shows strong sexual dimorphism (Datta et al., 2008). The Or67d+ ORNs project to DA1 glomeruli in the AL. The sizes of DA1 glomeruli are significantly larger in males than females. However, first (Or67d+ ORN) and second (DA1 PNs) order neurons are equally sensitive to cVA in males and females and thus can not account for the sexual dimorphic behaviors (Ruta et al., 2010). Recently, it was found that the axonal projection of DA1 PNs to LH also displayed sexual dimorphism and

formed synaptic connections with two different clusters of third order neurons (Kohl et al., 2013). Thus, the sexually dimorphic connections between second order PN and third order neurons generate behavioral dimorphism.

1.4 Trans-synaptic methods

Recently, major efforts have been devoted to anatomical reconstitution of entire neuronal wiring diagrams by automatic reconstruction of serial sections electron microscopy (EM). The idea of using EM to reconstruct a complete connectivity of a simple organism- *C. elegans*, which contains 302 neurons and 7,000 synapses, was proposed in the 1970s (White et al., 1986). A nearly complete draft was published in 1986 and, after an additional 25 year effort, a complete wiring diagram was published in 2011 (Varshney et al., 2011). An EM based connectome reconstruction provides high anatomical resolution (such as identification of electrical and chemical synapses) but does not allow functional manipulation. Moreover, the challenge of reconstruction is that serial sections of EM images need to be aligned properly in order for axonal and dendritic processes to be tracked back to the soma. Any misalignment of even a single side results in misleading results. Thus, EM methods are currently best suited for elucidating microcircuitry of small regions of the brain, rather than to map out long-range connections.

Classical lipophilic dyes are ideal to study axonal pathfinding. The spreading of injected dyes does not rely on active axonal transport but on lateral diffusion. Thus, the technique is also useful in fixed tissue (Balice-Gordon et al., 1993). Tracers such as biotinylated-dextran amine (BDA) (Reiner et al., 2000), fluorescence latex microspheres

(Katz and Iarovici, 1990), or phytohemagglutinin lectin (PHAL) are useful to trace long-range axonal projections. However, lipophilic dyes do not transfer from labeled cells to unlabeled cells unless the plasma membrane is disrupted. Therefore, the technique is not applicable to identify pre- or post-synaptic coupled neurons.

The idea of using neutrophilic viruses as trans-synaptic tracer was first introduced in 1960s. Genetically modified neutrophilic viruses are used to infect and replicate in molecularly defined neurons and then spread trans-synaptically (Callaway, 2008). The advantages of viral tracers include unidirectional spreading, self-replication and most importantly, genetic tractability. The direction of infection can be anterograde (HSV) (Garner and LaVail, 1999) or retrograde (Rabies virus) (Ugolini, 2008) and these approaches are useful for poly or uni-trans-synaptic labeling of defined sub-population of neural tissues. However, the delivery of viral tracer material to the target tissue requires surgical injection and therefore might be biased. Furthermore, a virus-based trans-synaptic labeling technique is not applicable in *Drosophila* because of animal size.

GFP reconstitution across synaptic partners (GRASP) was first developed in *C. elegans* (Feinberg et al., 2008) and adapted to *Drosophila melanogaster* (Gordon and Scott, 2009) and mammalian systems (Kim et al., 2012). GRASP is a powerful technique to monitor the synaptic contacts between two neurons. Two complementary non-fluorescent GFP fragments (1-10 and 11) bound to a trans-membrane protein are expressed in opposing neurons and functional GFP is reconstituted at the extracellular space of synaptic cleft. The GFP fragments are either fused to non-synaptic specific CD4 or synaptic-specific neurexin and neuroligin. GFP signal can be monitored *in vivo* or

amplified with a monoclonal antibody (Feinberg et al., 2008). The GRASP technique is best suited for examining and verifying if two neurons might form synaptic contacts.

The recently developed Tango system is an activity-dependent trans-synaptic tracing technique that detects the endogenous neurotransmitter activity in the flies (Inagaki et al., 2012; Jagadish et al., 2014). Ligand activation of a G-protein coupled receptor results in phosphorylation of specific serine and threonine residues at the cytoplasmic C-terminus, activating the G-protein and resulting in signal amplification. The signal is desensitized by arrestin as it competes with G-proteins for binding to the GPCR. The phosphorylated GPCR finally undergoes receptor endocytosis. In the Tango technique, Gal4 is fused to the GPCR with an intervening TEV protease cutting site (GPCR-TEV^{cs}-Gal4,) whereas TEV protease is linked with arrestin (Arr-TEV). When the GPCR is activated, recruitment of Arr-TEV mediates proteolysis at TEV^{cs}, releasing Gal4 and turning on the reporters (UAS-GFP) (Barnea et al., 2008). Transient receptor-ligand interaction thus generates a stable readout depending on the chosen reporters. However, the assay is limited to specific neurotransmitter types (for instance, Dopamine-Tango (Inagaki et al., 2012) and Histamine-Tango (Jagadish et al., 2014)) and cannot be generalized for all synaptically coupled neurons.

1.5 Binary expression system

To better label a subset of cells in a target tissue, fly genetics has been used to exogenously introduce transactivation systems from other organisms (yeast, bacterium and fungus). The Gal4/UAS system was developed first in 1993 (Brand and Perrimon, 1993; Fischer et al., 1988), whereas LexA/LexAop (Lai and Lee, 2006) and Q system

(Potter et al., 2010; Riabinina et al., 2015) are examples of recent additions (Figure 1.2). Although there are some minor differences in the systems, such as existence of repressible elements (Gal80 in Gal4/UAS and QS in Q system but not in LexA/LexAOP system), the general design logic is similar. There are two modules: the "driver" and "reporter". The driver is composed of trans-activator (transcription factor) under control of specific promoter region (for example, pan-neuronal Gal4). The reporter contains binding site of trans-activator and downstream effecter gene of interest (for example, UAS (upstream activation sequence)-GFP). The promoter targets the expression of trans-activator in specific tissue, resulting in transcriptional activation of the effecter gene (GFP expression in all neurons). Importantly, the trans-activators of certain binary systems (Gal4, LexA and QF) do not bind to the trans-activator binding sites of other systems (UAS, LexAop and QUAS, respectively) (Figures 1.2 A-1.2 C). Thus, one can simultaneously and independently express two reporters in the same organism by using two binary systems.

One of the best applications of using multiple binary systems is an intersectional strategy for manipulating effecter expression patterns. Drivers expressed in small neuronal populations are usually not available, especially in the central nervous system. Sometimes the neurons of interest can not be labeled specifically by a single binary system but can be labeled as the overlap of two independent systems sharing some commonalities. Thus, intersectional strategies employ genetically encoded logic gates between different binary expression systems to achieve specific expression of effecter genes in specific cells (Potter et al., 2010; Venken et al., 2011) (Figure 1.2 D).

1.6 Site-specific recombinase for genetic manipulations

Site-specific recombination has been a widely used method in DNA engineering. Two of the most widely used recombinases are Cre recombinase from the coliphage P1 and FLP recombinase from *Saccharomyces cerevisiae* (Turan et al., 2011). LoxP and FRT are the target sequences of Cre and FLP, respectively, and consist of 34 base pairs that are 13 base pair palindromes with an internal 8 base pair spacer. The recombinase target sequence (FRT for instance) and recombinase enzyme (FLP for instance) can induce chromosomal recombination either in *trans* or *cis* arrangements. In the *trans* arrangement, FLP induces chromosomal cross-over during mitosis between FRT sites of the two sister chromatids (Figure 1.3 A). This technique has been extensively used in generating mutant or mosaic clones, such as those involved in the MARCM technique (Lee and Luo, 1999). FRT can also be on the same chromosome in *cis* arrangement with the same or opposite orientations. When the two FRT sites are arranged in opposite orientation, the intervening sequence will be inverted, which has been used to produce random labeling of a variety of fluorescent proteins, such as Brainbow, dBrainbow and Flybow (Hadjieconomou et al., 2011; Hampel et al., 2011; Livet et al., 2007) (Figure 1.3 B). When the FRTs are arranged in tandem in the same orientation, the intervening sequence is excised and genes following the second FRT could be expressed (Figure 1.3 C).

FLP is derived from the yeast system, which has a physiological temperature (30 ºC) lower than the mammalian system (37 ºC). Previously, the application of FLP has been limited by its low efficiency compared to Cre recombinase at 37 ºC. By screening for thermostable variants using error-prone PCR, the optimized version (FLPe) contains

four mutations (P2S, L33S, Y108N and S294P) and is approximately 5 times more efficient in mammalian cells than wild-type FLP (Buchholz et al., 1998). However, FLPe still exhibits ~25% of the Cre recombination efficiency in transfection assays. By mouse codon-optimization, current FLP (FLPo) activity is comparable, or even superior, to Cre (Raymond and Soriano, 2007).

For proteins larger than 45 kDa, transportation into the nucleus requires a specific targeting sequence, called nuclear localization sequence (NLS) (Turan et al., 2011). The molecular weight of FLP is ~48 kDa, and a NLS would be necessary for proper function in the nucleus. Indeed, addition of NLS to FLPe increases the recombination efficiency by ~3 fold (Schaft et al., 2001). In contrast, Cre is only ~38 kDa and has been suggested to enter the nucleus by passive diffusion because addition of a NLS did not change the recombination efficiency (Glover et al., 2005). However, subsequent research revealed that Cre contains an intrinsic, bipartite NLS (two clusters of basic resides separated by 10 a.a.), which takes over the function of other extrinsic monopartite NLS.

1.7 Protein transduction domain

The ability of HIV-1 trans-activator protein (TAT) to enter the living cells was reported by two independent groups in 1988 (Frankel and Pabo, 1988; Green and Loewenstein, 1988). Analysis of the protein sequence revealed 11 amino acids (GRKKRRQRRRP) in the N-terminal portion responsible for the transduction ability (Schwarze et al., 2000). When tagged with beta-glactosidase and injected intraperitoneally, this sequence facilitated transduction into a variety of cell types, including liver, kidneys, brains and other tissues (Schwarze et al., 1999). Subsequently, a number of other peptides with

similar transduction abilities were identified, for instance the Antennapedia homeodomain transcription factor derived peptide (Anp) and the herpes-simplex-virus DNA binding protein VP22.

Protein transduction domains are short peptides (6-12 amino acids) of positively charged polypeptide sequences (containing multiple arginine and lysine residues). Possible mechanisms of cell entry include direct cell penetration, binding to heparan sulfate proteoglycan or clathrin-mediated endocytosis (Beerens et al., 2003). Despite intensive study, the exact mechanism remains unknown. Nevertheless, the ability to ferry large cargos (up to ~1000 a.a.) when tethered with PTD makes it an ideal tool to transfer proteins and DNA fragments into living cells for research purposes (Schwarze et al., 1999; Schwarze et al., 2000).

With the techniques and concepts mentioned above, I developed a pure genetically-encoded method that allows identification and functional studies of synaptically coupled neurons in a unbiased manner. The idea is based on trans-cellular delivery of site-specific reocmbinase from a starter neuron to its downstream target neuron(s), which is made possible by incorporation of protein transduction domain to the recombinase. Two binary systems, Gal4 and QF, endow the flexibility of manipulating separate components in the starter and downstream neurons, respectively. Thus, we provide a method to identify and manipulate downstream circuits with genetically defined pre-synaptic neurons (Chapter 3).

Figure 1.1

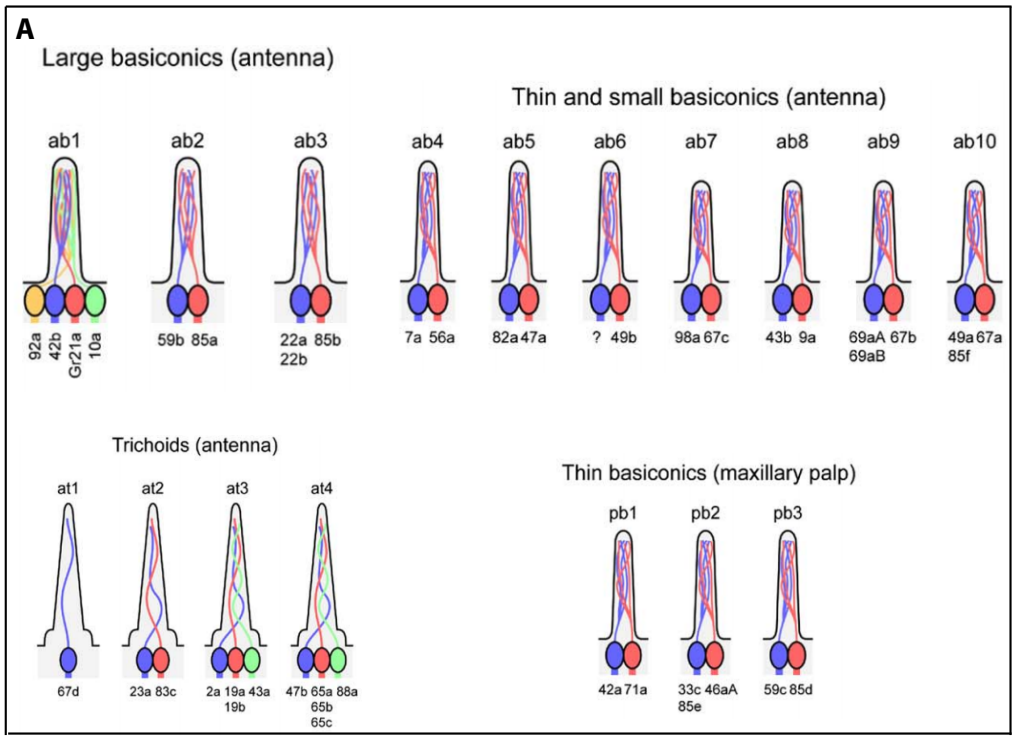

Couto et al., 2005 Current Biology

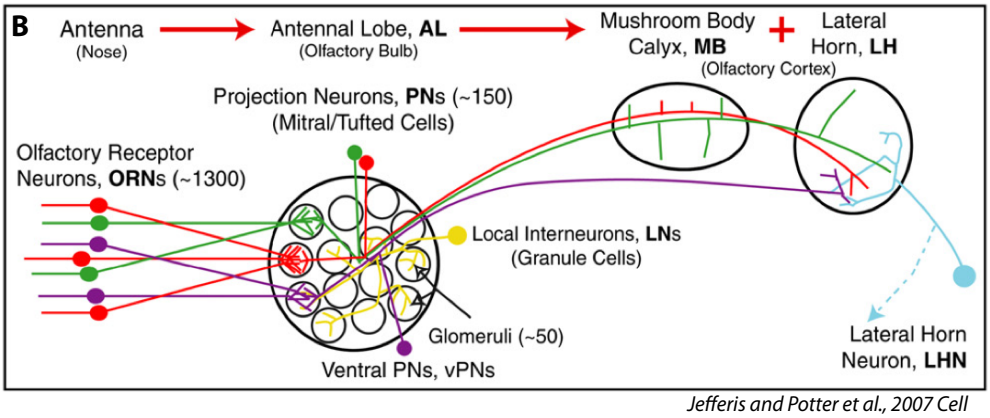

Jefferis and Potter et al., 2007 Cell

Figure 1.1 Basic organization of *Drosophila* olfactory system.

(**A**) Current classification of *Drosophila* sensilla. Shown here are two types: trichoid and basiconic sensilla (Couto et al., 2005). (**B**) Schematic of olfactory circuitry from periphery to central brain regions (Jefferis et al., 2007).

Figure 1.2

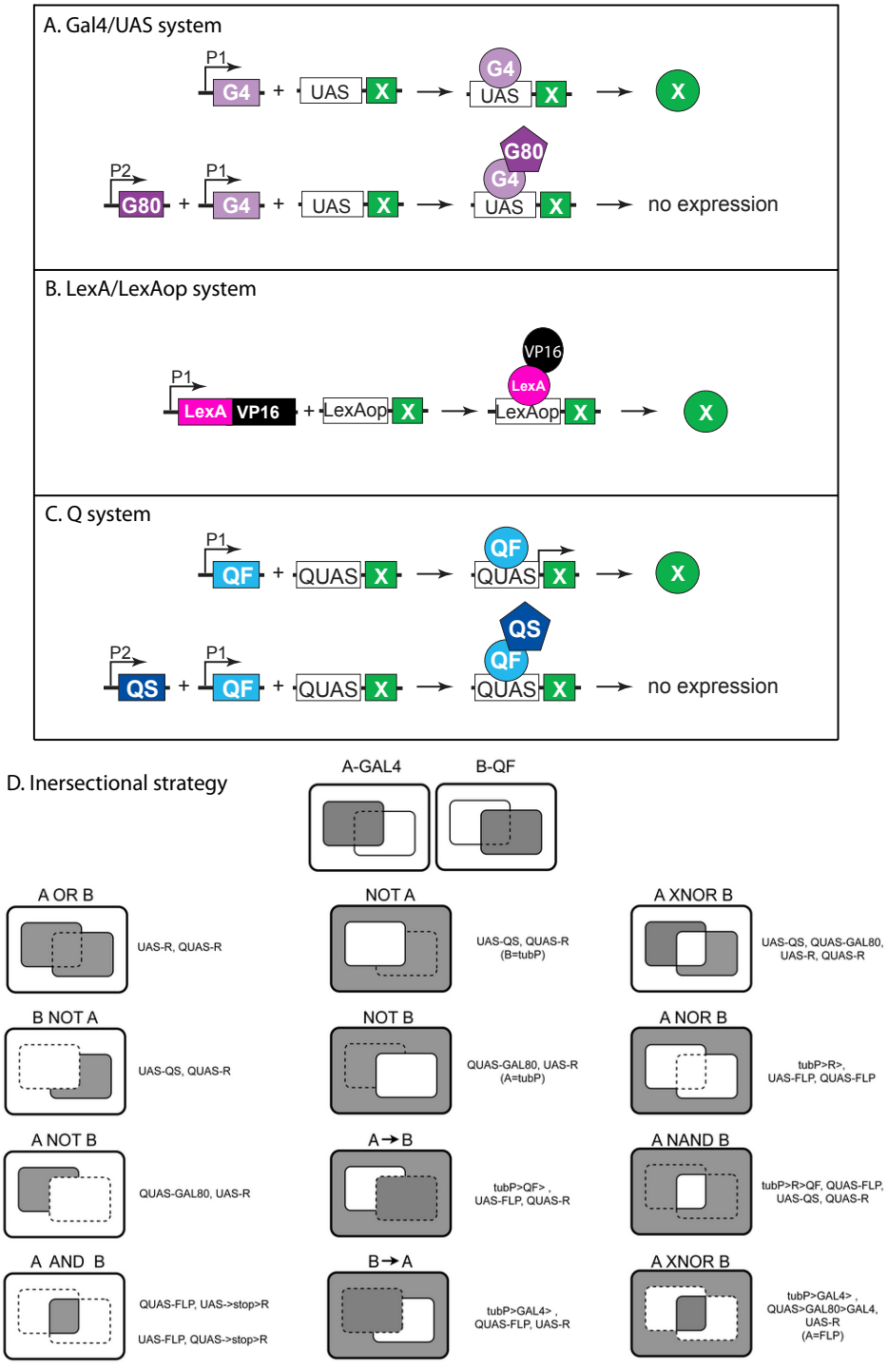
A. Gal4/UAS system
P1
G4
UAS
X
G4
UAS
X
X
P2
G80
P1
G4
UAS
X
G80
G4
UAS
X
no expression
B. LexA/LexAop system
P1
LexA
VP16
LexAop
X
VP16
LexA
LexAop
X
X
C. Q system
P1
QF
QUAS
X
QF
QUAS
X
X
P2
QS
P1
QF
QUAS
X
QS
QF
QUAS
X
no expression
D. Inersectional strategy
A-GAL4
B-QF
A OR B
UAS-R, QUAS-R
NOT A
UAS-QS, QUAS-R
(B=tubP)
A XNOR B
UAS-QS, QUAS-GAL80,
UAS-R, QUAS-R
B NOT A
UAS-QS, QUAS-R
NOT B
QUAS-GAL80, UAS-R
(A=tubP)
A NOR B
tubP>R>,
UAS-FLP, QUAS-FLP
A NOT B
QUAS-GAL80, UAS-R
A→B
tubP>QF> ,
UAS-FLP, QUAS-R
A NAND B
tubP>R>QF, QUAS-FLP,
UAS-QS, QUAS-R
A AND B
QUAS-FLP, UAS->stop>R
UAS-FLP, QUAS->stop>R
B→A
tubP>GAL4> ,
QUAS-FLP, UAS-R
A XNOR B
tubP>GAL4> ,
QUAS>GAL80>GAL4,
UAS-R
(A=FLP)

Figure 1.2 Schematics of binary expression systems.

(**A**-**C**) Cartoons of three major binary expression systems: Gal4/UAS, LexA/LexAOP and Q systems. Note that both Gal4 and QF have inhibitors: Gal80 and QS, respectively (**D**) Intersectional studies using Gal4/UAS and Q systems as example.

Figure 1.3

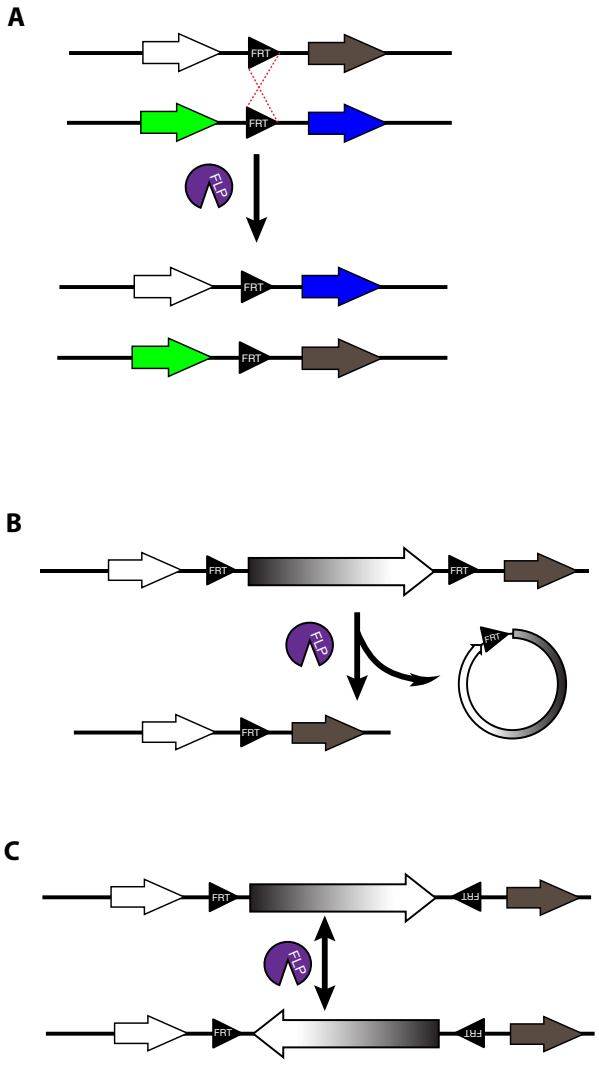

Figure 1.3 Site-specific recombination for genetic manipulation.

(**A**) When FRT sites are in *trans* arrangement, presence of FLP results in cross-over event. (**B**) When FRT sites are in *cis* arrangement with same orientation, intervening sequence will be excised. (**C**) If FRT sites are arranged in opposite orientation, the intervening sequence is inverted.

Chapter 2: Food odors trigger *Drosophila* males to deposit a pheromone that guides female oviposition decisions

2.1 Introduction:

Animals must navigate a complex and changing environment for survival and reproduction. Odorants function as molecular cues for objects in the environment, and the olfactory system translates these cues into appropriate behaviors (Laissue and Vosshall, 2008; Semmelhack and Wang, 2009; Stensmyr et al., 2012; Suh et al., 2004). Living organisms are also a source of odorants, broadly termed pheromones, which play important roles in olfactory communications between different organisms of the same species (Wilson, 1970). For instance, an alarm pheromone from the perianal area of male rats induces an autonomic stress response in recipients (Kiyokawa et al., 2004); and stingless bees (*Trigona spinipes*) lay a scent towards profitable food sources to induce a trailing marking behavior (Schorkopf et al., 2007). Despite a wealth of knowledge of pheromone identities and their physiological functions, how upstream environmental cues trigger pheromone signaling is not well understood.

With the rapid development of genetic and physiological tools, the vinegar fly *Drosophila melanogaster* provides a promising model system to dissect the neural basis of animal behaviors (Venken et al., 2011). Advances in the understanding of chemosensory receptors and neural circuitry of innate behaviors such as attraction, repulsion and feeding provide insight into sensory mechanisms utilized throughout evolution (Pool et al., 2014; Semmelhack and Wang, 2009; Stensmyr et al., 2012; Suh et al., 2004). Moreover, the effects of chemosensory systems on complex but stereotypic

behaviors such as courtship, aggression and oviposition are beginning to be elucidated (Alekseyenko et al., 2013; Wang et al., 2011; Yamamoto and Koganezawa, 2013; Yang et al., 2008).

A behavior that is largely mediated through pheromone signaling is population aggregation, which is hypothesized to ensure efficient use of resources (Karlson and Luscher, 1959; Wyatt, 2014). Aggregation behavior may reduce interspecific competition and also be important for finding mates (Hedlund et al., 1996). However, how aggregation pheromones are induced or deposited to mark certain geographical location and modulate animal behaviors remains largely unknown. In *Drosophila melanogaster*, aggregation behavior has been observed at locations that contain male flies and food substrates. The male specific pheromone cis-vaccenyl acetate (cVA) has been implicated as the key aggregation pheromone that attracts both males and females (Bartelt et al., 1985; Xu et al., 2005). However, cVA is manufactured and stored in an internal male organ (ejaculatory bulb) and transferred to females only during copulation (Brieger and Butterworth, 1970; Butterworth, 1969; Everaerts et al., 2010; Scott and Richmond, 1987), where it plays a role in inhibiting male courtship of previously mated females (Ejima et al., 2007). Little direct evidence supports the idea that cVA serves a behavioral role prior to the mating process (Everaerts et al., 2010). Furthermore, flies defective in sensing cVA exhibit residual aggregation behavior, suggesting the existence of an aggregation compound besides cVA from male flies (Xu et al., 2005).

Drosophila pheromones are typically cuticular hydrocarbons (CHCs) that are produced by specialized cells (oenocytes) in the fly abdomen and form a waxy layer on the body surface (Billeter et al., 2009; Ferveur, 2005; Wyatt, 2014). Given the chemical

nature of long chain hydrocarbons, most CHCs are not volatile and are instead detected by gustatory contact (Bray and Amrein, 2003; Ferveur, 1997; Jallon, 1984). For instance, 7-tricosene, an abundant male CHC, is a pheromone that functions as an aphrodisiac for females and anti-aphrodisiac for males that is sensed via the gustatory system (Lu et al., 2012; Thistle et al., 2012). Nonetheless, recent solid-phase micro-extraction gas chromatography experiments indicated the presence of volatile CHC pheromones, suggesting pheromone detection might be medicated through the olfactory system (Farine et al., 2012; Ferveur et al., 1997; Stocker, 1994). All together, these studies suggest an uncharacterized CHC functions as an aggregation pheromone, signaling via the olfactory system.

Here, we report the finding that male flies actively deposit a novel aggregation pheromone onto their surroundings upon food odor stimulation. The pheromone, 9-tricosene, is a volatile male-specific CHC and requires the olfactory, but not gustatory, system for detection. By electrophysiological and behavior studies, we identify the olfactory neurons necessary and sufficient for 9-tricosene pheromone detection. Behaviorally, 9-tricosene enhances courtship and modulates female oviposition site selection- a behavior that was previously considered a female exclusive decision (Joseph et al., 2009; Yang et al., 2008). Our study provides important insights into biological communication by identifying an olfactory mechanism that links together food-odor perception, male pheromone deposition, species aggregation, and female oviposition decision-making.

2.2 Results:

A Novel Chemosensory Assay Identifies a Post-Stimulus Aggregation Behavior

Traditional olfactory assays monitor either single flies (Semmelhack and Wang, 2009) or multiple flies in small spaces (Quinn et al., 1974) and might overlook important social behaviors. We modified a four-field olfactory arena and fly tracking system (Katsov and Clandinin, 2008; Ronderos et al., 2014; Semmelhack and Wang, 2009; Vet et al., 1983) to monitor large fly populations responding to odors over a large arena space. Flies are contained in a star-shaped arena between two glass plates (See Experimental Procedures for details) and tracked in a dark chamber using infrared illumination (which is invisible to flies), and detected by an infrared camera (Figure 2.1A). We validated our experimental design by monitoring attraction to apple cider vinegar (ACV), repulsion to citronellal (Kwon et al., 2010), and neutral responses to clean air (Figures 2.2A, 2.2B, and 2.2C). Flies mutant for *orco*, a necessary co-receptor for most olfactory receptor neurons (Larsson et al., 2004), showed reduced responses to control odorants, confirming the experimental design accurately assesses olfactory behaviors (Figures 2.2D and 2.2E).

During investigations with the food-odor ACV, we identified a novel olfactory behavior in which flies showed robust aggregation to the original odor quadrant for substantial time periods subsequent to odor application (Figures 2.1B, 2.1C, and 2.1G). In these experiments, flies were stimulated with ACV for 5 minutes, ACV odor was switched to clean air for 10 minutes, and flies tracked in an arena that had been rotated 90 degrees to rule out contamination in the odor delivery system (Figure 2.1B, Movies 1 and 2). Interestingly, this aggregation behavior in the absence of exogenous odor-stimulation persisted for >25 minutes (Figure 2.4A). We called this behavior "post-stimulus aggregation".

Post-Stimulus Aggregation is an Active Pheromone Deposition Process

Perfusion of ACV into the empty arena for 5 minutes in the absence of flies, and introduction of naïve flies into the arena, did not produce post-stimulus aggregation to the original quadrant (Figure 2.1D), suggesting the post-stimulus aggregation behavior is not due to residual ACV on the glass plates. Additionally, odorant levels returned to baseline in 2 minutes after cessation of odor application as analyzed by a photoionization detector (data not shown).

The bodies of flies are covered by cuticular hydrocarbons (CHCs) that can function as chemosensory pheromones (Amrein, 2004; Ferveur, 2005; Ferveur et al., 1997; van der Goes van Naters and Carlson, 2007). To rule out the possibility of passive pheromone deposition onto the glass plates due to congregation of many flies into a small space, flies were corralled into the odor quadrant by attraction to humidified air and monitored for post-stimulus aggregation after 10 minutes of clean air. Under these conditions, there was no detectable post-stimulus aggregation (Figures 2.1E and 2.1F). All together, these data suggest that flies actively and selectively deposit a pheromone(s) in response to the food-odor ACV. Different concentrations of ACV generated post-stimulus aggregation responses of different potencies (Figure 2.4B).

Post-Stimulus Aggregation Behaviors are Stimulated by Food-Odors

To determine if post-stimulus aggregation could be induced by other food odors, we tested two additional food odors, banana and yeast paste (Figure 2.2A). These stimuli were highly attractive to flies and also induced post-stimulus aggregation. As a further

test, we examined stimulus attraction by prominent monomolecular odorants of ACV, ethyl acetate (EA) and acetic acid (AA). Although these odorants were highly attractive, they failed to generate post-stimulus aggregation behaviors (Figure 2.2A). Together, these data suggest that post-stimulus aggregation behaviors are guided specifically by food odors, and possibly by food odor perceptions. As such, a particular combination of monomolecular odorants might mimic food odor perception. Indeed, simultaneous perfusion of EA (~0.001%) and AA (0.33%) at physiological concentrations as in ACV created an ACV-like post-stimulus attractive behavior (Figures 2.3A and 2.3C).

Males are the Source of the Aggregation Pheromone and Detection Requires *Orco*

Intra-species communications via pheromones are often sex-specific. We used different combinations of flies (mixed genders, virgin females, or males) as potential pheromone secretors upon ACV stimulation, and new naïve mixed genders as detectors for the presence of the pheromone (Figure 2.2B). Only in the presence of male secretor flies did detector flies show post-stimulus aggregation (Figure 2.2C). This indicates that male flies are the source of the pheromone. The aggregation pheromone was equally attractive to both virgin and mated males and females (Figure 2.4D).

Pheromones are detected by the olfactory and gustatory systems (Amrein, 2004; Lu et al., 2012; Thistle et al., 2012; Wyatt, 2014). Since the pheromone is deposited onto the glass plates, it might be detected by either chemosensory system. We utilized genetic mutants that are defective in specific modes of chemosensory signaling as detectors. *Poxn* mutants, which exhibit no functional gustatory receptor neurons (Awasaki and Kimura, 2001), were as attracted as wild-type animals (Figure 2.2D), suggesting that the

gustatory system is not necessary for post-stimulus aggregation. Pickpocket channel 23 (ppk23), a Degenerin/epithelial sodium channel, is necessary for the detection of a male-predominant CHC, 7-tricosene (Lu et al., 2012; Thistle et al., 2012). However, *ppk23* mutants exhibited similar post-stimulus aggregation compared to wild-type animals (Figure 2.2D), suggesting ppk23 function is not necessary for aggregation and that 7-tricosene is unlikely to be the aggregation pheromone. Most insect olfactory receptors require a coreceptor(s) for normal olfactory responses: *Orco* for Odorant Receptors (Larsson et al., 2004) and *Ir8a* or *Ir25a* for ionotropic receptors (Abuin et al., 2011; Benton et al., 2009). The *Ir8a* and *Ir25a* double mutant flies exhibited normal post-stimulus aggregation, showing that most ionotropic receptors are not required for the pheromone attraction (Figure 2.3E). Interestingly, in *orco* mutant flies, attraction behavior to the pheromone was completely abolished and instead repelled by the ACV quadrant. This repulsion is likely due to acid sensing of minimal residual acetic acid on the quadrant mediated by the *Ir8a*/*Ir64a* complex (Ai et al., 2010)(Figure 2.4E). Indeed, the *orco*, *Ir8a* double mutant was no longer repelled by the odor quadrant (Figure 2.3E), and the use of neutralized ACV as the stimulus eliminated the post-stimulus repulsion demonstrated by *orco* mutants (Figure 2.4F). Interestingly, neutralized ACV retains the ability to stimulate post-stimulus aggregation behaviors in wild-type flies (Figure 2.4G). These data suggest that detection of the food-odor-induced pheromone is mediated through the *orco*-dependent olfactory system.

cVA has been suggested to be a male-derived aggregation pheromone in *Drosophila melanogaster* (Bartelt et al., 1985). cVA binds to and induces a conformational change of the odorant binding protein LUSH, which enhances the

activation of Or67d/Orco complexes (Laughlin et al., 2008; Xu et al., 2005). Furthermore, the Drosophila melanogaster CD36 homologue, sensory neuron member protein (Snmp), likely works in concert with the odorant receptor and is essential for Or67d neuronal activation (Benton et al., 2007). cVA can also activate Or67d/Orco complexes directly (Gomez-Diaz et al., 2013). However, mutations of the key components in the signaling pathway (*Or67d*, *lush*, *snmp*) do not alter the post-stimulus aggregation behavior (Figure 2.3F), suggesting that cVA is not the food-odor induced aggregation pheromone.

9-Tricosene is a Food-Odor Induced Aggregation Pheromone

Since most insect pheromones are lipophilic carbohydrates dissolvable in hexane (Scott and Richmond, 1988; van der Goes van Naters and Carlson, 2007), we reasoned that hexane might extract the active pheromone off the glass surface in the food-odor-induced quadrant. We induced wild-type flies to deposit the food-odor induced pheromone onto the glass plate and dissolved the deposited molecules into hexane. We then painted the hexane extract onto a new glass plate in a letter 'E' pattern. Naïve new flies were able to trace and follow the E pattern but do not follow control hexane extracts of flies stimulated by humidified air painted in the same pattern (Figures 2.5A, 2.5B, 2.6 and Movie 3). These experiments demonstrated that an active pheromone component(s) was successfully preserved during the pheromone extraction. Behavioral results suggested the pheromone was volatile because: 1) it required the olfactory system for detection (Figure 2.3E); 2) constant air flushing reduced behavioral attraction after ~25 minutes (Figure 2.4A); and 3) heating the pheromone-containing arena to 32˚C to

increase odor volatility eliminated post-stimulus behaviors (Figure 2.4H). Recently, five CHCs were identified as male-specific volatile pheromones: 7-docosene, 5-tricosene, 23-methyldocosane, cVA and 9-tricosene (Farine et al., 2012). To identify the nature of the pheromone molecule(s), we performed gas chromatography-mass spectrometry (GC-MS) analyses of hexane extracts from quadrants stimulated with ACV alone, with humidified air (HA) and flies, and with ACV and flies. Consistent with our behavior results that cVA is unlikely to be the food-odor induced pheromone (Figure 2.3F), cVA was not detected in pheromone extracts from the glass plates (Figure 2.5C; Figure 2.17). 7-docosene and 23-methyldocosane were also not detected, while 5-tricosene was detected at trace amounts (Figure 2.5C and Figure 2.17). The levels of 7-tricosene were increased in the experimental conditions, but as 7-tricosene is a highly abundant male CHC (Everaerts et al., 2010), its presence likely reflects passive deposition of pheromones onto the glass plate. In addition, our behavioral results excluded 7-tricosene as the food-odor-induced pheromone (Figure 2.3D; also see below and Figure 2.10B). Interestingly, only one other peak was significantly enriched in the experimental but not HA+flies control group: (Z) 9-tricosene (9-T) (Figure 2.5C, Figure 2.17). Little is known regarding the function of 9-tricosene in *Drosophila melanogaster* besides its presence as a male-specific volatile pheromone (Everaerts et al., 2010; Farine et al., 2012). To determine if 9-tricosene was attractive to *Drosophila*, as would be predicted for the food-odor induced aggregation pheromone, we used 9-tricosene as the stimulus in the 4-field olfactory assay. Indeed, 9-tricosene was attractive at dilutions of 1:1000 (Figure 2.5D). These data suggest that 9-tricosene is likely a key aggregation pheromone deposited upon food-odor stimulation.

9-Tricosene is a member of CHCs produced by oenocytes on the fly abdominal wall (Billeter et al., 2009; Everaerts et al., 2010). 9-Tricosene and other CHC components, but not cVA, can be genetically eliminated by specifically ablating oenocytes (Billeter et al., 2009). Oenocyte-less males mixed with wild-type females no longer produced a post-stimulus aggregation behavior, suggesting that an oenocyte-derived CHC is essential for post-stimulus aggregation (Figure 2.4I), consistent with the identification of 9-tricosene as a food-odor induced pheromone.

The Or7a Receptor is Necessary and Sufficient for 9-tricosene Activation

The *Drosophila* antenna utilizes three different receptors for the detection of odorants and they can be classified as those that require either *orco* (odorant receptors expressed in basiconic, intermediate, trichoid and ac3 sensilla) (Couto et al., 2005; Larsson et al., 2004) or those that are *orco*-independent (ionotropic receptors expressed in coeloconic sensilla and gustatory receptors expressed in the ab1C neuron) (Abuin et al., 2011; Benton et al., 2009; Suh et al., 2004). To determine which odorant receptors are required for 9-tricosene responses, we performed electroantennogram (EAG) recordings, which measure global detection of odor-induced antennal responses, in WT and *orco* mutants (Figure 2.7A). The *orco* mutants completely lacked responses to 9-tricosene (Figures 2.7A and 2.7B). This suggests that 9-tricosene activates an *orco*-dependent odorant receptor, and does not require signaling from *Ir* or *Gr* receptors, consistent with our behavioral data (Figure 2.3E).

We next identified the *orco*-positive olfactory receptor neurons (ORNs) in the antenna and maxillary palps that respond to 9-tricosene by using fluorescence guided

Single Sensillum Recording (SSR), which detects the activity of olfactory neurons within single sensory sensilla. Previously characterized volatile pheromones typically activate trichoid or intermediate sensillar neurons (Ronderos et al., 2014; van der Goes van Naters and Carlson, 2007). Surprisingly, 9-tricosene did not stimulate the activity of these sensillar neurons (Figure 2.7C). We found that 9-tricosene elicits rapid and robust firing patterns in the antennal basiconic ab4 sensillum, which houses two neurons (ab4A and ab4B) that express Or7a (ab4A) or Or56a receptors (ab4B) (Figure 2.7C) (Couto et al., 2005; Fishilevich and Vosshall, 2005; Stensmyr et al., 2012). 9-Tricosene stimulates spiking of the larger amplitude neuron indicating the 9-tricosene-responsive ORNs are ab4A, which express Or7a receptors (Figure 2.7D). To determine if the Or7a receptor is sufficient for 9-tricosene responses, we misexpressed Or7a in an olfactory neuron that lacks an odorant receptor in ab3A sensillar neurons (Dobritsa et al., 2003). Expression of Or7a endowed ab3A neurons the ability to respond to 9-tricosene comparable to the 9-tricosene activation pattern as detected in the endogenous Or7a-positive ab4 sensillum (Figures 2.7D and 2.7E). These data indicate that the Or7a receptor responds to 9-tricosene. This is unexpected since basiconic sensilla were traditionally considered food odor detectors (Fishilevich and Vosshall, 2005; Jones et al., 2007; Laissue and Vosshall, 2008; Larsson et al., 2004; Suh et al., 2004). Both male and female ab4A/Or7a neurons responded equally to 9-tricosene (Figure 2.7E), consistent with 9-tricosene being attractive to both males and females (Figure 2.4D). Or7a neurons did not respond to cVA (Figures 2.8A and 2.8B).

To further verify that Or7a was responsible for the 9-tricosene responses of ab4A neurons, we generated *Or7a* mutants using homologous recombination (Figure 2.8C and

S4D). Ab4 sensilla in *Or7a* mutants were identified based on their shape and the specific response of the ab4B neuron to geosmin (Stensmyr et al., 2012). No spontaneous or 9-tricosene stimulated ab4A spiking activity was observed in *Or7a* mutant flies (Figures 2.8F and 2.8G), indicating that Or7a is necessary for 9-tricosene activation in ab4 sensilla.

The Or7a Receptor is Necessary for Pheromone and 9-tricosene Induced Aggregation

Or7a-GAL4 specifically drives effector expression only in olfactory neurons that target the DL5 antennal lobe glomerulus (Figure 2.9A) (Couto et al., 2005). We thus could use the *Or7a-GAL4* line to specifically ablate $Or7a^{+}$ neurons and test for changes in behavior. Aggregation responses to both the naturally deposited food-odor induced pheromone (Figures 2.9B and 2.9C) and to 9-tricosene (Figures 2.9D and 2.9E) were completely abolished in Or7a neuron-ablated flies obtained using *Or7a-Gal4+UAS-hid* (Figure 2.9) and *Or7a-Gal4+UAS-DTI* (Figure 2.10A). Ablation of other odorant receptors (*OrX-Gal4+UAS-hid*) did not affect aggregation (Figure 2.9C). Similarly, *Or7a* mutants completely lacked attraction to the naturally deposited food-odor-induced pheromone and to 9-tricosene (Figures 2.9B-2.9E). To verify that aggregation behavior is specific to 9-tricosene, we repeated the experiments using the 9-tricosene pheromone isomer 7-tricosene (7-T), which contains an identical carbon chain length to 9-tricosene but a double bond at an alternate location. Interestingly, 7-tricosene induced a neutral to slightly repulsive behavior in WT flies (AI=-0.07 ± 0.026, Figure 2.10B). These data

suggest that aggregation behavior to the naturally deposited food-odor-induced pheromone depends on 9-tricosene and proper function of the *Or7a* receptor.

9-Tricosene Enhances Courtship Behaviors and Subsequently Increases Egg Production

Many behaviors occur at food sources, including courtship and egg-laying, but the molecular signals that help guide these behaviors remain poorly characterized (Wyatt, 2014). Since 9-tricosene effectively aggregates flies to sites of food-odor perception, we asked whether 9-tricosene is a major olfactory mechanism for catalyzing these behaviors.

Egg-laying by females is a highly regulated process involving many sensory cues (Joseph et al., 2009; Yang et al., 2008). We therefore asked if 9-tricosene could stimulate egg-laying production in females (Figure 2.10C). There was no significant change in egg laying production by females in the presence of 9-tricosene. However, if males were also present, egg-production significantly increased more than 2-fold (Figure 2.10C). This suggests that simultaneous presence of 9-tricosene and males increase egg production. This might be a result of increased courtship, which has been previously shown to increase egg production (Herndon and Wolfner, 1995; Monsma et al., 1990). We performed courtship assays in the presence or absence of 9-tricosene and found that, in the presence of 9-tricosene, the successful mating rate was about 2-fold higher than control groups (Figures 2.10D and 2.10E). These data suggest that 9-tricosene functions as an aphrodisiac to stimulate female courtship and thereby egg production.

9-Tricosene Guides Oviposition Site Selection via Or7a Neurons

Drosophila preferentially lay their eggs in food sources so as to increase survival of their progeny (Dweck et al., 2013; Joseph et al., 2009; Schwartz et al., 2012). Female flies utilize a complex decision making process to determine appropriate locations for egg laying (Joseph et al., 2009; Yang et al., 2008). Since 9-tricosene acts as a geographical marker for food, it could function as a male-generated guide for female egg-laying decisions. We modified our 4-field arena by spreading a thin layer of 1% agarose onto one of the glass plates that served as a substrate for the secreted pheromone and an appropriate medium for female egg-laying (Figure 2.11A). In order to rule out a potentially confounding role of males in this behavior, only previously mated females were assayed in the arena. Under conditions in which the food-odor-stimulated pheromone was deposited onto the agarose (Figure 2.11A'), females laid five-fold more eggs in the pheromone quadrant. This suggests that a deposited pheromone could guide female egg-laying site selection decisions. We next generated an arena in which one quadrant contained 9-tricosene (Figure 2.12A). Female flies also laid significantly more eggs in locations containing only 9-tricosene (Figure 2.11B'). The 9-tricosene egg-laying preference was abolished when Or7a neurons were ablated (*Or7a-Gal4/UAS-hid* or *Or7a-Gal4/UAS-DTI*) (Figures 2.11C' and 2.12B-C). The 9-tricosene guided egg laying preference was also abolished in *Or7a* mutant flies (Figure 2.11D). The oviposition preference for the 9-tricosene quadrant was not due to the innate attraction to 9-tricosene because females spent similar time in the four quadrants over the course of the 23 hour egg-laying assay (Figure 2.11E). Hydrocarbons could be potential food sources for larvae and female flies might thus preferentially lay eggs in locations containing CHCs. To verify that oviposition guidance is specific to 9-tricosene, we repeated the oviposition

experiments using the 9-tricosene pheromone isomer 7-tricosene (7-T), the most abundant CHC in male flies (Everaerts et al., 2010). Female flies did not preferentially oviposit in the 7-T quadrant (Figure 2.11F). Interestingly, total egg numbers laid were significant higher in *Or7a* mutant and Or7a neuron ablated flies, implying a potential connection of oviposition site selection and egg production number (Figure 2.11G). These data suggest that male derived 9-tricosene specifically guides female egg-laying preferences, and this decision-making process requires proper Or7a neuronal function.

The Or7a Receptor Is Evolutionarily Divergent

Evolving the ability to detect an olfactory niche might alleviate direct competition among different species, especially for behaviors essential for species survival like oviposition site selection. Closely-related species can exhibit very different preferences for oviposition sites (R'Kha et al., 1991; Ramdya and Benton, 2010). Since the Or7a is a critical olfactory receptor for oviposition site selection, we asked if the Or7a protein is evolutionarily conserved in *Drosophilids* or represents a recent adaptation. A rapidly evolving receptor might endow a species-specific ability to find an oviposition niche. We performed comprehensive comparisons of the amino acid changes that occur among the odorant receptors versus the time since 12 different *Drosophila* species diverged and found that different odorant receptors evolve at distinct rates (Figures 2.13A, 2.13B and Figure 2.18). Odorant receptors that exhibit highly conserved functions showed the least amount of evolutionary divergence: *e.g,* olfactory co-receptors Orco (Larsson et al., 2004), Ir8a, and Ir25a (Abuin et al., 2011); and CO_2 receptors Gr21a and Gr63a (Suh et al., 2004). In contrast, the Or7a receptor has undergone one of the most rapid amino acid

substitutions during evolution of *Drosophilids*. It also showed positive selection by a codon-based Z test (p=0.0003), indicating that the Or7a receptor is likely under selective pressure to evolve new functions. Indeed, the Or7a receptor was recently found to exhibit variation in ligand affinity among different *Drosophilid* species (Stensmyr et al., 2012).

Reclassification of sensilla types in *Drosophila melanogaster*

By using fluorescence-guided SSR, we are able to directly locate the ORNs of interest to the target sensillum for recording (OrX-Gal4>UAS-mCD8GFP) (Figure 2.20A). During the comprehensive screening, we accidentally found that some of the sensilla types were previously misclassified (Couto et al., 2005). For example, there are only two types of trichoid sensilla: at1 (containing only Or67d ORN) and at2 (containing Or47b, Or65a/b/c and Or88a). Other "trichoid" sensilla are actually intermediate sensilla (ai2 (Or23a and Or83c) and ai3 (Or2a, Or19a/b and Or43a)) (Figure 2.20B).

2.3 Discussion:

We have identified a phenomenon in which *Drosophila* males actively deposit the pheromone 9-tricosene in response to food-odor stimulation. This male-predominant cuticular hydrocarbon acts as an aggregation pheromone to attract animals, as an aphrodisiac to enhance courtship, and as a chemosensory cue to influence female oviposition site selection (Figure 2.13C). This study introduces a number of important findings to *Drosophila* pheromone signaling: (1) environmental cues, such as food-odors, can act as upstream regulators to stimulate pheromone deposition; (2) 9-tricosene is a key aggregation pheromone deposited upon food-odor stimulation; (3) 9-tricosene is the first

Drosophila cuticular hydrocarbon demonstrated to function via the olfactory system; (4) a male-derived pheromone affects multiple female decisions such as courtship and egg-laying site selection. This work provides insight into the mechanisms by which pheromones link environmental cues to behavioral choices.

Aggregation Behavior Guided by Food-Odor Perception

"Undercrowding" of a conspecific population can increase vulnerability to predators and lower reproductive rates (Allee effect) (Allee, 1931; Courchamp et al., 1999). In addition to a protective effect, aggregation behavior brings both sexes to the resource so that mating can happen. Aggregation behavior is mediated primarily by pheromone chemosensory cues and maximum production of an aggregation pheromone in many species requires the presence of food (Wyatt, 2014). However, the exact mechanisms of how food odors trigger aggregation pheromone signaling remained unclear.

Animals attracted to a food site might utilize multiple strategies in depositing an aggregation pheromone. Animals could passively deposit pheromones onto their surroundings, and abundance of the aggregation pheromone at a food-site would reflect the general attractiveness of the food site. An alternative strategy would be to specifically deposit a pheromone by certain behaviors only in the presence of an optimal food-source, as has been observed in ants and termites (Fitzgerald and Edgerly, 1982; Holldobler and Wilson, 1978). We have found that *Drosophila* likely utilize the second strategy for aggregation pheromone deposition. In addition, aggregation at a food-site is strongly influenced by the olfactory perception of an optimal food source. We found that the aggregation pheromone 9-tricosene is only deposited upon food-odor stimulations, such

as ACV, ripe banana or yeast. Attractive odorant components alone (EA and AA) found in ACV are not sufficient for pheromone deposition, suggesting that attraction *per se* to an odor is not sufficient for aggregation pheromone deposition. Only upon mixture of these two components was pheromone deposition recapitulated, suggesting that combinatorial sensory perception mimics an optimal food-source and triggers pheromone signaling. Indeed, introduction of a repellant odor with ACV can abolish aggregation pheromone deposition (data not shown). These studies also present a new genetic model in which precise individual odorant components and conditions are "bound" to a perception (Crick, 1995; Shadlen and Movshon, 1999). Ablating Or42b olfactory receptor neurons, which is a major class of olfactory neurons for EA attraction and detection (Semmelhack and Wang, 2009), abolishes the pheromone deposition process (data not shown). This identifies at least one necessary olfactory signal required for food-odor perception and subsequent pheromone deposition. Future studies will determine the combination of olfactory signaling necessary and sufficient to connect an odor perception to a physiological response.

cVA has been suggested as the aggregation pheromone in *Drosophila melanogaster*. However, in contrast to the aggregation pheromones identified in other *Drosophila* species (Bartelt et al., 1985; Hedlund et al., 1996), cVA attracts flies only when coupled with food or food-derived odor (Bartelt et al., 1985). cVA is not normally present on the cuticle and so can not play a olfactory role before being transferred to females during copulation (Everaerts et al., 2010). Our study demonstrates that mutating key components in cVA signaling pathway does not affect the food-odor induced aggregation behavior. Moreover, GC-MS analysis of the active aggregation pheromone

extract found no evidence that cVA was deposited. Therefore, cVA is likely not responsible for the aggregation behaviors triggered by food odors. Nonetheless, it remains possible that, under natural conditions, cVA is used as a long distance co-attractant with food odors at mating sites while 9-tricosene is used as a short-range aggregation pheromone to modulate social behaviors at food sites.

9-Tricosene Is an Important Close-Range Social Pheromone

Food searching behaviors rely on volatile chemosensory cues, which create long-distance odor plumes or homogeneous odor clouds to guide foraging behaviors (Budick and Dickinson, 2006). In contrast, 9-tricosene, as a low volatility olfactory pheromone, might be ideally suited as a close-range olfactory marker, and may be utilized to convey social information regarding environmental interactions. This is supported by the variety of functions 9-tricosene exhibits in other species. For instance, 9-tricosene is a sex attractant for female houseflies (*Haematobia irritans*) (Carlson et al., 1971); female Asian longhorned beetles (*Anoplophora glabripennis*) attract males to their locations by pheromone trails containing 9-tricosene (Hoover et al., 2014); mate-searching male spiders (*Pholcus beijingensis*) utilize 9-tricosene to stimulate female courtship behaviors (Xiao et al., 2010); and honey bee waggle dancers (*Apis mellifera L.*) use a pheromone cocktail that includes 9-tricosene to communicate with nest mates about the locations of food sources (Thom et al., 2007). Given its widespread use among different species, the 9-tricosene signal might be recognized by non-conspecific organisms. This suggests that 9-tricosene might function predominately to modulate behaviors directed by other species-specific sensory cues.

Pheromones Can Activate Basiconic Sensillar Neurons

The olfactory organs of insects contain sensory hairs called sensilla that house olfactory receptor neurons (ORNs). Three basic-types of olfactory sensilla have been classified based on their size, shape, and predicted functions (Couto et al., 2005; Venkatesh and Naresh Singh, 1984). ORNs housed in basiconic sensilla tend to be strongly activated by food odors; ORNs in intermediate/trichoid sensilla tend to be activated by pheromones, and ORNs in coeloconic sensilla are activated by amines, ammonia, water vapor and putrescine (Goldman et al., 2005; Ha and Smith, 2006; Hallem and Carlson, 2006; Yao et al., 2005). Only a couple of exceptions are known—phenylacetic acid is a food odor that activates coeloconic Ir84a+ neurons (Grosjean et al., 2011); and carbon dioxide is detected by basiconic neurons expressing Gr21a/Gr63a (Jones et al., 2007; Kwon et al., 2007). 9-tricosene represents the first CHC pheromone that, to our knowledge, activates a *Drosophila* basiconic sensilla. Therefore, basiconic sensilla are responsive to a greater range of stimuli than previously appreciated, and investigations attempting to link pheromone responses to underlying olfactory neurons should not be restricted to examination of intermediate/trichoid sensilla.

A comprehensive SSR survey of odorant-receptor activities had identified multiple other ligands for Or7a receptors (Hallem and Carlson, 2006). Many of these odorants are highly volatile and exhibit high vapor pressures (Figure 2.19). 9-Tricosene, however, likely functions as a short-range pheromone with limited volatility. Factoring in volatility to calculate the number of molecules reaching the antennae, previously identified Or7a odorants require approximately 10^2 to 10^6 more molecules than 9-

tricosene to generate a similar neuronal response (Figure 2.19). For example, the previously identified strongest ligand for Or7a, E2-hexenal, has ~3.4 x 10^3 fold more molecules reaching the antennae than 9-tricosene. This suggests that Or7a receptors are over 1000 times more sensitive to 9-tricosene than to E2-hexenal (Figure 2.19, Figure 2.14).

Male Pheromones Influence a Female Oviposition Decision

Oviposition site selection is a model system to study simple decision-making in *Drosophila* (Joseph et al., 2009; Yang et al., 2008). The behavior comprises three steps—an ovipositor motor program, a clean/rest period and a search-like behavior. The ovipositor motor program that leads to egg deposition is relatively short (6-7 seconds) as compared to clean/rest and search-like behaviors (100-130 seconds) (Yang et al., 2008). Rapid egg-laying associated with an extended positional search is consistent with our observations that over long time periods there were no detectable positional preferences in the 9-tricosene pheromone quadrant even though female flies preferentially laid eggs in this quadrant (Figure 2.11). These findings also suggest that 9-tricosene might mediate two temporally distinct responses in our experimental design. A short-term aggregation behavior that lasts for ~25 minutes and a long-term oviposition site selection behavior that lasts for hours. A possible mechanism underlying these different behaviors could be that detection thresholds for the two behaviors are different, *i.e.* high concentrations of 9-tricosene triggers aggregation whereas low 9-tricosene concentrations affect oviposition. This hypothesis suggests different strategies of 9-tricosene sensory coding which could be addressed by future studies.

In many insects, eggs are vulnerable and larvae have restricted motility, thus oviposition site selection is a crucial decision for progeny survival. The hypothesis of "mother-knows-best" stipulates that female egg-laying decisions evolved to oviposit in places offering the best survival of offspring (Jaenike, 1990; Soto et al., 2014). As expected, oviposition decisions require multiple sensory modalities, such as visual, olfactory, gustatory and proprioception (Azanchi et al., 2013; Joseph et al., 2009; Schwartz et al., 2012; Yang et al., 2008). For instance, flies will prefer to lay eggs in fermenting fruit since the main component of fermentation- ethanol- protects larvae from natural parasites as well as help larva develop into healthier adults (Geer et al., 1993; Milan et al., 2012). Expected larva foraging costs also affect female oviposition site selection. When larva foraging cost is high, female flies tend to lay eggs directly upon the food source (Schwartz et al., 2012). Our study further expands understanding of oviposition site selection by showing that a previously considered female-only decision can in fact be modulated by a male-deposited pheromone. Since 9-tricosene is enriched only upon food-odor stimulation, and acts to aggregate and increase courtship, it could be a mechanism used by *Drosophila* males to increase the likelihood that their progeny will be laid in an optimal location. Thus, in addition to "mother-knows-best", this suggest that "father" may have co-opted a female's olfactory system in order to influence an egg-laying decision for maximizing progeny survival.

We demonstrate that basiconic Or7a+ neurons are responsible for 9-tricosene guided oviposition decisions (Figures 2.11C and 2.11D). Recently, it was found that flies prefer citrus fruit as oviposition substrates detected by Or19a+ olfactory neurons (Dweck et al., 2013). Both Or7a and Or19a receptors have undergone rapid amino acid

substitution over time (Figures 2.13A and 2.13B). Rapid evolution of these ORs might be beneficial for species survival since acquiring new ligand-receptor affinities may help individuals detect oviposition niches. Using odor-cues for establishing new species-specific oviposition preferences might thus prevent interspecies competition and facilitate species survival.

Food odors and pheromone signals have been shown to project to non-overlapping divisions in higher brain regions in *Drosophila*, suggesting that distinct brain divisions may be involved in mediating different biological functions (Jefferis et al., 2007). Might these disparate olfactory signals for oviposition decision converge in the female brain? ORNs expressing the same ORs converge onto the same glomeruli and synapse with second order projection neurons, which relay the olfactory information to higher brain regions (mushroom body calyx and lateral horn) (Marin et al., 2002; Wong et al., 2002). Interestingly, the Or7a DL5 and Or19a DC1 projection neurons share highly similar axonal projection patterns in the lateral horn that are distinct from previously described food and pheromone regions (Figure 2.16) (Jefferis et al., 2007; Ronderos et al., 2014). This suggests that oviposition site-selection might be strongly guided by a dedicated olfactory processing brain center. Characterizing the olfactory circuits in higher olfactory centers activated by Or7a+ and Or19a+ neurons (Jefferis et al., 2007) might reveal how chemosensory cues are integrated in a decision-making process. Furthermore, similar olfactory centers might be evolutionally conserved in other insects such as mosquitoes, and could be potential targets for intervention.

Some ORs are specifically expressed in the *Drsosphila* larval olfactory system. 14 of 25 larval ORs are stage-specific and replaced in adult ORNs. The segregation of larvae

and adult specific ORs might be important for detecting ecological niches in different development stage- larval ORs are tuned to sense much higher concentrations of odors since they are in direct contact with food. We analyzed evolutionary rate of the larval-specific ORs and found that 12 out of 14 (except Or45a and Or49a) are evolutionarily conserved (rate between 0.5-1.3 m/Myr) (Figure 2.15). The data suggest that larval specific ORs are under lower selection pressure possibly because consistent environment.

2.4 Experimental procedures:

Fly stocks:

Wildtype flies are isogenized w^{1118} (*IsoD1* w^{1118}) and *IsoD1* w^{+}. Sources of the lines used in the study: *poxn* mutant, *ppk23*$^{-}$ (Thistle et al., 2012), *Ir8a*$^{-}$ (Abuin et al., 2011), I*r25a*$^{-}$ (Benton et al., 2009), *Ir64a-Gal4* (Ai et al., 2010), *snmp1* mutant (Benton et al., 2007), *lush* mutant, constitutive active *lush* (Laughlin et al., 2008), *Or67d-Gal4* (Kurtovic et al., 2007), *Δhalo/CyO; UAS-Or7a, Δhalo; Or22a-Gal4* (Hallem and Carlson, 2006), *PromE(800)-Gal4, Tub-Gal80ts/TM6B* (Billeter et al., 2009), *Or7a-Gal4* (BS#23907 (Couto et al., 2005)), *orco* mutant (BS# 23130 (Larsson et al., 2004)), *Or83c-Gal4* (BS#23910), *Or43a-Gal4* (BS#9974), *Or88a-Gal4* (BS#23138). Before any behavioral analyses were performed, mutant or transgenic stocks were backcrossed at least 5 generations to *IsoDI* w^{1118}.

Generation of Or7a transgene:

5' and 3' homology arms of the *Or7a* gene were generated by PCR amplifying from bacterial artificial chromosome (C.H.O.R.I, RP98-39F18) and *WT* genomic DNA, respectively and subcloned into the pTV^{Cherry} vector (Baena-Lopez et al., 2013). 5' homologous sequence immediately 5' to the ATG start site of Or7a (A of ATG is included) (4199 b.p.) was subcloned between NheI and KpnI restriction sites. A 4304 b.p sequence starting from 1368 base pairs downstream to the ATG start codon of Or7a was cloned between SpeI and BglII sites. In-Fusion cloning was used for subcloning into the pTV vector (Clontech Laboratories, Inc.) (Figure 2.8C).

Primers used for PCR (Vector specific sequence in red, Or7a specific sequence in blue; lowercase letters indicate designed b.p. to preserve restriction sites):

5' homology arm: 5'Or7a_FOR, GCT ACC GCG GGC TAG cCA ACA TGC CGA TTA TGT CG; 5'Or7a_REV, AGT TGG GGC ACT ACG gta ccT GGC TGA TGG ACT TTT GAC G

3' homology arm: 3'Or7a_FOR, CGA AGT TAT CAC TAG tAG CCA AGT TCT CGT TTT CGC; 3'Or7a_REV, TTA TGC ATG GAG ATC tTT TGG CAT TGT GTG TTG CAC

Generation of Or7a deletion mutant:

Accelerated homologous recombination was performed according to Baena-Lopez LA et al. (Baena-Lopez et al., 2013). Briefly, P-element insertion lines containing the Or7a knockout construct were crossed to *hs-Flp, hs-SceI* (BS#25679) and heat-shocked at 48 and 72 hours after egg-laying (1 hour duration each time). Female progeny with mottled eyes were crossed to *ubi-Gal4[pax-GFP]* (Baena-Lopez et al., 2013) in order to select against flies containing non-homologous recombination events. Stocks were generated from candidate flies that contained both w^+ and GFP markers. *Or7a* mutants were verified by single sensillum recordings and PCR (Figures 2.7F, 2.7G, 2.8C and 2.8D). In order to identify the ab4 sensillum, 30 µl of geosmin (Sigma #16423-19-1), an odor that specifically activates only ab4B (Or56a) (Stensmyr et al., 2012), was used (Figures 2.7F and 2.7G).

Primers used for verification: G4polyA_FOR: TCG ATA CCG TCG ACT AAA GCC; gOr7a_REV:TCG CCG TTG AGT TTT CAG AG

Imaging and Immunohistochemistry:

Confocal images were taken on a LSM 700 Confocal Microscope (Zeiss). The procedures for fixation, immunochemistry and imaging were as described previously (Wu and Luo, 2006). Primary antibodies used were Rat anti-CD8 (Caltag Laboratories, 1:200) and Mouse anti-nc82 (DSHB, 1:25).

Four-quadrant behavioral assay: A four-quadrant olfactometer (Semmelhack and Wang, 2009; Vet et al., 1983) was used to track the olfactory responses of multiple flies at 30 frames/second (Katsov and Clandinin, 2008). Central air passed through a carbon filter before being split into multiple channels each regulated by a high-resolution flowmeter (Cole-Parmer). Electronically controlled 3-way solenoid valves (Automate Scientific, Berkeley, CA) regulated if clean air leaving the flowmeters expelled into the room or entered into custom made odor chambers (Lundstrom et al., 2010). Teflon tubing was used for odor delivery. The Teflon fly arena is 19.5 cm by 19.5 cm, with a thickness of 0.7 cm. Glass plates were secured onto the arena using clamps. The airflow of each quadrant was maintained at a rate of 100 ml min^{-1} and verified by an electronic flowmeter before each experiment. ACV was diluted in H_2O to make the final concentrations of 6.25% (1/16), 1.56% (1/64) and 0.39% (1/256) and acetic acid in water to make final concentration of 0.33%. Ethyl acetate and 9-tricosene (Sigma #859885) were diluted in paraffin oil for final concentration of 0.001% and 0.1%. When paraffin oil was used as solvent in the odor chamber, paraffin oil alone used in the three non-odor control chambers. 40-50 flies with an isogenized genetic background (*IsoD1* w^{1118}) were

used. At the time of the assay, flies were 4-6 days old and had been starved in vials containing 1% agarose for 40-42 hours to increase locomotor activity. The dark arena was illuminated by 2 infrared LED arrays (AL4554-880; Advanced Illumination, Rochester, VT), monitored by an infrared camera (Sony XC-EI50), and flies tracked by previously described software (Katsov and Clandinin, 2008). Data was analyzed by custom Matlab scripts. On average, each fly generates approximately 1800 tracked positional data points per min. If two flies intersect, their respective previously continuous tracks are considered completed, and new independent tracks begun once they move apart. This assures continuously labeled tracks originated from the same fly. An Attraction Index (AI) is defined as $(Ot_5\text{-}Cavgt_5)/ (Ot_5+Cavgt_5)$, in which Ot_5 is the number of tracked positional data points in the odor quadrant and $Cavgt_5$ is average number of tracked positional data points in non-odor control quadrants over a 5 min testing period. An AI = 1 indicates all flies were tracked to the odor quadrant, and an AI = 0 indicates flies were equally distributed to all four quadrants.

Pheromone extraction: A 1:1 mixture of 40-44-hour starved 50 male:female flies were stimulated with humidified air (HA) or apple cider vinegar (ACV) for 5 minutes to deposit substrates onto cleaned glass plates. ACV stimulation alone (without flies) was used as a negative control. Odors were followed by clean air perfusion for another 5 minutes. To generate a hexane pheromone extract, the glass plates were treated 3× with 500 μl hexane solvent. The ACV-stimulated pheromone extract was used to pipette a pattern onto a new clean glass plate or stored at -20 ºC for GC-MS analysis. The HA-stimulated hexane extract was used as a negative control in the hexane painting. In GC-

MS experiments, to monitor extraction efficiency, 750 ng of internal standard controls (hexacosane (Sigma #241687) and triacontane (Sigma #263842) as dissolved in hexane) were added on to the glass plates immediately before pheromone extraction procedures.

Gas Chromatography/Mass Spectrometry (GC/MS). A sample volume of 2 μL of the hexane extract was injected in splitless mode into a Thermo Scientific ISQ single quadrupole GC/MS (Waltham, MA) with Xcalibur software (ThermoElectron Corp.) for separation and analysis of the deposited hydrocarbons. The GC/MS was equipped with a Stabilwax column, 30 m × 0.32 mm with 1.0 μm film thickness (Restek Corp., Bellefonte, PA). The injection port was set at 230°C. The oven temperature was set to 60°C, raised to 180°C at 6°C min^{-1}, held at 180°C for 20 min, and then raised to 220°C at 6°C min^{-1} where it was maintained for an additional 20 min. Helium carrier gas constantly flowed at 2.5 mL min^{-1}. The mass spectrometer was operated at an ionizing energy of 70 eV with a 2 scan/sec rate over a scan range of *m/z* 40–400 and an ion source temperature of 200°C. Identification of structures/compounds was performed using the National Institute of Standards and Technology library, as well as comparisons with known literature compounds and commercially available standards. Relative retention times were obtained by comparison of sample hydrocarbons to authentic standards. All standards were purchased from Sigma or Cayman Chemical Company at the highest available purity.

Electroantennography (EAG): Electroantennograms were recorded with capillary glass electrodes (1.5mm outer diameter) containing *Drosophila* saline plus Triton X-100

(188mM NaCl, 5mM KCl, 2mM $CaCl_2 \cdot 2H_2O$, 0.02% Triton X-100). The reference electrode was placed in the head capsule close to the base of the antenna. A polished large diameter (~40-50 μm) recording electrode was capped onto the anterior distal region of the *Drosophila* third antennal segment. Control odorant stimulations (1% and 10% cVA; data not shown) were used to verify that the recording electrode was properly sealed onto the distal antenna, 30 μl of different dilutions of 9-tricosene in mineral oil on filter paper was used as the pheromone stimulus. Electrical signals were acquired with a Syntech Intelligent Data Acquisition Controller IDAC-4-USB and quantified by measuring the mV value at the greatest deflection in the EAG trace.

Fluorescence Guided Single Sensillum Recording (SSR): Sensillum of targeted ORNs was identified using green fluorescence signals by crossing *OrX-Gal4* to *15xUAS-IVS-mCD8GFP* (Bloomington Stock #32193) (Pfeiffer et al., 2010). Extracelluar activity was recorded by inserting a glass electrode to the base of the sensillum of 4-10 day-old flies. Signals were amplified 100X (USB-IDAC System; Syntech, Hilversum, The Netherlands) and inputted into a computer via a 16-bit analog-digital converter and analyzed off-line with AUTOSPIKE software (USB-IDAC System; Syntech). The low cutoff filter setting was 50Hz, and the high cutoff was 5kHz. Stimuli consisted of 1000 ms air pulses passed over odorant sources (Dobritsa et al., 2003).

Courtship Behavior: Virgin male flies were collected 0-6 hours after eclosion and transferred to individual fly vials (1.5 ml Eppendorf tubes containing 500 μl of fly food). Virgin females were collected and kept in regular vials in groups of 15-20. Both male and

female flies were aged for 4 days at room temperature with 12:12 light dark cycle before behavior testing. During courtship behavior experiments, images were digitally captured by a Sony Handycam (HDR-CX260V) and a courtship index (unilateral wing extension and copulations lasting >2 minutes) were scored by human eye. In 9-tricosene stimulation experiments, 1 μl of 0.1% 9-tricosene (hexane as solvent) was added to a 1mm × 3mm paper strip and placed into the behavior chamber right before introducing male and female flies, whereas in control experiments, strips treated with 1 μl of hexane solvent were used (as shown in Figures 2.10D and 2.10E).

Egg laying stimulation test: Control agarose gel was made by pouring 70 ml of a 1% agarose gel onto a glass plate assembled onto the 4-field arena. 9-tricosene or 7-tricosene gel was made by mixing 0.8 mg pure 9-tricosene (Sigma #859885) or 7-tricosene (Cayman Chemical Company #9000313) into 70 ml of 1% agarose gel (temperature = ~50 ºC). One quadrant of the control gel or 9-tricosene or 7-tricosene gel was cut out and transferred to a Petri dish. 4-day old mixed populations of 15 males and 15 females or 15 mated females only were transferred onto the Petri dishes and allowed to oviposit at room temperature for 22-23 hours (as shown in Figure 2.10C).

Four-quadrant egg laying behavior assay and positional recording: The schematic of the hybrid 9-tricosene or 7-tricosene gel is as shown in Figure 2.12A. Control, 7-tricosene, and 9-tricosene agarose gels were prepared as described above. In order to increase egg production, mixed population of male and female flies were pre-induced in vials with wet yeast paste (yeast + 0.5% propionic acid) overnight. Mated females from

premixed population were rapidly separated by cooling on ice and transferred to the arena gel. The egg laying behavior was performed in a dark enclosure at room temperature for 22-23 hours. Simultaneous recordings of the fly positions were performed using the same setup for tracking of the four-quadrant behavior assay described above except that the frame rate was set at 1 frame/5 sec due to the large file size generated over the extended time period. On average, each fly generated approximately 16560 tracked positions per experiment. The recorded data was analyzed with custom Matlab programs and analyzed for the AI as defined above.

Estimation of molecule numbers reaching the antennae in SSR experiments:

According to Raoult's law, the partial vapor pressure of each component of the liquid is equal to the vapor pressure of the pure component multiplied by its mole fraction in the mixture.

Therefore,

(1) $Pi=Pi^*Xi$

Pi is the partial vapor pressure of the component i in the gaseous mixture

Pi^* is the vapor pressure of the pure component i

Xi is the mole fraction of the component i in the mixture

In the SSR experiments in Hallem and Carlson (Hallem and Carlson, 2006), chemicals were diluted in paraffin oil to a final concentration of 1%. The average molecular weight of paraffin oil is 262 and the density is 0.83.

MWi= molecular weight of component i; Di=density of component i

Therefore,

$$Xi = \frac{\frac{1\% \times Di}{MWi}}{\frac{1\% \times Di}{MWi} + \frac{99\% \times 0.83}{262}} \quad (2)$$

Pi can thus be calculated accordingly using (1).

According to ideal gas law, $PV=nRT$

P is the pressure of the gas (in atm)= the *Pi* in (1)

V is the volume of the gas (in liter); the volume of the pipette is ~0.01L

n is the amount of the gas (in mole)

R is Boltzmann constant (=0.082 L·atm/mol·K)

T is the temperature of the gas (in Kelvin); experiments were conducted at ~25 °C, which equals to (273+25) °K

Therefore,

$$n = \frac{P \cdot V}{R \cdot T} = \frac{Pi \times 0.01}{0.082 \times 298}$$

Evolution rate calculations:

The protein sequences of 49 odorant receptors analyzed in the study were downloaded from FlyBase. Each sequence was used as a query to BLAST other species homologues using the NCBI server. Multiple sequence alignment was then performed using ClustalW2 from the EMBL-EBI website and aligned outputs were further analyzed with the MEGA6 program (Tamura et al., 2013). Briefly, the observed number of difference in the aligned length (n) was calculated (p-distance) and transformed into actual change numbers (m) by the following equation (Dickerson, 1971; Zuckerkandl and Pauling, 1965):

$m = -100 \cdot \ln (1- n/100)$

n = observed amino acid changes per 100 residues

m = corrected amino acid changes per 100 residues

Divergence dates (Myr) of *Drosophila* species with *Drosophila melanogaster* are 2.3 (*D. sechellia*), 2.3 (*D. simulans*), 6.1 (*D. erecta*), 6.1 (*D. yakuba*), 12.8 (*D. ananassae*), 24.9 (*D. persililis*), 24.9 (*D. pseudobscura*), 36.3 (*D. willistoni*), 39.2 (*D. grimshawi*), 39.2 (*D. virillis*) and 39.2 (*D. mojavensis*) based on the *Adh* molecular clock (Guo and Kim, 2007; Russo et al., 1995). The data were then plotted and regression lines were generated accordingly.

Figure 2.1

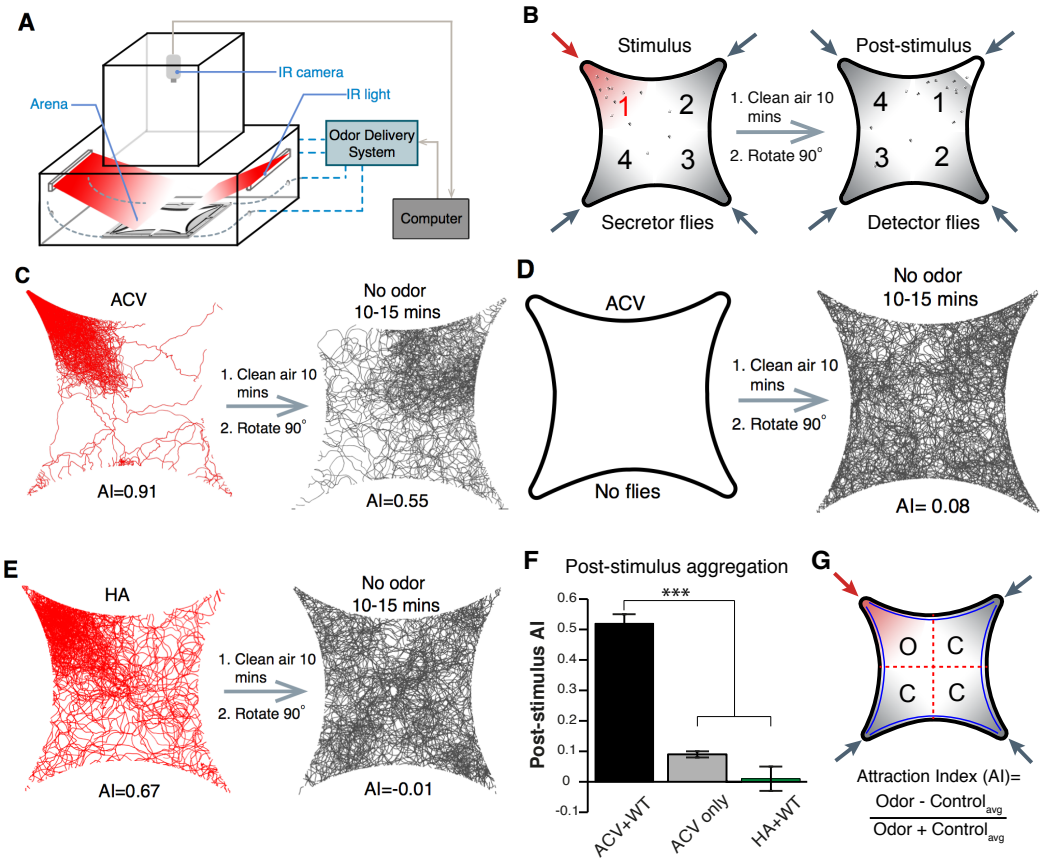
A
IR camera
IR light
Arena
Odor Delivery System
Computer
B
Stimulus
Post-stimulus
1
2
4
3
1. Clean air 10 mins
2. Rotate 90°
Secretor flies
Detector flies
C
ACV
No odor 10-15 mins
1. Clean air 10 mins
2. Rotate 90°
AI=0.91
AI=0.55
D
ACV
No odor 10-15 mins
1. Clean air 10 mins
2. Rotate 90°
No flies
AI= 0.08
E
HA
No odor 10-15 mins
1. Clean air 10 mins
2. Rotate 90°
AI=0.67
AI=-0.01
F
Post-stimulus aggregation
***
Post-stimulus AI
0.6
0.5
0.4
0.3
0.2
0.1
0
-0.1
ACV+WT
ACV only
HA+WT
G
O
C
C
C
Attraction Index (AI)=
Odor - Control avg
Odor + Control avg

Figure 2.1. Identification of an odor induced post-stimulus aggregation behavior. (**A** and **B**) Schematic of behavior setup and experimental design. (**C**) Fly tracking for 5-minutes of 25 male and 25 female wild-type flies. Flies are highly attracted to apple cider vinegar food odor (ACV), which gives rise to a post-stimulus aggregation behavior in the absence of exogenous odorants (right). (**D**) The lack of flies with ACV stimulation (left) led to a lack of a post-stimulus aggregation (right). (**E**) Humidified air (HA) versus dry air is attractive (left), but does not lead to a post-stimulus aggregation (right). (**F**) Post-stimulus response summary (p=0.0002 and 0.00001 for ACV only and HA+WT, respectively; t-test, n=3-6 per trial) (**G**) Definition of attraction index, A.I. Error bars indicate ± s.e.m. throughout. See also Figure 2.2 and Movies 1 and 2.

Figure 2.2

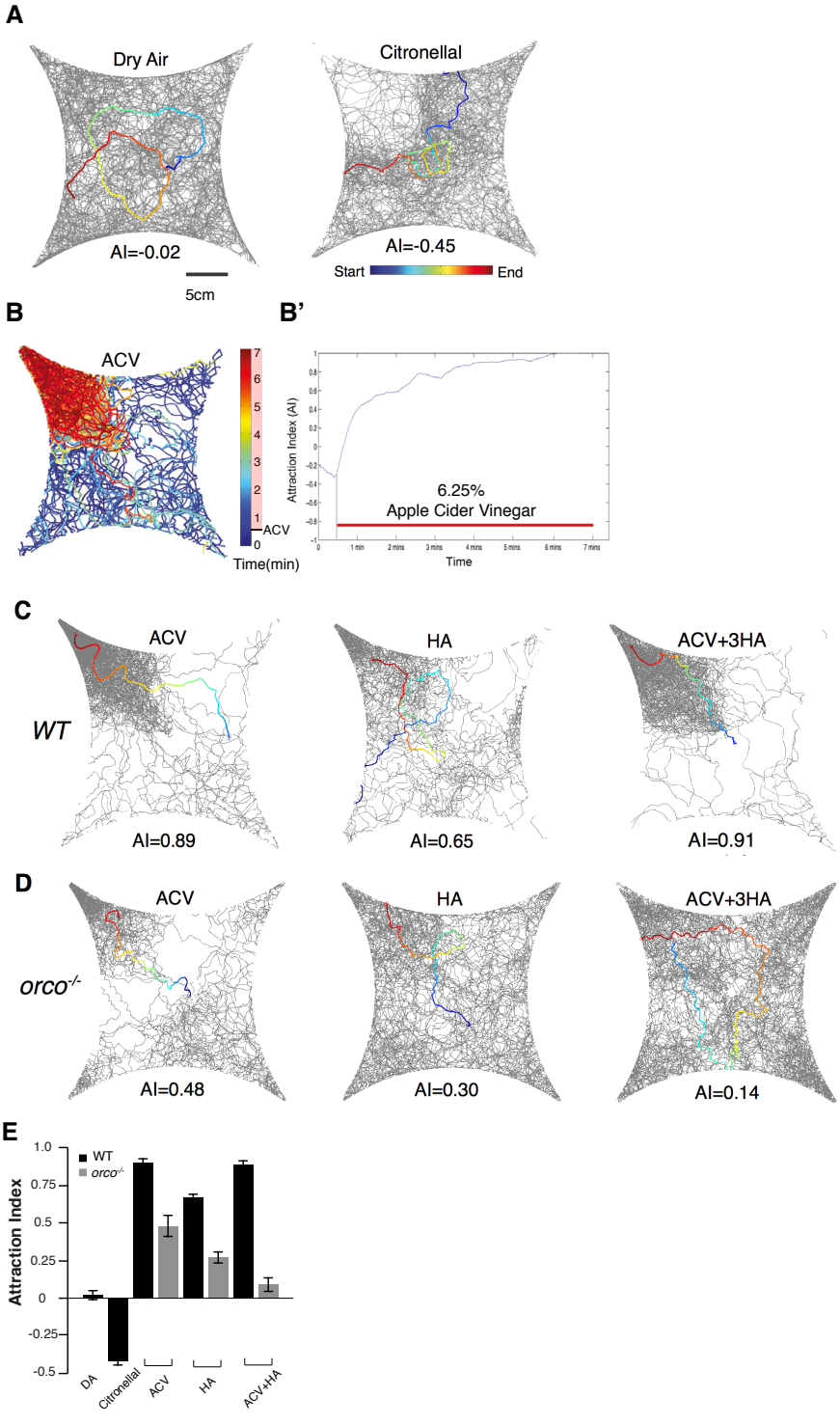
A
Dry Air
AI=-0.02
5cm
Citronellal
AI=-0.45
Start
End
B
ACV
Time(min)
B'
Attraction Index (AI)
6.25%
Apple Cider Vinegar
Time
C
WT
ACV
AI=0.89
HA
AI=0.65
ACV+3HA
AI=0.91
D
orco-/-
ACV
AI=0.48
HA
AI=0.30
ACV+3HA
AI=0.14
E
Attraction Index
WT
orco-/-
DA
Citronellal
ACV
HA
ACV+HA

Figure 2.2. Basic characterization of the four-field olfactometer.

(**A**) Fly tracking for 5-minutes of 25 male and 25 female wild-type flies to dry air (left) and insect repellent citronellal (right). Example single fly tracks within the dataset are shown color-coded from start (blue) to end (red) of a continuous track. (**B**) Colormap of all fly trajectories from 0 minute to 7 minutes. ACV was applied at 0.5 minute. (B') Attraction index over time is shown. (**C**) Wild-type flies stimulated with apple cider vinegar (ACV), humidified air (HA), and ACV with HA perfusion in the other 3 quadrants (ACV+3HA). (**D**) *Orco* mutant flies responding to ACV, HA and ACV+3HA. (**E**) Response summary of wild-type and *orco* mutant flies to ACV, HA and ACV+3HA. n=4-6 for each condition ±s.e.m.

Figure 2.3

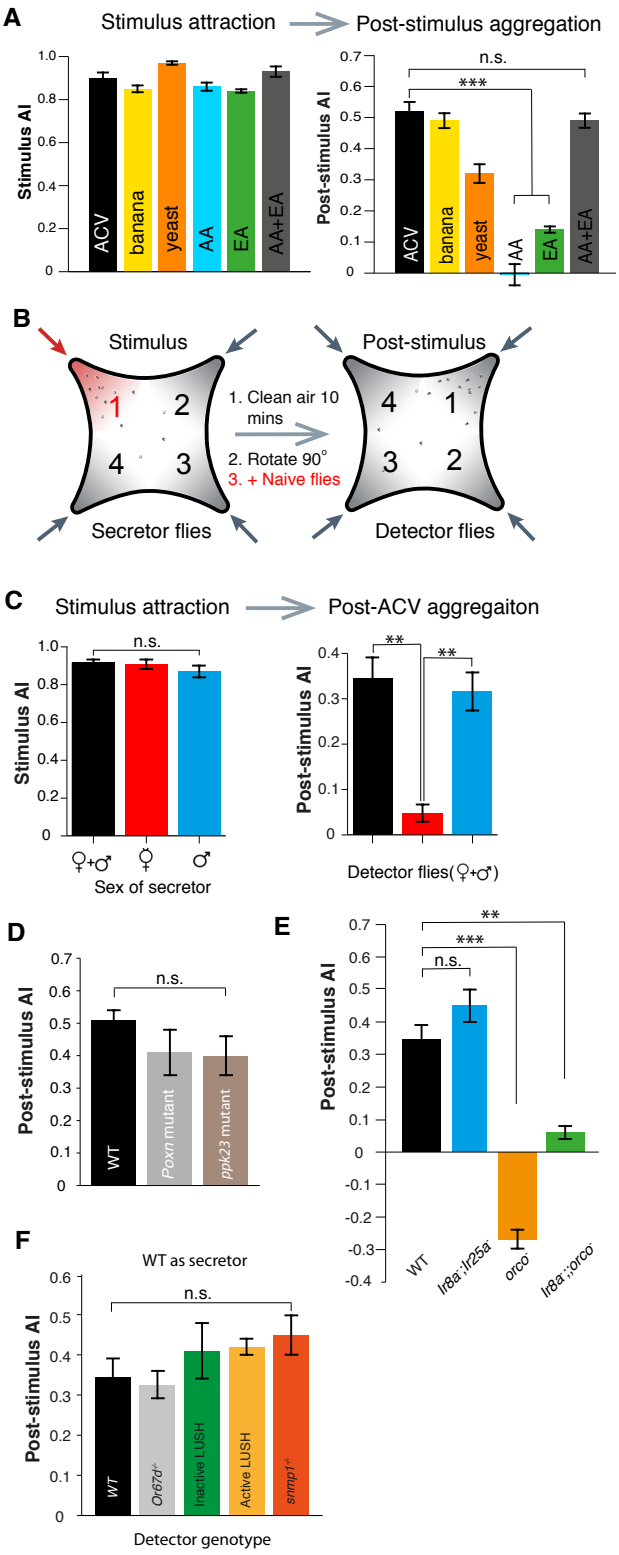
A
Stimulus attraction
Post-stimulus aggregation
Stimulus AI
Post-stimulus AI
n.s.
***
ACV
banana
yeast
AA
EA
AA+EA
B
Stimulus
Post-stimulus
1. Clean air 10 mins
2. Rotate 90°
3. + Naive flies
Secretor flies
Detector flies
C
Stimulus attraction
Post-ACV aggregaiton
**
Sex of secretor
Detector flies(♀+♂)
D
Post-stimulus AI
WT
Poxn mutant
ppk23 mutant
E
Ir8a::Ir25a
orco
Ir8a::orco
F
WT as secretor
Detector genotype
WT
Or67d-/-
Inactive LUSH
Active LUSH
snmp1-/-

Figure 2.3. Post-stimulus aggregation is food-odor specific and requires Orco-dependent olfactory signaling.

(**A**) Quantification of post-stimulus aggregation by food-odors (ACV, banana and yeast), ACV mono-moleculars (EA and AA) and combination of mono-moleculars (EA+AA) ($p<0.001$ for post-stimulus phase of AA and EA; $p=0.4689$ for post-stimulus phase of AA+EA; t-test, n=4-5 per odor stimulation). (**B**) Schematic of 4-quadrant arena using different populations of secretor and detector flies. (**C**) Different secretor fly populations (females+males, females only, males only) were used as pheromone sources and assayed for post-stimulation aggregation by female+male detector flies ($p=0.003$; t-test, n=3-5 per combination). (**D**) Post-stimulus aggregation responses by gustatory receptor (*Poxn;* $p=0.2258$; t-test) and *ppk-23* mutants ($p=0.0951$; t-test, n=4-5 per trail). (**E**) Post-stimulus aggregation responses by olfactory receptor (*orco*), and Ionotropic receptor (*Ir8*, *Ir25a*) mutants ($Ir8a^{-/-};Ir25a^{-/-}$: $p=0.1524$; $orco^{-/-}$: $p<0.001$; $Ir8a^{-/-};;orco^{-/-}$: $p=0.004$; t-test, n=4-6 per genotype). Wild-type flies were used as pheromone secretors. (**F**) Quantification of post-stimulus aggregation in mutants of key components in the cVA signaling pathway ($p=0.4405$, one-way ANOVA test, n=3 for each trial). Error bars indicate ± s.e.m. throughout. See also Figure 2.4.

Figure 2.4

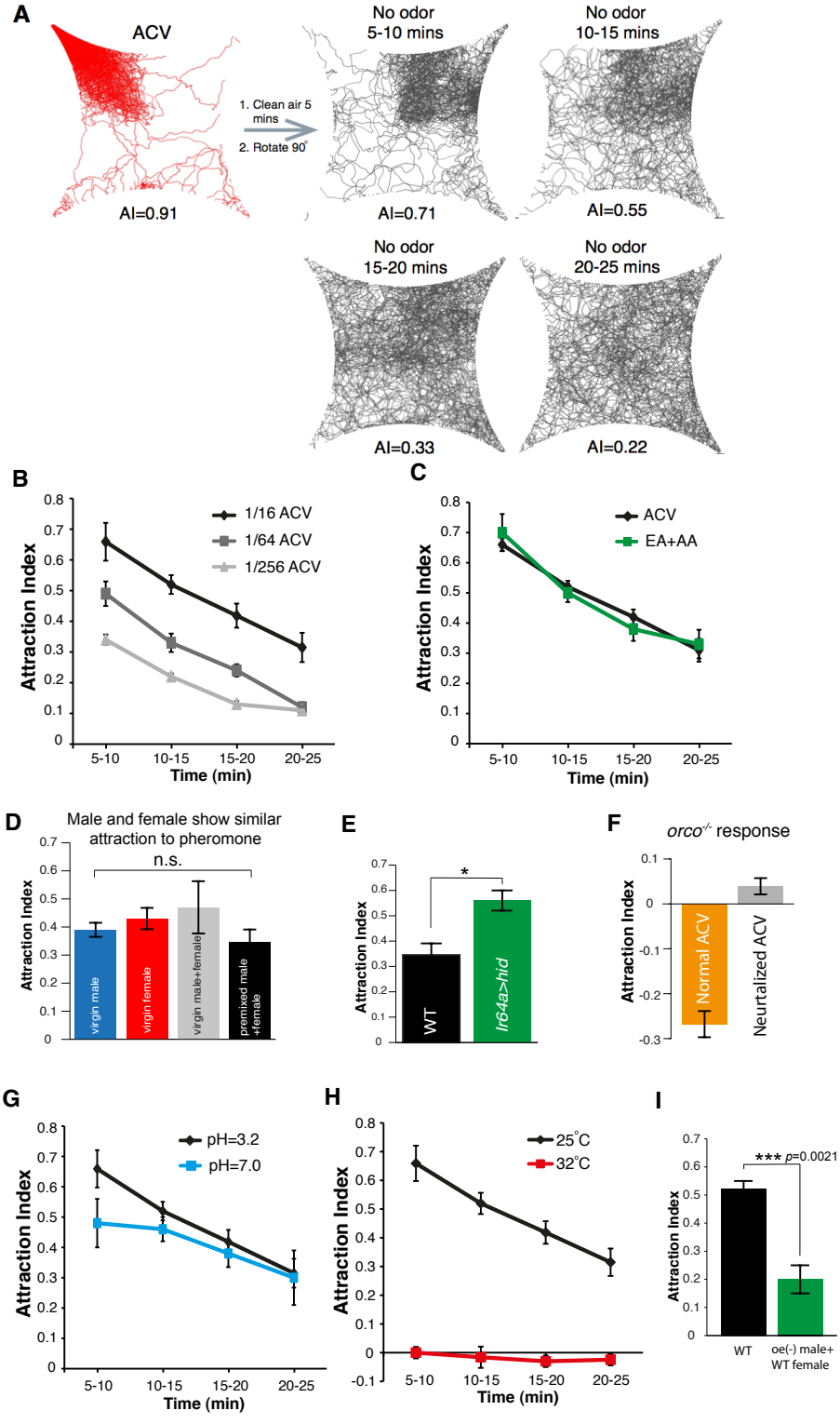
A
ACV
1. Clean air 5 mins
2. Rotate 90°
No odor 5-10 mins
No odor 10-15 mins
No odor 15-20 mins
No odor 20-25 mins
AI=0.91
AI=0.71
AI=0.55
AI=0.33
AI=0.22
B
1/16 ACV
1/64 ACV
1/256 ACV
Attraction Index
Time (min)
C
ACV
EA+AA
D
Male and female show similar attraction to pheromone
n.s.
virgin male
virgin female
virgin male+female
premixed male +female
E
*
WT
Ir64a>hid
F
orco-/- response
Normal ACV
Neurtalized ACV
G
pH=3.2
pH=7.0
H
25°C
32°C
I
*** p=0.0021
WT
oe(-) male+ WT female

Figure 2.4. The aggregation pheromone produced by oenocytes is volatile, heat-sensitive, and is similarly attractive to male and female flies.

(**A**) Recordings of post-stimulus aggregation in 5-minute intervals up to 25 minutes post clean air perfusion. (**B**) Post-stimulus aggregation was assayed using different dilutions of ACV. (**C**) Post-stimulus aggregation responses to 0.0001% ethyl acetate (EA)+ 0.33% acetic acid (AA) recapitulates that of natural ACV. (**D**) Post-stimulus aggregation to natural pheromone is similar among virgin males, virgin females, virgin male + virgin females (1:1) and premixed males+females (1:1). (**E**) Post-stimulus attraction responses of flies are increased when acid-sensing olfactory neurons are removed (*Ir64a-Gal4/UAS-hid*)(p=0.021; t-test, n=3-4 per trial ±s.e.m.). (**F**) Post-stimulus repulsive behavior is abolished in *orco* mutant flies assayed with neutralized ACV (pH=7.0). (**G**) Post-stimulus responses using neutralized ACV (pH=7). (**H**) To determine effects of heat on pheromone stability, the arena was maintained at 32 ºC for the entire testing period (red). The wild-type response at 25 ºC is shown for comparison. (**I**) Post-stimulus behavior is reduced when using mixtures of oenocyte-negative males (*UAS-hid; PromE(800)-Gal4,Tub-Gal80ts*) with wild-type females as the source of the aggregation pheromone (p=0.0021; t-test, n=4 per trial ±s.e.m.).

Figure 2.5

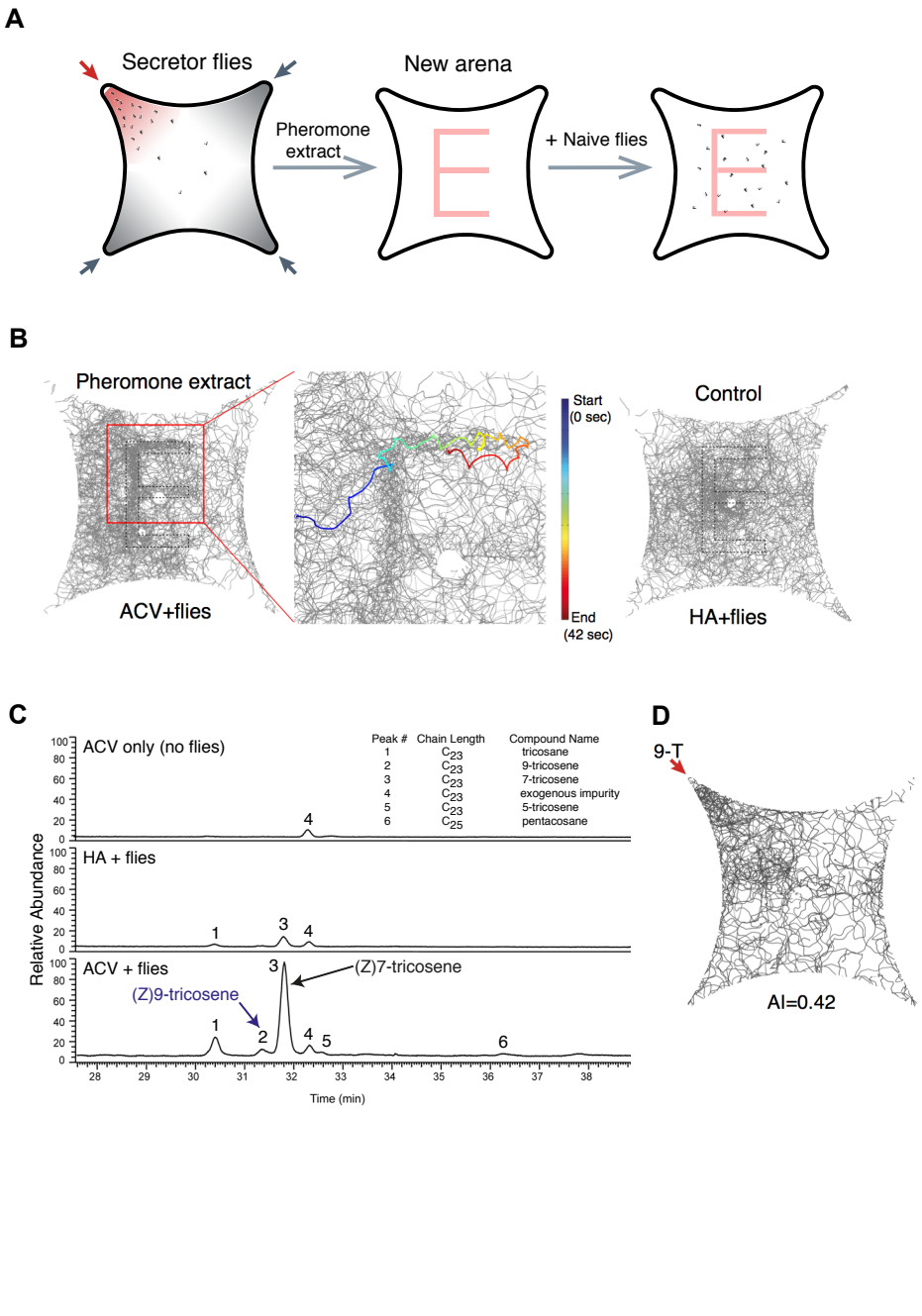
A
Secretor flies
Pheromone extract
New arena
+ Naive flies
B
Pheromone extract
ACV+flies
Start (0 sec)
End (42 sec)
Control
HA+flies
C
ACV only (no flies)
HA + flies
ACV + flies
(Z)9-tricosene
(Z)7-tricosene
Relative Abundance
Time (min)
Peak # Chain Length Compound Name
1 C23 tricosane
2 C23 9-tricosene
3 C23 7-tricosene
4 C23 exogenous impurity
5 C23 5-tricosene
6 C25 pentacosane
D
9-T
AI=0.42

Figure 2.5. 9-Tricosene is a food-odor induced pheromone.

(**A**) Schematic of pheromone extract paint experiment. (**B**) Hexane extracts of the pheromone quadrant were used to paint the letter "E" onto the glass plate. Shown are traces of naïve new flies in the painted arenas by deposited pheromone extract (ACV+secretor flies) or control (humidified air+flies). The blue to red color trace indicates a single fly track from start to end of tracking. (**C**) GC-MS results of hexane extracts from quadrants stimulated by ACV-only, humidified air and flies, and ACV with flies. Peak #2 is (Z)9-tricosene. 9-Tricosene exhibited a 2.8 fold enrichment on the glass plates upon food-odor stimulation. D) Olfactory behavioral response of flies to 0.1% 9-tricosene. See also Figure 2.6, Figure 2.17 and Movie 3.

Figure 2.6

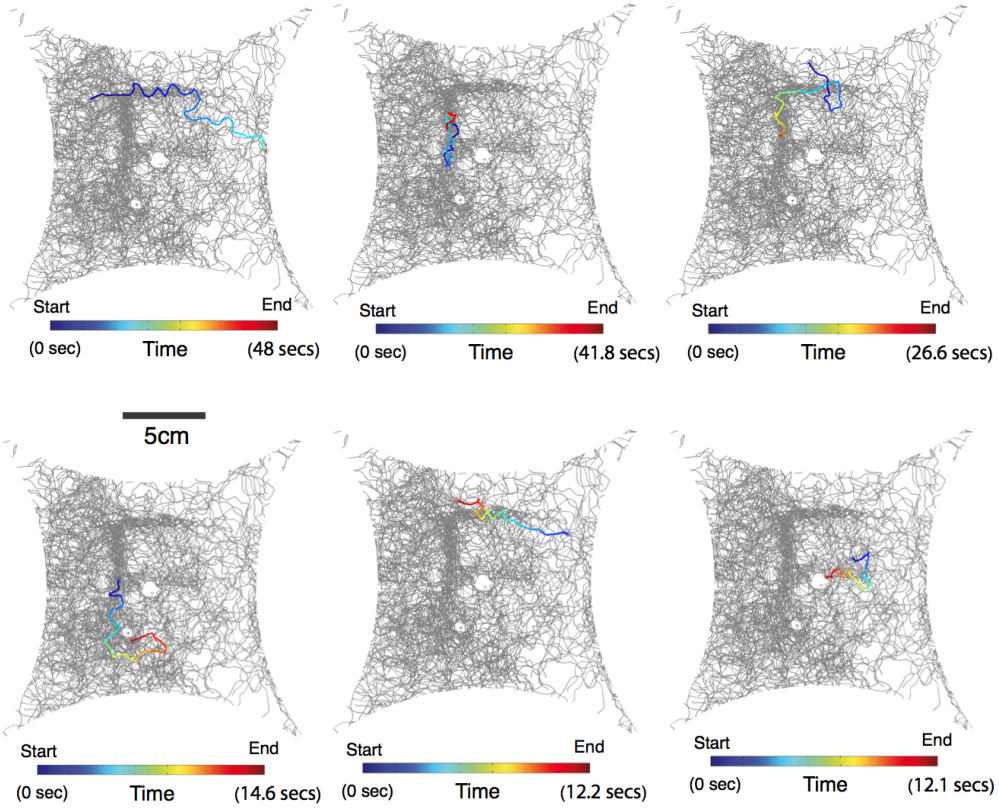
Start
End
(0 sec)
Time
(48 secs)
Start
End
(0 sec)
Time
(41.8 secs)
Start
End
(0 sec)
Time
(26.6 secs)
5cm
Start
End
(0 sec)
Time
(14.6 secs)
Start
End
(0 sec)
Time
(12.2 secs)
Start
End
(0 sec)
Time
(12.1 secs)

Figure 2.6. Single fly trajectories of painted “E” experiment.

The blue to red color trace indicates a single fly track from the start to end of one continuous track.

Figure 2.7

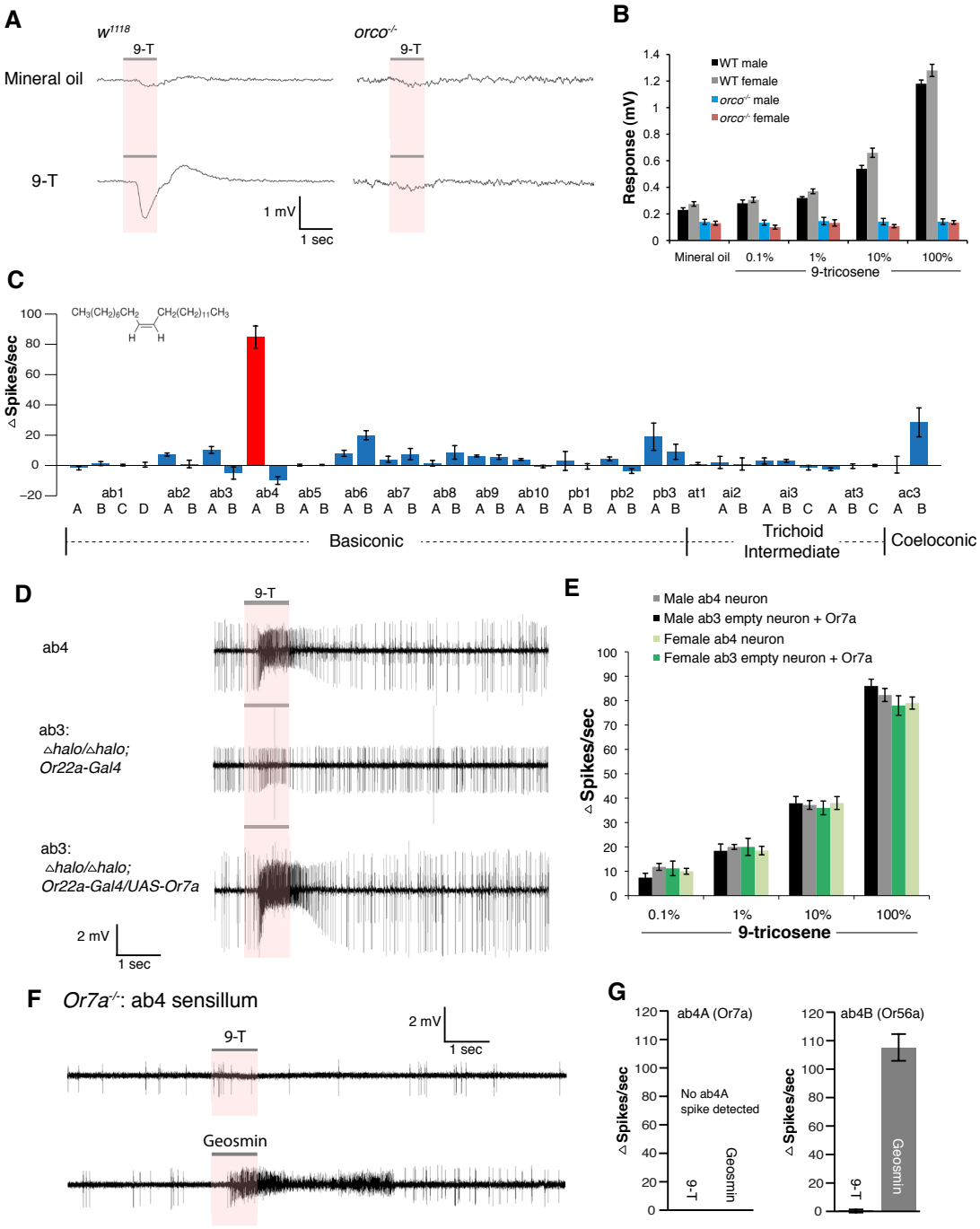
A
w1118
orco-/-
9-T
Mineral oil
9-T
1 mV
1 sec
B
WT male
WT female
orco-/- male
orco-/- female
Response (mV)
Mineral oil
0.1%
1%
10%
100%
9-tricosene
C
△Spikes/sec
ab1 ab2 ab3 ab4 ab5 ab6 ab7 ab8 ab9 ab10 pb1 pb2 pb3 at1 ai2 ai3 at3 ac3
Basiconic
Trichoid
Intermediate
Coeloconic
D
9-T
ab4
ab3:
△halo/△halo;
Or22a-Gal4
ab3:
△halo/△halo;
Or22a-Gal4/UAS-Or7a
2 mV
1 sec
E
Male ab4 neuron
Male ab3 empty neuron + Or7a
Female ab4 neuron
Female ab3 empty neuron + Or7a
△Spikes/sec
0.1%
1%
10%
100%
9-tricosene
F
Or7a-/-: ab4 sensillum
9-T
2 mV
1 sec
Geosmin
G
ab4A (Or7a)
No ab4A
spike detected
9-T
Geosmin
ab4B (Or56a)
9-T
Geosmin
△Spikes/sec

Figure 2.7. Electrophysiological results identify Or7a as the receptor for 9-tricosene. (**A**) Electroantennography (EAG) traces of wild-type and *orco*$^{-/-}$ flies stimulated with 100% 9-tricosene. (**B**) EAG response summaries of different 9-tricosene concentrations in different sexes of wild-type and *orco*$^{-/-}$ flies (n=5-7 per stimulation) (**C**) Single sensillum recording (SSR) in all *orco*-positive antennal and maxillary palp sensilla. n=3-6 per sensillum. (**D**) SSR traces of ab4 (9-tricosene responsive), ab3 empty neuron (*halo*/*halo;Or22a-Gal4*), and ab3 rescue (*halo*/*halo;Or22a-Gal4*/*UAS-Or7a*) sensilla. (**E**) SSR response summary of native ab4 and rescued ab3 sensilla in different sexes. n=7-8 per sensillum. (**F** and **G**) SSR trace responses and quantitative summary of ab4 sensillum of *Or7a*$^{-/-}$ mutant flies stimulated with 100% 9-tricosene and geosmin (n=4). Error bars indicate ± s.e.m. throughout. See also Figure 2.8.

Figure 2.9

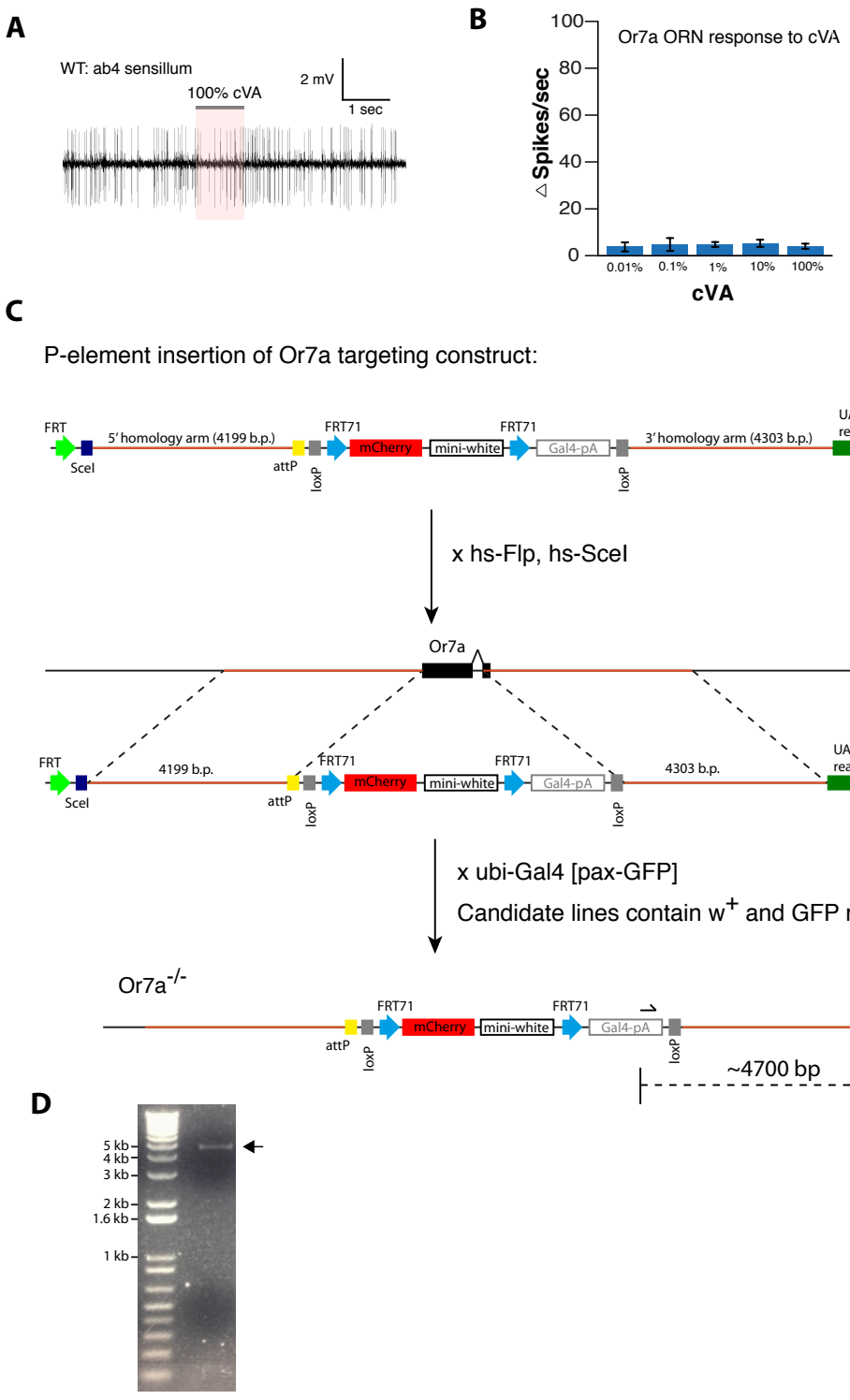
A
WT: ab4 sensillum
100% cVA
2 mV
1 sec
B
Or7a ORN response to cVA
△ Spikes/sec
100
80
60
40
20
0
0.01%
0.1%
1%
10%
100%
cVA
C
P-element insertion of Or7a targeting construct:
FRT
5' homology arm (4199 b.p.)
FRT71
mCherry
mini-white
FRT71
Gal4-pA
3' homology arm (4303 b.p.)
UAS-reaper
FRT
SceI
attP
loxP
loxP
SceI
x hs-Flp, hs-SceI
Or7a
FRT
4199 b.p.
FRT71
mCherry
mini-white
FRT71
Gal4-pA
4303 b.p.
UAS-reaper
FRT
SceI
attP
loxP
loxP
SceI
x ubi-Gal4 [pax-GFP]
Candidate lines contain w+ and GFP markers
Or7a-/-
FRT71
mCherry
mini-white
FRT71
Gal4-pA
attP
loxP
loxP
~4700 bp
D
5 kb
4 kb
3 kb
2 kb
1.6 kb
1 kb

Figure 2.8. Response of ab4 sensillum to cVA and generation of *Or7a* mutant. (**A**) SSR response traces and (**B**) activity summary of WT ab4 sensillum to different dilutions of cVA (n=4 per concentration ±s.e.m.). (**C**) Schematic of constructs and crosses utilized for accelerated homologous recombination of the *Or7a* locus (See Experimental Procedures for details). (**D**) PCR verification of *Or7a* mutant. Primer locations are diagramed in (**C**).

Figure 2.9

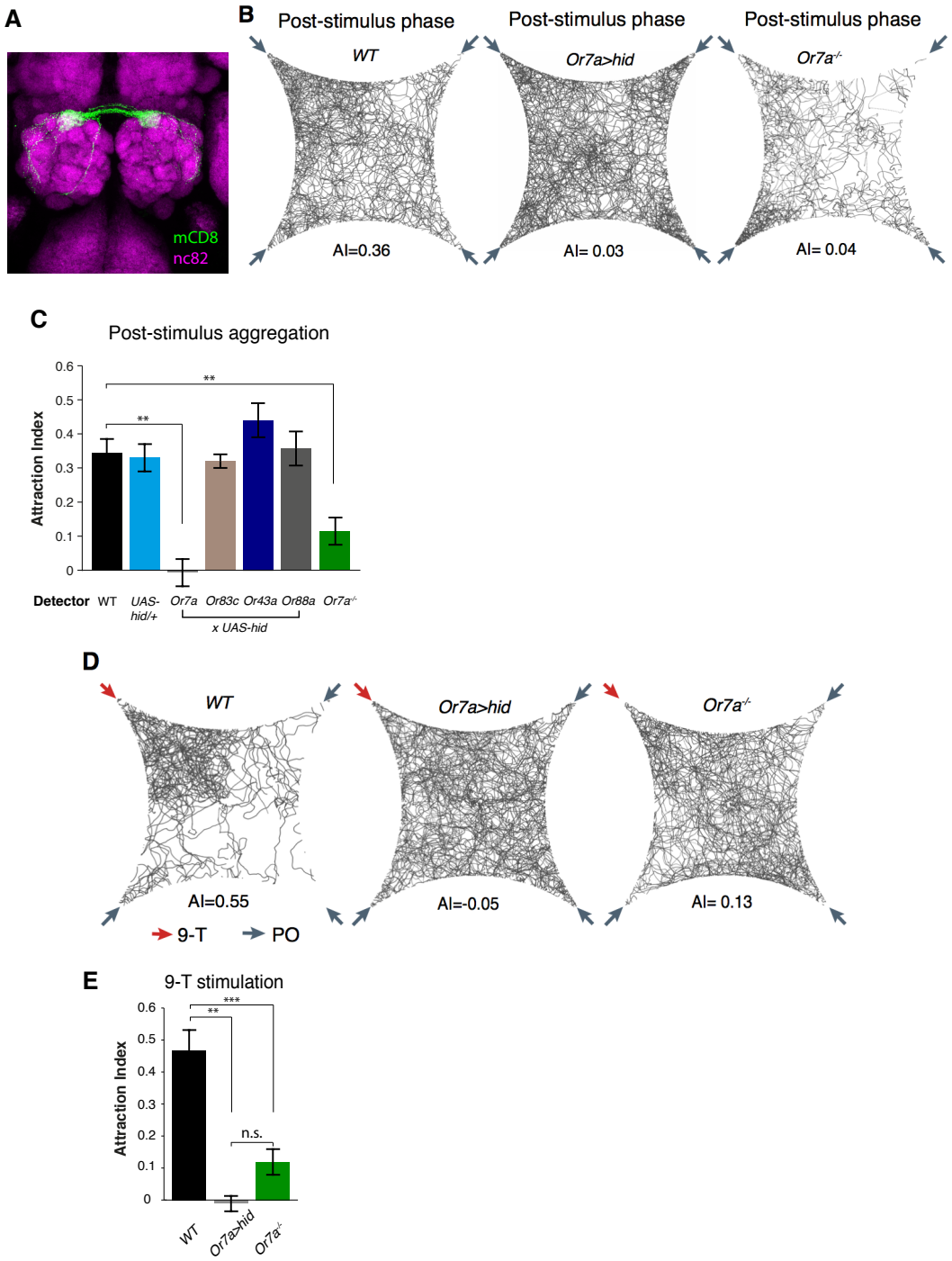
A
mCD8
nc82
B
Post-stimulus phase
WT
AI=0.36
Post-stimulus phase
Or7a>hid
AI= 0.03
Post-stimulus phase
Or7a-/-
AI= 0.04
C
Post-stimulus aggregation
Attraction Index
0.6
0.5
0.4
0.3
0.2
0.1
0
**
**
Detector
WT
UAS-hid/+
Or7a
Or83c
Or43a
Or88a
Or7a-/-
x UAS-hid
D
WT
AI=0.55
9-T
PO
Or7a>hid
AI=-0.05
Or7a-/-
AI= 0.13
E
9-T stimulation
Attraction Index
0.6
0.5
0.4
0.3
0.2
0.1
0
***
**
n.s.
WT
Or7a>hid
Or7a-/-

Figure 2.9. Or7a neurons are necessary for the behavioral response to naturally deposited aggregation pheromone and 9-tricosene.

(**A**) Immunostaining of Or7a-expressing neurons innervating the DL5 glomerulus in the antennal lobe (*Or7a-Gal4/UAS-mCD8GFP*). (**B-C**) Four-field behavior responses of WT, *Or7a* mutant, Or7a-neuron ablated, and control OrX-neuron ablated flies (*Or83c, Or43a* and *Or88a-Gal4 x UAS-hid*) to naturally deposited pheromone (p=0.0012 and 0.006 comparing WT to Or7a neurons ablated and $Or7a^{-/-}$ flies; t-test, n=4-6 per experiment). (**D-E**) Behavioral response of WT, *Or7a* mutant, and Or7a neuron ablated flies to 9-tricosene (0.1%) (p<0.001; t-test; n=4-5 per trial). Error bars indicate ± s.e.m. throughout. See also Figure 2.10.

Figure 2.10

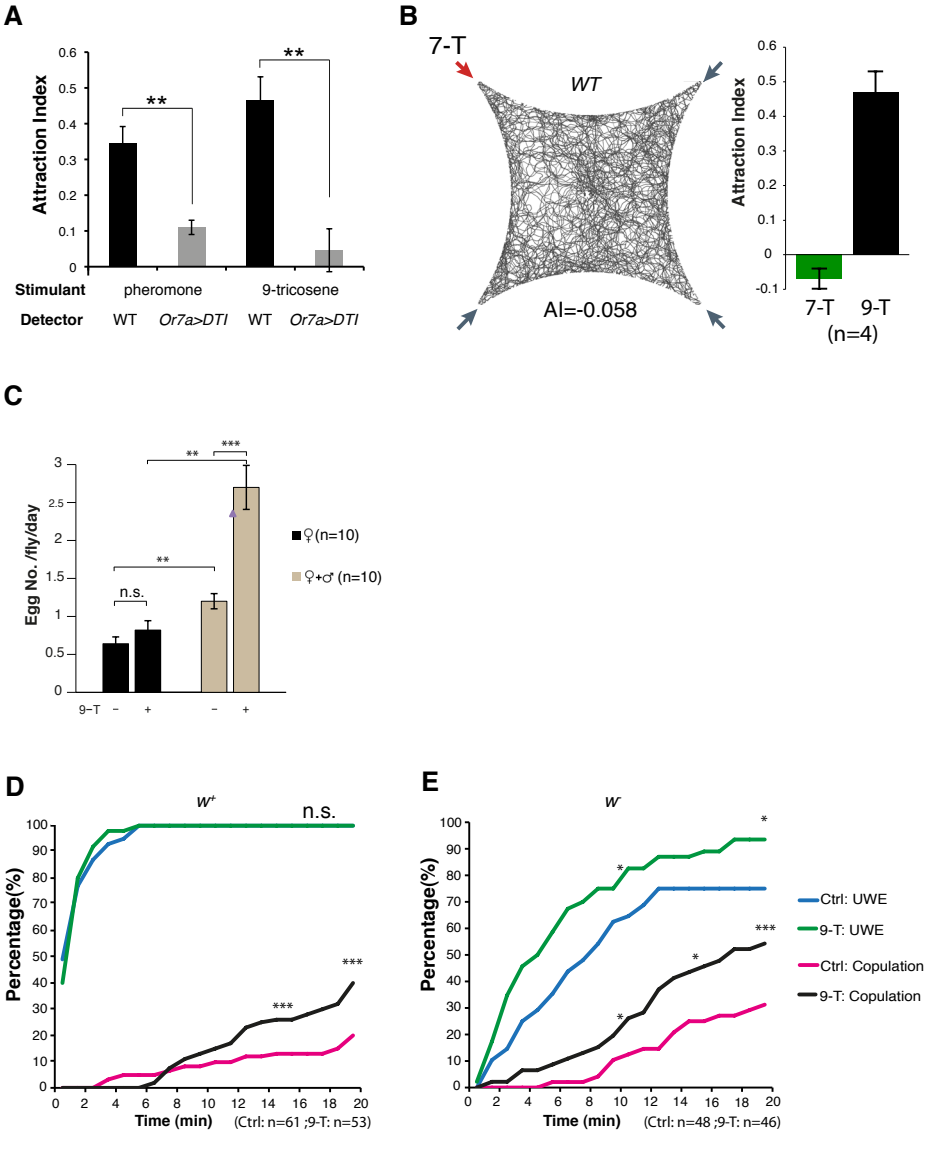
A
Attraction Index
0.6
0.5
0.4
0.3
0.2
0.1
0
**
**
Stimulant
pheromone
9-tricosene
Detector
WT
Or7a>DTI
WT
Or7a>DTI
B
7-T
WT
AI=-0.058
Attraction Index
0.6
0.5
0.4
0.3
0.2
0.1
0
-0.1
7-T
9-T
(n=4)
C
Egg No. /fly/day
3
2.5
2
1.5
1
0.5
0
**
***
**
n.s.
♀(n=10)
♀+♂ (n=10)
9–T
–
+
–
+
D
w+
n.s.
***
***
Percentage(%)
100
90
80
70
60
50
40
30
20
10
0
0
2
4
6
8
10
12
14
16
18
20
Time (min)
(Ctrl: n=61 ;9-T: n=53)
E
w-
*
*
***
*
*
Percentage(%)
Time (min)
(Ctrl: n=48 ;9-T: n=46)
Ctrl: UWE
9-T: UWE
Ctrl: Copulation
9-T: Copulation

Figure 2.10. Determining the effects of 9-tricosene on *Drosophila* aggregation, courtship, and egg-laying behaviors.

(**A**) Post-stimulus aggregation response of wild-type or Or7a neuron ablated flies (*Or7a-Gal4/UAS-DTI)* to natural pheromone (p=0.0014; t-test, n=4-5 per stimulation) and 0.1% 9-tricosene (p=0.0049; t-test, n=4-5 per stimulation). Error bars indicate ± s.e.m. (**B**) Four-field behavior response (left) and summary (right) of wild-type flies to 0.1% 7-tricosene (n=4 per odor ±s.e.m.). (**C**) The number of eggs laid by females was assayed in the absence or presence of 0.001% 9-tricosene (left, p=0.0534; t-test; n=10 per condition), or with the addition of males (brown bars, p=0.0002; t-test; n=10 per condition). (**D and E**) Courtship index monitoring unilateral wing extension (UWE) and copulation in the presence or absence of 0.1% 9-tricosene in the arena in w^+ (**D**) and w^- (**E**) flies. (**D**) No significant difference is detected in UWE percentage. As to copulation percentage, p=0.1623, <0.0001 and 0.0004, when compared with 9-tricosene absence group at 10-min, 15-min and 20-min time points; χ^2 test. (**E**) As to UWE percentage, p=0.049, 0.0611 and 0.0392 compared with 9-tricosene absence group at 10 min, 15-min and 20-min time points respectively; χ^2 test. As to copulation percentage in the presence or absence of 0.1% 9-tricosene, p=0.0306, 0.0107 and 0.0006 compared with 9-tricosene absence group at 10-min, 15-min and 20-min time points; χ^2 test.

Figure 2.11

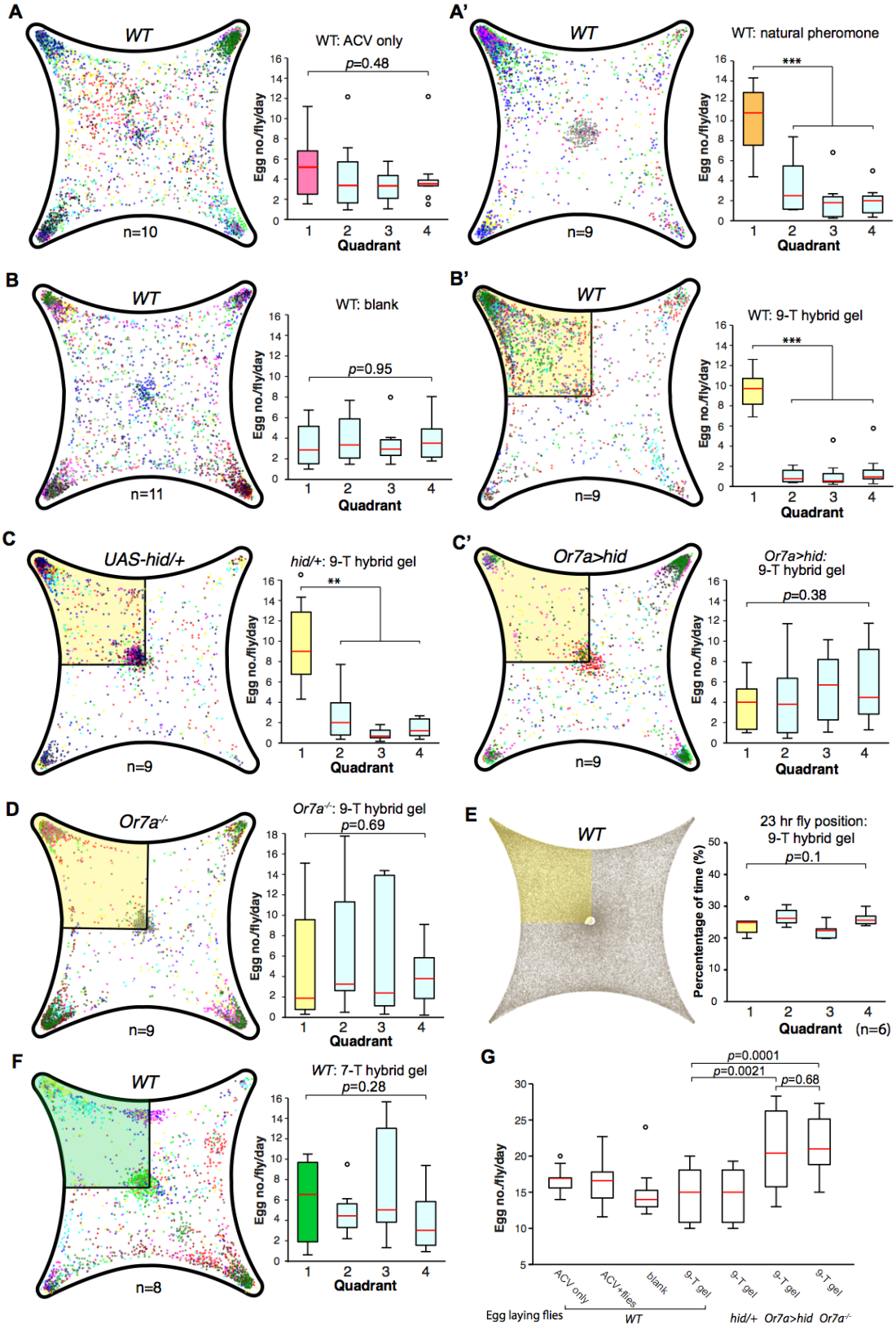
A
WT
n=10
WT: ACV only
p=0.48
Egg no./fly/day
Quadrant
A'
WT
n=9
WT: natural pheromone
***
B
WT
n=11
WT: blank
p=0.95
B'
WT
n=9
WT: 9-T hybrid gel
***
C
UAS-hid/+
n=9
hid/+: 9-T hybrid gel
**
C'
Or7a>hid
n=9
Or7a>hid:
9-T hybrid gel
p=0.38
D
Or7a-/-
n=9
Or7a-/-: 9-T hybrid gel
p=0.69
E
WT
23 hr fly position:
9-T hybrid gel
p=0.1
Percentage of time (%)
Quadrant (n=6)
F
WT
n=8
WT: 7-T hybrid gel
p=0.28
G
p=0.0001
p=0.0021
p=0.68
ACV only
ACV+flies
blank
9-T gel
Egg laying flies
WT
hid/+
Or7a>hid
Or7a-/-

Figure 2.11. 9-Tricosene modulates female oviposition site selection.

(**A**) Quantification and positions of eggs laid over ~23 hours in the 1% agarose arena with ACV-only control or naturally deposited aggregation pheromone (A: p=0.4836; n=10; A': p<0.001; n=9; one-way ANOVA test) (**B**) Quantification and positions of eggs laid over ~23 hours in the agarose arena in blank control or with 9-tricosene (yellow, 0.001%) (B: p=0.9499; n=11; p<0.001; t-test, n=9 per trial, One-way ANOVA test). (**C**) The effect of 9-tricosene on female oviposition site selection was assayed in Or7a neuron ablated flies (C: *UAS-hid*/+, p<0.001, n=9 per trial; C': *Or7a-Gal4*/*UAS-hid*, p=0.384; n=9, One-way ANOVA test). (**D**) 9-Tricosene guided oviposition site selection assayed in $Or7a^{-/-}$ mutant flies (p=0.69; n=9, One-way ANOVA test). (**E**) Positional recording throughout the 23 hr course of female oviposition behavior with a 9-tricosene hybrid gel (p=0.1; n=6, One-way ANOVA test). (**F**) Oviposition site selection using a 7-tricosene hybrid gel. (p=0.28; n=8, One-way ANOVA test). (**G**) Box plots indicating the total number of eggs laid in **A-D** (p=0.0021 comparing WT and *Or7a>hid*, p=0.0001 comparing WT and $Or7a^{-/-}$, p=0.68 comparing *Or7a>hid* and $Or7a^{-/-}$; t-test ; n=9-11). In all panels, colored dots indicate actual egg locations. Different colors represent different experiment trials. Error bars indicate ± 2.5 s.e.m. throughout. Data points not within this range are plotted as circles. See also Figure 2.12.

Figure 2.12

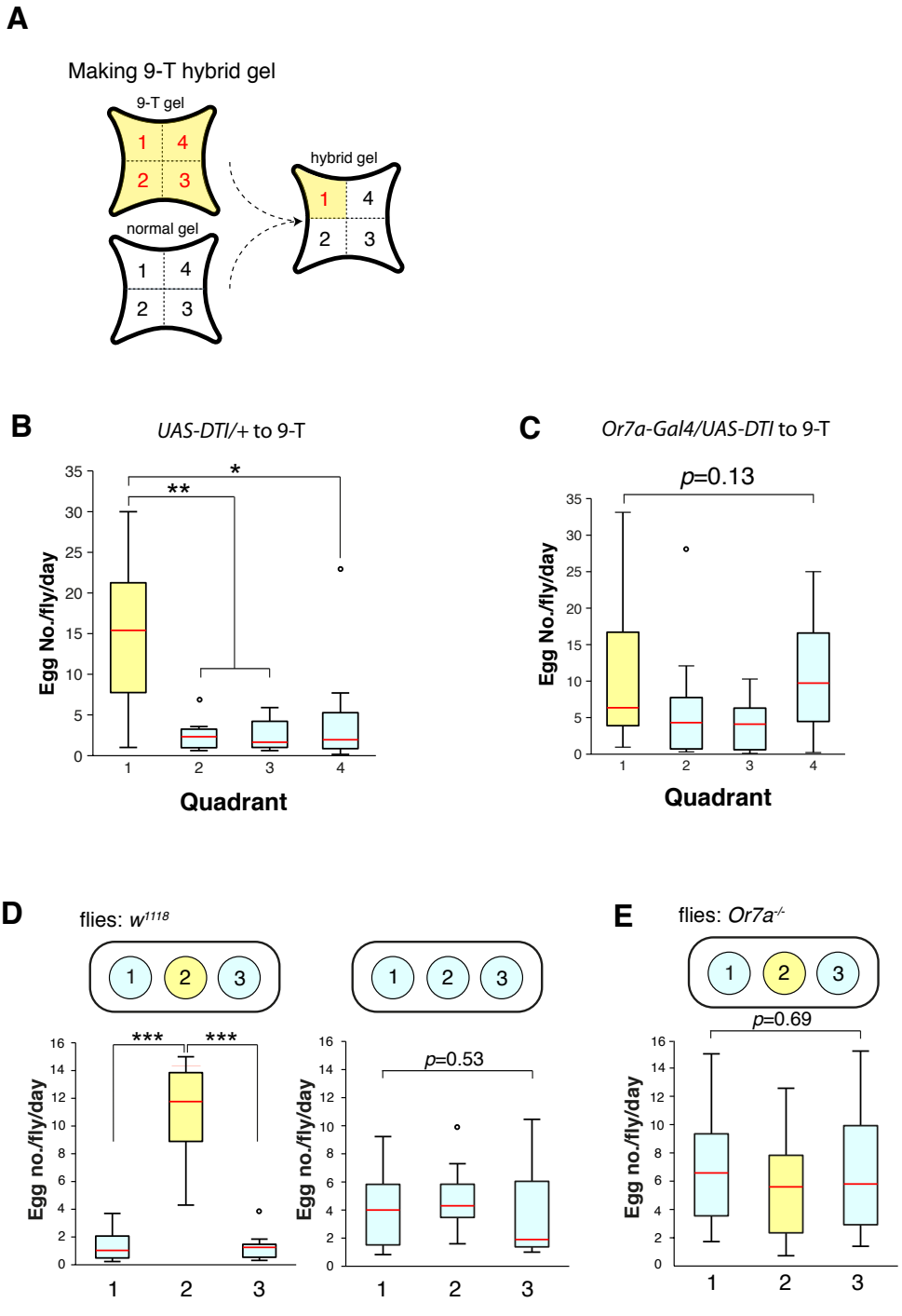
A
Making 9-T hybrid gel
9-T gel
1
4
2
3
normal gel
1
4
2
3
hybrid gel
1
4
2
3
B
UAS-DTI/+ to 9-T
*
**
Egg No./fly/day
Quadrant
C
Or7a-Gal4/UAS-DTI to 9-T
p=0.13
Egg No./fly/day
Quadrant
D
flies: w1118
1
2
3
***
***
Egg no./fly/day
1
2
3
p=0.53
Egg no./fly/day
1
2
3
E
flies: Or7a-/-
1
2
3
p=0.69
Egg no./fly/day
1
2
3

Figure 2.12. Oviposition guidance to 9-tricosene as assayed by two different behavioral methods

(**A**) Schematic of making hybrid 9-tricosene gel. Concentration of 9-tricosene in the agarose gel is ~0.001%. (**B**) Egg laying preference summary to the 9-tricosene quadrant in control (*UAS-DTI*/+, p= 0.0028, 0.0028 and 0.0353 to 9-tricosene quadrant; t-test, n=8) and (**C**) Or7a neuron ablated flies (*Or7a-Gal4*/*UAS-DTI*, p=0.1349; one-way ANOVA test, n=11). (**D**) The effects of 9-tricosene guidance on egg-laying using a 3-well spot plate (34x85 mm) containing 9-tricosene in a 1% agarose gel (yellow, 0.001%; p<0.001; t-test, n=12) or control 1% agarose gel (blue) (p=0.53, One-way ANOVA test, n=17). (**E**) Egg laying preference of $Or7a^{-/-}$ mutant flies in the 3-well spot 9-tricosene egg laying assay (p=0.69, One-way ANOVA test, n=15). For box plots (**B**-**E**), error bars indicate ± 2.5 s.e.m. Data points not within this range are plotted as circles.

Figure 2.13

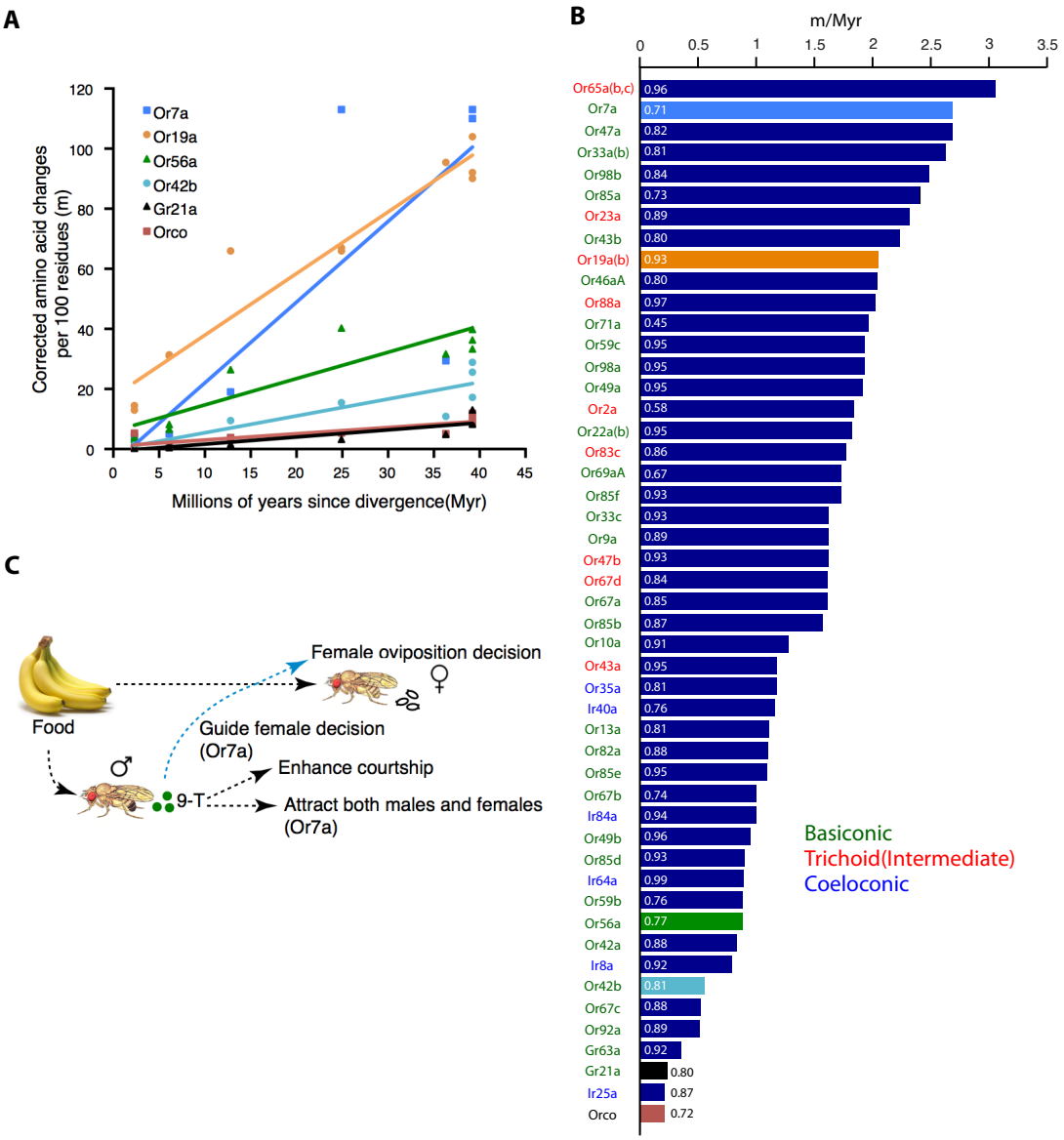
A
Corrected amino acid changes per 100 residues (m)
Millions of years since divergence(Myr)
Or7a
Or19a
Or56a
Or42b
Gr21a
Orco
B
m/Myr
Basiconic
Trichoid(Intermediate)
Coeloconic
C
Food
Female oviposition decision
Guide female decision (Or7a)
Enhance courtship
9-T
Attract both males and females (Or7a)

Figure 2.13. Comprehensive molecular evolution analysis reveals rapid amino acid substitution rate in Or7a.

(**A**) Corrected amino acid changes of Or7a, Or19a, Or56a, Or42b, Gr21a and Orco receptors over time (Myr). Regression lines of each receptor types are shown. (**B**) Comprehensive analysis of orco-dependent olfactory receptors, Grs and representative Irs expressed in the adult olfactory system. Numbers within the bars are the R^2 values of each regression line. Names of olfactory receptors are color-coded based on the sensillum types they reside in (green: basiconic, red: trichoid/
intermediate, blue: coeloconic). (C) Model of food-odor induced aggregation pheromone behavioral response. See also Figure 2.18.

Figure 2.14

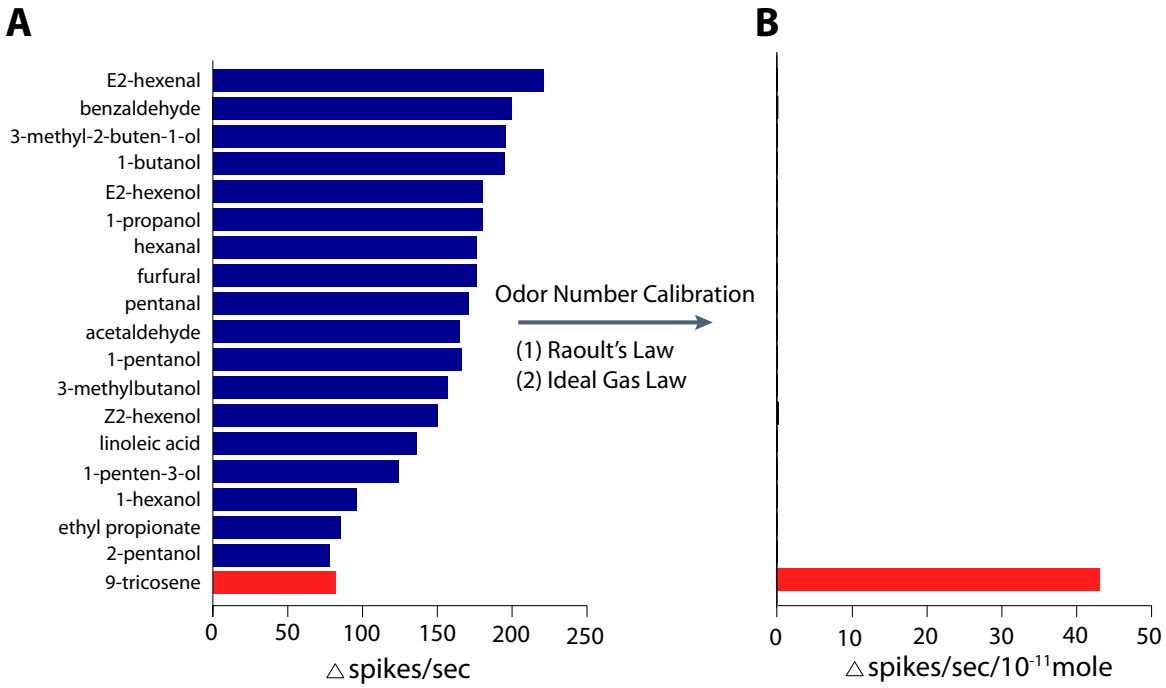
A
B
E2-hexenal
benzaldehyde
3-methyl-2-buten-1-ol
1-butanol
E2-hexenol
1-propanol
hexanal
furfural
pentanal
acetaldehyde
1-pentanol
3-methylbutanol
Z2-hexenol
linoleic acid
1-penten-3-ol
1-hexanol
ethyl propionate
2-pentanol
9-tricosene
0
50
100
150
200
250
△spikes/sec
Odor Number Calibration
(1) Raoult's Law
(2) Ideal Gas Law
0
10
20
30
40
50
△spikes/sec/10-11mole

Figure 2.14. Calibration of Or7a neuron activity to number of stimulating odor molecules.

Ab4A (Or7a) firing frequencies of known Or7a ligands (blue) (Hallem and Carlson, 2006) and 9-tricosene (red) before (**A**) and after molecule number calibration (**B**). See Figure 2.19 and Experimental Procedures for details.

Figure 2.15

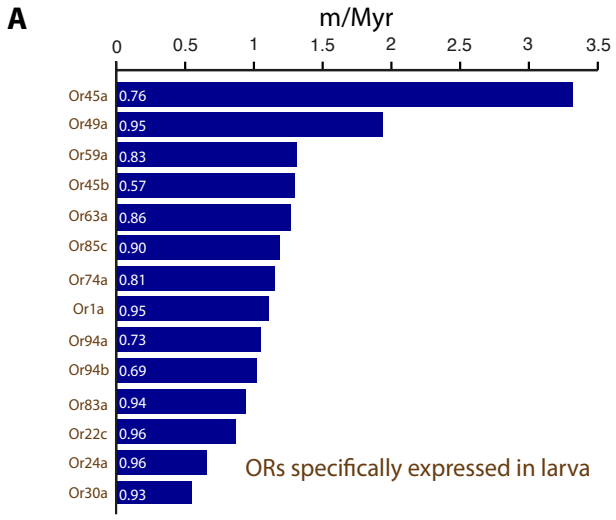

Figure 2.15 Molecular evolution analysis of larva-specific odorant receptors

Figure 2.16

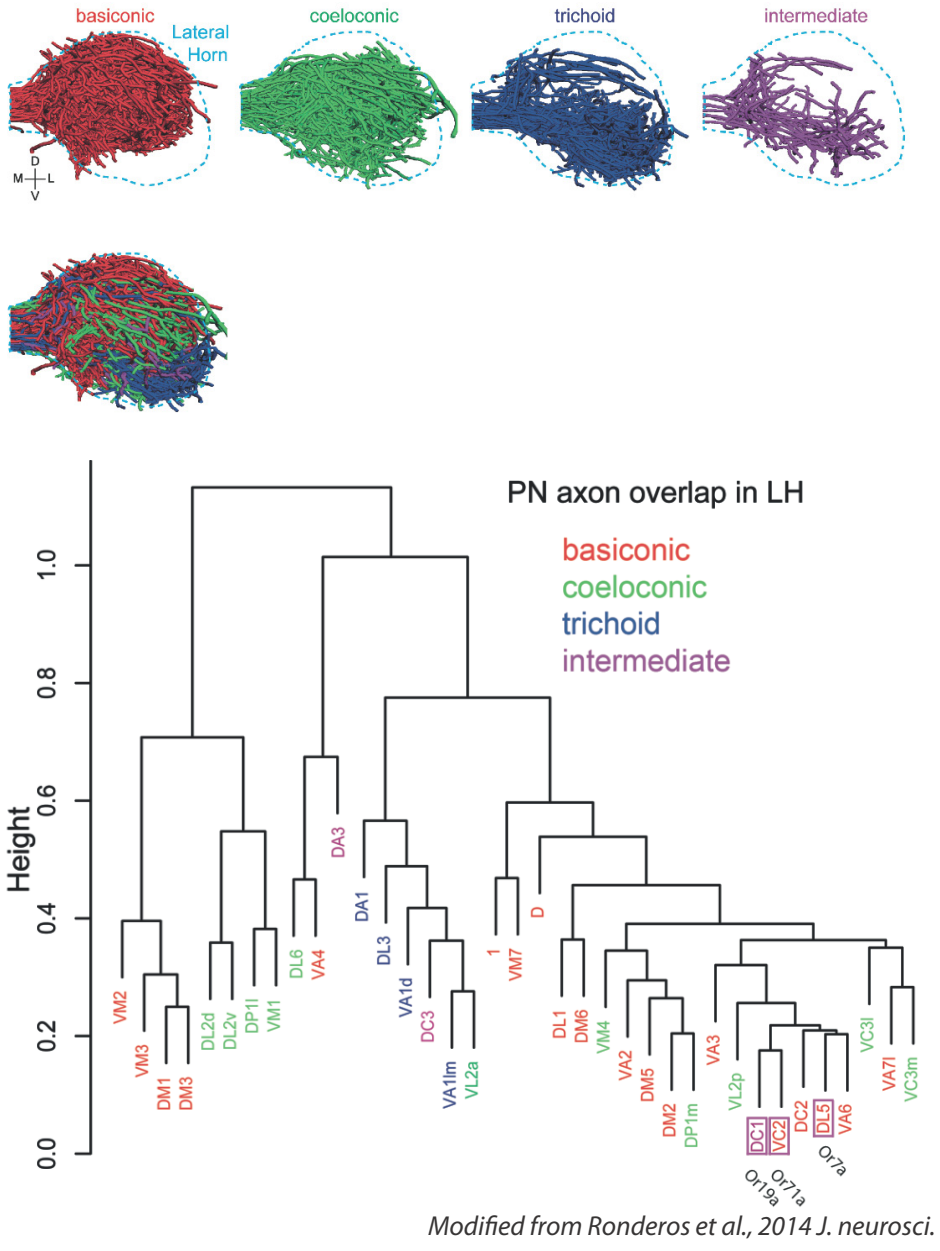

Modified from Ronderos et al., 2014 J. neurosci.

Figure 2.16 Clustering analysis of axonal projections to the lateral horn.
Analysis of axonal arborizations of 37 classes of projection neurons to the lateral horn shows that circuits responsible for oviposition decisions are highly similar.

Figure 2.17.

Volatile Pheromone	ACV-only	HA+flies	ACV+flies	Fold Enriched
cis-vaccenyl acetate (cVA)	N.D. [b]	N.D.	N.D.	-
7-docosene (7-D)	N.D.	N.D.	N.D.	-
5-tricosene (5-T)	N.D.	trace [c]	trace	-
9-tricosene (9-T)	N.D.	15.2 ± 3 .2	42.2 ± 14	**2.8**
2-methyldocosane (23-Br)	N.D.	N.D.	N.D.	-
7-tricosene (7-T) [d]	N.D.	158.6 ± 36	552.9 ± 225	**3.5**

[a] values normalized by internal standard (hexacosane n-C26)
[b] N.D., not detected;
[c] trace, not detected on TIC; detected only by characteristic ion (*m/z* 97)
[d] male-enriched but not specific

Figure 2.17. Volatile male-specific and male-enriched pheromones detected by GC-MS under control and experimental conditions. [a]

9-Tricosene is an enriched male volatile pheromone deposited upon food-odor stimulation. Shown are concentrations normalized to an internal standard (hexacosane) for 5 volatile male-specific and 1 male-enriched (7-tricosene) pheromones deposited onto the odor quadrant as detected by GC-MS in hexane extracts. 9-Tricosene is enriched ~3 fold upon ACV food-odor stimulation. Stimuli as shown in Figure 2.1. ND, not detected. Trace, not detected by TIC, but detected by characterstic ion (m/z 97).

Figure 2.18. Calculated evolutionary rates of odorant receptors among 12 *Drosophila* species.

Receptor	m/Myr	R^2
Or2a	1.84	0.58
Or7a*	2.69	0.71
Or9a	1.62	0.89
Or10a	1.18	0.91
Or13a	1.1	0.81
Or19a	2.09	0.93
Or22a	1.82	0.95
Or23a	2.32	0.89
Or33a	2.63	0.81
Or33c	1.62	0.93
Or35a	1.16	0.81
Or42a	0.83	0.88
Or42b	0.56	0.81
Or43a	1.18	0.95
Or43b	2.24	0.8
Or46aA	2.04	0.8
Or47a	2.69	0.82
Or47b	1.61	0.93
Or49a	1.92	0.95
Or49b	0.95	0.96
Or56a	0.88	0.77
Or59b	0.88	0.76
Or59c	1.93	0.95
Or65a	3.06	0.96
Or67a	1.57	0.85
Or67b	1	0.74
Or67c	0.52	0.88
Or67d	1.61	0.84
Or69aA	1.73	0.67
Or71a	1.97	0.45
Or82a	1.09	0.88
Or83c	1.77	0.86
Or85a	2.41	0.73
Or85b	1.28	0.87
Or85d	0.9	0.93
Or85e	1.06	0.95
Or85f	1.73	0.93
Or88a	2.03	0.97
Or92a	0.51	0.89

Or98a	1.93	0.95
Or98b	2.49	0.84
Orco	0.21	0.72
Gr21a	0.24	0.8
Gr63a	0.53	0.92
Ir8a	0.79	0.92
Ir25a	0.21	0.87
Ir40a	1.11	0.76
Ir64a	0.89	0.99
Ir84a	1	0.94

***** Test of positive selection using codon-based Z test (MEGA6) (Tamura et al., 2013) reveals statistically significant positive selection (p=0.0003).

Figure 2.19. Activity of known ligands for the Or7a receptor factoring in odorant volatility. Mole is the calculated number of molecules reaching the antenna in the SSR experiments (Based on Raoult's law and ideal gas law, see Experimental Procedures for details).

Chemical	Vapor pressure[a]	Density (g/ml)	Mol. Weight	Mole (10^{-11})	Δspikes/ sec[b]	Δspikes/sec/ mol (10^{-11})	Ratio[c]
E2-hexenal	4.62	0.84	98	$6.62x10^3$	221	0.03	1292
benzaldehyde	1	1.04	106	$1.63x10^3$	200	0.12	352
3-methyl-2-buten-1-ol	1.4	0.853	86	$2.31x10^3$	196	0.08	508
1-butanol	7	0.81	74	$1.27x10^4$	195	0.02	2812
E2-hexenol	3.42	0.843	100	$4.82x10^3$	180	0.04	1155
1-propanol	21	0.803	60	$4.63x10^4$	180	0.004	11091
hexanal	11	0.814	100	$1.50x10^4$	176	0.01	3673
furfural	2	1.16	96	$4.00x10^3$	176	0.04	979
pentanal	36	0.809	86	$5.65x10^4$	171	0.003	14241
acetaldehyde	760	0.788	44	$2.21x10^6$	165	0.00007	577980
1-pentanol	1.5	0.814	88	$2.31x10^3$	166	0.07	601
3-methylbutanol	3	0.809	88	$4.60x10^3$	157	0.03	1264
Z2-hexenol	0.608	0.85	100	$8.64x10^2$	150	0.2	248
linoleic acid	44.6	0.9	288	$2.37x10^4$	136	0.006	7516
1-penten-3-ol	11.18	0.839	86	$1.82x10^4$	124	0.007	6318
1-hexanol	1	0.813	102	$1.33x10^3$	96	0.07	599
ethyl propionate	36	0.88	102	$5.19x10^4$	85	0.002	26340
2-pentanol	6	0.812	88	$9.23x10^3$	78	0.008	5107
9-tricosene	0.0000353	0.806	322	1.9	82	43	1

[a], Temperature ranging from 20 ˚C to 25 ˚C. Unit: mmHg.

[b], All data are from Hallem and Carlson (Hallem and Carlson, 2006) except for 9-tricosene (this work). All the chemicals were dissolved in paraffin oil and final concentration is 1% except for 9-tricosene (100%).

[c], Ratio is the values of Δspikes/sec/mole of 9-tricosene divided by that of identified ligands. Ratio signifies the relative sensitivity to Or7a receptor. Higher value indicates lower sensitivity.

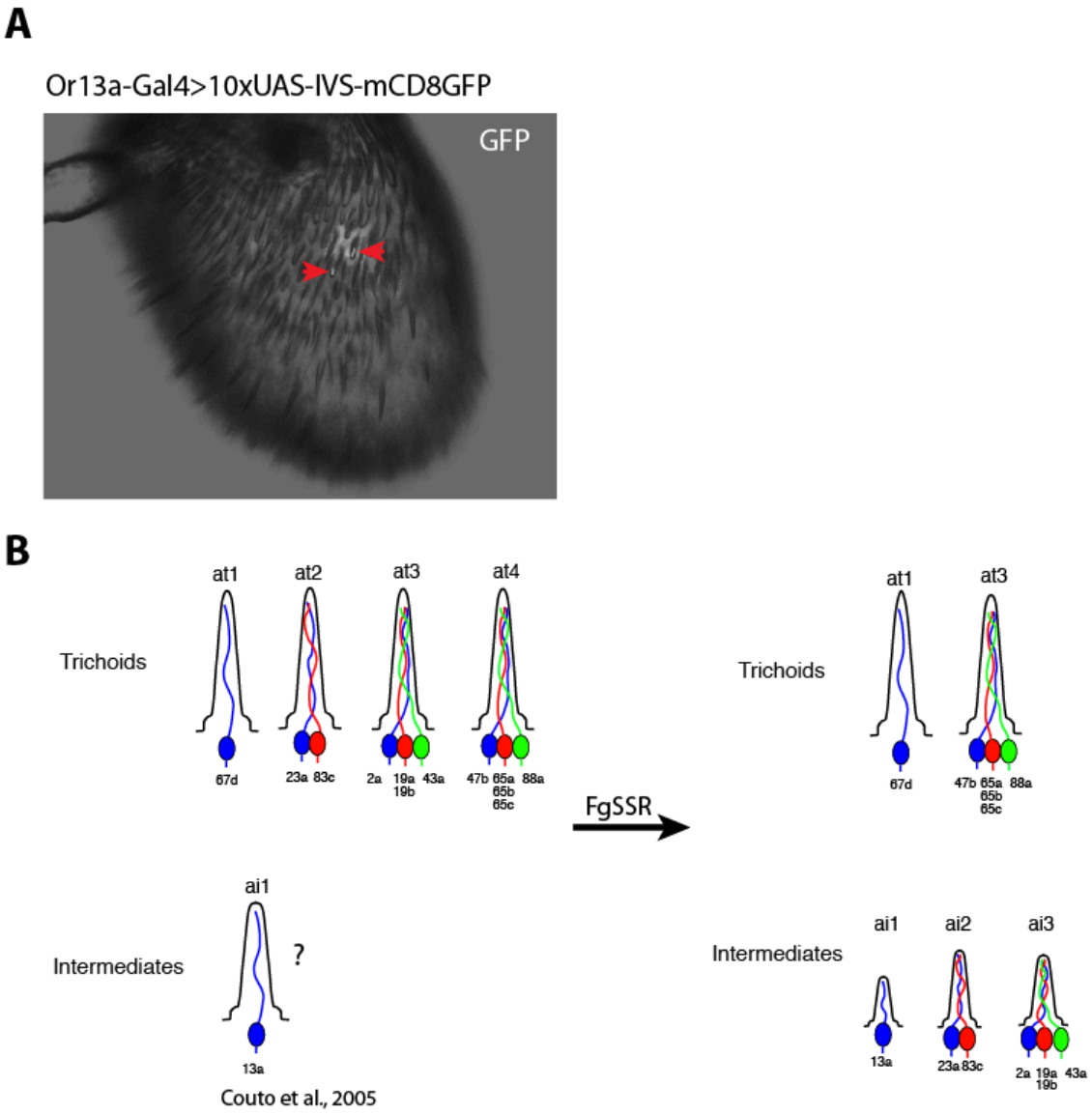

Figure 2.20. Reclassification of trichoid and intermediate sensilla types.

(**A**) Representative image of fluorescence guided single sensillum recording by using Or13a-Gal4 driving 10xUAS-IVS-mCD8GFP (**B**) Diagram of trichoid/intermediate classification from the published data (Couto et al., 2005) and our current updated modification.

Chapter 3: The CLAMP system: a genetically encoded trans-synaptic tool for circuit identification and manipulation

3.1 Introduction:

We demonstrated that Or7a+ neurons are responsible for 9-tricosene guided oviposition decisions. Recently, it was found that flies utilized Or19a+ neurons to detect citrus fruit as oviposition substrates (Dweck et al., 2013). Interestingly, the Or7a DL5 and Or19a DC1 projection neurons (PNs) share highly similar axonal projection patterns in the higher olfactory brain region (later horn) that are distinct from previously described food and pheromone regions (Ronderos et al., 2014). Characterizing the olfactory circuits in higher olfactory centers that are activated by Or7a+ and Or19a+ neurons would reveal how chemosensory cues are processed in the oviposition decision-making process. Furthermore, similar olfactory centers might be evolutionally conserved in other insects such as mosquitoes, and could be potential targets for intervention. We therefore sought to decipher the connectivity and functions of higher olfactory brain regions.

A pivot question in neuroscience is to understand how an ensemble of neural circuitry generates corresponding behaviors. To achieve this, it is necessary to first characterize neuronal connectivity of specific input and output neurons. Specifically manipulating the neuronal activity (with opto- or thermogenetic tools) would establish the linkage between anatomical data and functional behavior results (Venken et al., 2011). Serial electron microscopy-based connectome reconstruction provides superior anatomical resolution but does not allow functional manipulation (Takemura et al., 2013; White et al., 1986). Besides, EM methods are currently best suited for elucidating

microcircuitry of small regions of the brain, rather than mapping out long-range connections. Classical anterograde tracers such as biotinylated-dextran amine (BDA), fluorescence latex microspheres, or phytohemagglutinin lectin (PHAL) provide useful information as to long-range axonal projections of the neurons, but the injected lipophilic dyes are confined into the neuron and cannot be applied to identify pre- or post-synaptic coupled neurons (Katz and Iarovici, 1990; Reiner et al., 2000). In order to simultaneously specify anatomical structure and manipulate the function, incorporation of genetic tools is necessary.

This can be achieved by virus-based trans-synaptic tracing techniques. The advantages of using viral tracers include unidirectional spreading, self-replication and, most important, genetic tractability (Callaway, 2008). The retrograde and anterograde viruses are useful for poly or uni-trans-synaptic labeling. However, both virus and lipophilic dye injection require surgical injection and therefore might be biased. Furthermore, virus-based trans-synaptic labeling technique is not applicable in *Drosophila* because of small animal size and lack of appropriate viruses. We therefore need tools that are entirely genetically encoded.

GFP reconstitution across synaptic partners (GRASP) was first developed in *C. elegans* to monitor potential synaptic contacts between two neurons (Feinberg et al., 2008). Two complementary non-fluorescent GFP fragments (1-10 and 11) bound to a trans-membrane protein CD4 are expressed in opposing neurons, and functional GFP is reconstituted at the synaptic cleft. This method is useful to understand if two neurons form close apposition of pre- and post-synaptic membranes but can not be used to characterize unknown upstream or downstream neurons.

The recently developed Tango system is an activity-dependent trans-synaptic tracing technique that detects endogenous neurotransmitter activity in flies. Transient receptor-ligand interaction generates a stable readout depending on the chosen reporters. However, the assay is limited to specific neurotransmitter types and cannot be generalized for characterization of all synaptically coupled neurons (Barnea et al., 2008; Inagaki et al., 2012; Jagadish et al., 2014). To our knowledge, no existing genetically encoded tool in *Drosophila* or mammalian systems can be used for simultaneous identification and manipulation of downstream neurons with genetically defined pre-synaptic neurons.

The key idea of our trans-synaptic method is to design a cell-permeable fusion protein that can be specifically released at the synaptic cleft, cross to the next order neuron and turn on expression of an effecter gene (Figure 3.1). With the powerful genetic tools in *Drosophila melanogaster*, we utilize two binary expression systems and site-specific recombinase to achieve this goal. The use of site-specific recombinase (FLP/FRT, Cre/LoxP) and binary expression systems (Gal4/UAS, LexA/LexAop, QF/QUAS) has allowed targeting of genetically encoded markers to molecularly defined neuronal populations in flies (Brand and Perrimon, 1993; Buchholz et al., 1998; Fischer et al., 1988; Lai and Lee, 2006; Potter et al., 2010; Raymond and Soriano, 2007; Turan et al., 2011). The recombinase target sequence (FRT for instance) and recombinase enzyme (FLP for instance) can induce chromosomal recombination either in trans or cis arrangement (Turan et al., 2011). In our method, we make use of the fact that when the FRTs are arranged in tandem in the same orientation, the intervening sequence is excised and genes following the second FRT can be expressed. Previously, the application of FLP

has been limited by its low efficiency compared to Cre recombinase. By screening for thermostable variant (Buchholz et al., 1998) and codon optimization (Raymond and Soriano, 2007), current FLP (FLPo) activity is comparable, or even superior to, Cre (Turan et al., 2011).

In order for the recombinase to traverse the membrane and enter opposing neurons, we fused FLPo to a Protein transduction domain (PTD). This short polypeptide PTD domain, found in such proteins as HIV-1 TAT, antennapedia and VP22, is a positively charged polypeptide sequence (containing multiple arginine and lysine residues) that allows transversion across lipid bilayers of mammalian and insect cells (Schwarze et al., 1999; Schwarze et al., 2000). Although the exact mechanism remains unknown, the ability to ferry large cargos (up to ~1000 a.a.) when tethered with PTD makes it an ideal tool to transfer proteins and other molecules into living cells for research purposes (Beerens et al., 2003). Here, we have developed a novel genetically-encoded method to map downstream neurons in a unbiased manner. We provide a method to identify and manipulate downstream circuits with genetically defined pre-synaptic neurons.

3.2 Results:

Basic Principles of Developing CLAMP

In the second part of my thesis work, I have developed a novel genetically-encoded method to map downstream neurons in a unbiased manner. **CLAMP** (**C**ell **L**abeling **A**cross **M**embrane **P**artners) allows for the identification and functional manipulation of downstream neurons. The CLAMP system is based upon trans-cellular

delivery of FLPo (codon-optimized FLPase) from a starter neuron to its downstream target neuron(s), taking advantage of the proximity of the pre- and post-synaptic membranes (~20 nm) (Figure 3.1). Two binary systems, Gal4 and QF, are used in the starter and downstream neurons, respectively. The Q system is a binary system similar to the Gal4/UAS system (Brand and Perrimon, 1993; Fischer et al., 1988), where QF is the transcription factor that binds to *QUAS* (QF upstream activating sequence), analogous to Gal4 binding and activation of *UAS effecer genes* (Potter et al., 2010).

Under Gal4/UAS control, the pre-synaptic starter neuron expresses a fusion protein consisting of FLPo fused to PTD and a TEV (tobacco etch virus) protease cutting site (TEV^{cs}) (Pauli et al., 2008). Under control of the Q system, the post-synaptic receiver neurons express TEV-protease. Inspired by the idea of GRASP, in which GFP can be successfully reconstituted at the synaptic cleft, both pre-synaptic and post-synaptic components were tethered with human T cell protein CD4 (Feinberg et al., 2008; Gordon and Scott, 2009) (pre-synaptic: *UAS-CTP-FLPo-*TEV^{cs}*-CD4*; post-synaptic: *QUAS>TEV protease-CD4-Stop>mCD8-GFP*) (Figure 3.1, Figure 3.2). The effecters or reporters driven by QF are not active unless the stop cassette is removed by the site-specific FLP recombinase (QUAS>TEV protease stop>mCD8GFP, > is the FRT sequence; TEV protease is discussed below). Once the Flp-out event occurs, reporter expression is "turned on" and no longer relies on trans-cellular delivery of FLPo from the upstream neurons (an once-for-all and irreversible event) (Figure 3.1).

The pre-synaptic component is driven by a well-characterized X-Gal4 line, whereas the post-synaptic component is expressed in candidate neurons or in all neurons (via *nsyb-QF2,* which expresses pan-neuronally (Riabinina et al., 2015)). To ensure

synapse-specificity, the size of the linkers are designed so that only at the synapse is the TEV from the post-synaptic neuron able to cleave at the TEV^{cs} on the pre-synaptic neuron, releasing CTP-FLPo, which transverses the plasma membrane of the downstream neuron. FLPo then mediates excision of the '>TEV protease-CD4-stop>' cassette (flp-out), allowing for expression of GFP in the downstream neuron (Figure 3.1, Figure 3.2). Since we are in the midst of developing CLAMP, we have generated different 3 versions, which represent increasing expression levels (20xUAS, preCLAMP II), cleavage efficiency (adding poly-glycine, post-CLAMP II) and specific synaptic targeting (utilizing Cac and TLCN, pre- and post-CLAMP III) (Figure 3.2).

CLAMP Allows Trans-synaptic Identification of Olfactory Secondary Neurons

As a proof-of-principle, we tested CLAMP in the well-characterized olfactory system. Axons of olfactory receptor neurons (ORNs) project to the antennal lobes (AL), where they form synapses with projection neurons (PNs) (Couto et al., 2005; Fishilevich and Vosshall, 2005) (Figure 3.3). The latter relay olfactory information to higher brain centers such as the mushroom body (MB) or lateral horn (LH) (Jefferis et al., 2007). We used *pebbled-Gal4* to label ORNs and gustatory receptor neurons, and *GH146-QF2* to potentially label most PNs (~60%, Figure 3.3). As shown in Figure 3.4A, CLAMP specifically labels PNs synaptically coupled with the ORNs, allowing visualization of the PN's dendrites in the AL and axon processes in the MB and LH. Targeting TEV protease to the membrane with CD4 tag is necessary for this process since no neuron is labeled if TEV protease is not expressed on the membrane of post-synaptic neurons (Figure 3.4B). This was the first indication that FLPo-PTD could be released outside the neuron

terminals, enter a post-synaptic neuron, and function on a genetically encoded FLP-out cassette. PNs are not the only post-synaptic neurons of ORNs in the antennal lobe. Local interneurons (LNs) are wired diversely with ORNs axons and PN dendrites in the AL (Figure 3.3B). LN cell bodies are located in two clusters: a large and continuous cluster lateral to the AL and a separate cluster ventral to AL (Chou et al., 2010). By using pan-neuronal driver *nsyb-QF2*, we successfully identified the lateral cluster LNs (Figures 3.4C and 3.4D). Interestingly, since both pre- and post-synaptic components are co-expressed in the pre-synaptic neurons (*pebbled-Gal4* and *nsyn-QF2* in this case), this self-labeling phenomenon is observed in the ORNs and gustatory neurons (Figures 3.4C and 3.4D) as is predicted by *pebbled-Gal4* expression pattern. This could serve as an internal control for monitoring if two systems are present in the same neurons but can be easily eliminated by adding *UAS-QS* to suppress Q system activity in the Gal4-positive neurons (or reciprocally, *QUAS-Gal80* to suppress Gal4 activity in the QF-positive neurons). In summary, the results suggest that CLAMP could be a useful technique for morphological characterization of post-synaptic neurons.

Restricted Starter Lines Fails to Label Cognate Neurons in CLAMP I

We next ask if a single class of ORNs is sufficient to label the cognate post-synaptic PNs. In our previous initial experiments, the pre-synaptic component was driven by a pan-ORN Gal4 (*pebbled-Gal4*), which covers ~1300 ORNs projecting to more than 50 glomeruli in the antennal lobes (Fishilevich and Vosshall, 2005). By using a single class of ORNs to express pre-synaptic components, we should be able to assess the trans-synaptic efficiency of our technique. After several different combinations of trials, self-

labeling was reliably noted but there was no success for trans-synaptic labeling (pre-synaptic: *Or42b-Gal4* or *Or67d-Gal4*; post-synaptic: *GH146-QF2* or *nsyb-QF2*) (Figure 3.5). Since the construct was driven by *5xUAS* and the fusion protein was distributed equally to the cell membrane by CD4, we reasoned that insufficient CTP-FLPo release at the synaptic clefts might be the cause of low trans-synaptic labeling events.

Expression Level Correlates with Success Rate and Unspecific Labeling

In order to increase potency, we modified the construct by using *20xUAS-IVS* (Pfeiffer et al., 2010) to drive the *CTP-FLPo-TEV^{cs}-CD4* (*20xUAS-IVS-CTP-FLPo-TEV^{cs}-CD4,* preCLAMP II, Figure 3.2). In addition, to increase the opportunity for the TEV protease active domain (located at the C-terminal) to cleave at the TEV^{cs}, a poly-glycine-serine $(GGGGS)_3$ linker sequence was added at the junction between TEV protease and CD4 (*10xQUAS>TEV protease-PG-CD4>mCD8GFP*, postCLAMP II, Figure 3.2). By using *Or42-Gal4* to drive the pre-synaptic component and *GH146-QF2* to label the post-synaptic component, Or42b DM1 PN was successfully labeled (Figures 3.6A and 3.6B). The cell body location of DM1 PN and the axonal arborization to the MB and LN are comparable with previously published results (Jefferis et al., 2007) (Figures 3.6B and 3.6B'). Interestingly, one multi-glomeruli neuron ventral to the AL was also identified (Figure 3.7C). This is considered specific labeling because the dendritic arborization of the novel PN also covers DM1 glomeruli (Figures 3.7A and 3.7C). However, non-specific labeling of Ir75d VL1 PNs was also noted (Figures 3.7A and 3.7B). This could be due to the close proximity of axonal projections between Or42+ and the Ir75d+ ORN circuits from the antenna causing non-specific cleavage and

resulting in CTP-FLPo leakage to the VL1 PN. Although CLAMP II can successfully label post-synaptic neurons using restricted starter *OR-Gal4* lines, non-specific labeling prompted us to design synapse specific CLAMP III.

Synapse-specific CLAMP Version Increases Efficiency and Reduces Non-specificity

To increase specificity and efficiency, we developed CLAMP III by using CD4-Cacophony (Cac) for targeting proteins to pre-synaptic membrane terminals and Telencephalin (TLCN)/ICAM5 to target proteins to post-synaptic terminals (kindly suggested and provided by Steven Stowers, Montana State University; *5xUAS-SP-CTP-FLPo-TEV^{cs}-CD4-Cac, 10xQUAS>TEV protease-PG-TLCN>mCD8GFP,* Figure 3.1 and 3.2). By using pan-ORNs as starter neurons and PNs as receiver neurons shown in Figure 3.8A and 3.8B, CLAMP III specifically labels PNs synaptically coupled with the ORNs, allowing visualization of the PN's dendrites in the AL and axon processes in the MB and LH. The successful labeling rate is higher than CLAMP I and II. Or56a+ ORNs are specifically activated by Geosmin, the odor of mold, which generates aversive behavior. Or56a+ ORNs relay the information to DA2 PNs, which subsequently projects to a repulsive region in the LH (Stensmyr et al., 2012). Previous attempts to identify the DA2 PN circuit utilized photoactivatable GFP (PA-GFP), but the resulting resolution of axonal arborization in the lateral horn was poor (Stensmyr et al., 2012) (Figure 3.8). We generated *GH146-QF2* with the core promoter region (4274 b.p.), which labels a few more PNs than the *GH146-Gal4* enhancer trap line (Figure 3.9). With *GH146-QF2*, we tested if CLAMP III could specifically label DA2 PN by using Or56a+ ORNs as the labeled starter neurons (*5xUAS-SP-CTP-FLPo-TEV^{cs}-CD4-Cac; Or56a-Gal4, GH146-*

QF2/10xQUAS>TEV protease-PG-TLCN>mCD8GFP). Indeed, a DA2 PN was successfully labeling using CLAMP III and the axonal arborizaiton was consistent with previous predictions, forming the cup-shape repulsive region in the lateral horn (Figure 3.8E and 3.8F).

Deciphering Unknown Central Gustatory Circuitry

The application of the CLAMP system is not limited to the olfactory system- we have also mapped previously unknown potential second order neurons in the *Drosophila* gustatory system. The secondary gustatory receptor neurons are currently not known. Although some candidate neurons display arborizations in the primary taste center subesophageal ganglion (SOG), none have been demonstrated to have direct synaptic connection with gustatory receptor neurons (GRNs) (Melcher and Pankratz, 2005). Gr5a+ gustatory receptor neurons are the primary neurons responsible for sweet sensation in *Drosophila* (Marella et al., 2006). By using Gr5a+ neurons as the CLAMP starter and pan-neuronal line as the CLAMP receiver, we identified 1-2 neurons located ventrolateral to the AL that connect the SOG and AL (Figure 3.10). One pair of neurons bilaterally innervates each AL and covers the glomeruli at the ventral part of AL, suggesting that olfactory and gustatory sensory stimuli might be modulating each other through these interneurons. By characterizing the identities of these glomeruli and corresponding ligands, we would be able to understand which and how specific olfactory signal might be interacting with gustatory sweet sensation. Future experiments include behavior and electrophysiological experiments to determine if olfactory sensory outputs might be affected by gustatory stimuli or vice versa.

3.3 Discussion:

Our data demonstrate that CLAMP can be used in circuit analyses to identify and characterize unknown neurons downstream of a defined starter neuron. CLAMP allows visualization of the full morphology (cell body, dendrites and axon projections) of target neurons, providing valuable information about these cells. This is in contrast to GRASP, which only labels points of contact between two neurons. By using the *Drosophila* olfactory system as a proof of principle, second order projection neurons and local interneurons were successfully identified. Furthermore, we have identified candidate second order gustatory neurons, which send projections to communicate with some glomeruli in the antennal lobe. This new technique could transform how circuit mapping is accomplished in *Drosophila*, and might be adaptable to other genetic systems, such as mice.

In the *Drosophila* olfactory system, ~50-100 ORNs project to one glomerulus, forming synapses with ~1-8 PNs. This represents a strong pre-synaptic input. Even with such strong pre-synaptic inputs, pan-ORNs starters typically label only a subset of PNs (~25% on average). Using single classes of ORNs as starter neurons, ~5% of the brains contain correct post-synaptic labeling in synaptic specific CLAMP III. Successful trans-synaptic events might be correlated with synaptic inputs and organization between opposing neurons. Therefore, the efficiency of CLAMP might be too low if the synaptic strength is weak between input and output neurons. The ultimate goal of developing CLAMP is to establish functional causation of circuitry and behavior. To achieve this, post-synaptic neurons of the flies must be reliably labeled (indicating a successful trans-

synapic event) in order for activity to be manipulated. With low trans-synaptic success rates, results would be difficult to interpret in population behavior assays (a 4-field behavior usually requires 50 flies per experiment). We aim to improve the trans-synaptic efficiency by modification of (A) type and number of protein transduction domains and (B) expression level of the pre-synaptic and post-synaptic components (for example, by increasing *UAS* copy number or by increasing GAL4/QF driver expression).

Higher brain regions are usually specialized into different functional areas. With circuit analyses and behavior readouts, the *Drosophila* lateral horn region is divided into food, pheromone and repulsive subdomains. Oviposition channels Or7a DL5 and Or19a DC1 projection neurons share highly similar axonal arborizations in the lateral horn distinct from previously subdomains; therefore, there seems to be a region specialized for oviposition decisions. The establishment of connections between a peripheral chemical-receptor pair to the central wiring diagram is usually difficult since it depends on using correct and specific transgenic lines. Labeling subclasses of the peripheral sensory neurons follows the logic of receptor types. However, mapping candidate second or third order neurons (and beyond) depends on tedious transgenic line screening. With the CLAMP technique, it will be straightforward to map out central circuitry using peripheral-specific drivers.

In the future, we plan to generate additional *QUAS>TEV protease-TLCN-stop> effector* (such as *dTrpA1*, *shi^{ts}*, *CsChrimson*) transgenic lines, to facilitate functional manipulation of the post-synaptic neurons with temperature and light. Together with behavioral assays, we will be able to unravel the circuit basis for olfactory behaviors. In addition, by including a *QUAS>TEV protease-TLCN-stop>CTP-FLPo-TEV^{cs}-CD4-Cac-*

T2A-GFP transgene, post-synaptic neurons are endowed with ability to express CTP-FLPo fusion protein and labeling would no longer be limited to the first post-synaptic neurons but could be able to continue down along the entire circuit (Figure 3.11)

3.4 Experimental procedures:

Fly stocks:

Or42b-Gal4 (BS#9971), *Or56a-Gal4* (BS#23896), *nsyb-QF2* (BS#51955), *pebbled-gal4* (gift from Liqun Luo), *Gr5a-Gal4* (gift from Craig Montell), *GH146-QF2* (unpublished reagent, C.-C. Lin and C. Potter)

Generation of CLAMP constructs:

preCLAMP fusion protein was cloned into pUAST construct using InFusion cloning technique. postCLAMP components were cloned into custom-made 10xQUAS>>>stop>>> construct (> is FRT site, the construct consists of 3 tandem FRT repeats to increase cutting efficiency).

CTP DNA sequence: GGCGGACGTCGCGCCCGTAGGCGCCGTCGACGC (GGRRARRRRRR).

TEV^{cs} sequence (3 repeats):

AGGGCTAGAGAGAATTTGTATTTTCAGGGTGCTTCTGAAAACCTTTACTTCCA AGGAGAGCTCGAAAATCTTTATTTCCAGGGAGCTAGC (RARENLYFQGASENLYFQGELENLYFQGAS)

TEV protease was PCR amplified from *UAS-NLS-V5-TEV-NLS2* (gift from Kim Nasmyth, Oxford University(Pauli et al., 2008)). Codon-optimized FLP (FLPo) was acquired from Addgene (#13792 (Raymond and Soriano, 2007)). CD4 construct was a gift from Kristin Scott (UC-Berkeley (Gordon and Scott, 2009)). 20xUAS-IVS was PCR

amplified from pJFRC7-20xUAS-IVS-mCD8GFP (Addgene #26220 (Pfeiffer et al., 2010)). CD4-Neurexin-Cac and TLCN/ICAM5 are gifts from Steve Stowers (Montana State University).

Figure 3.1

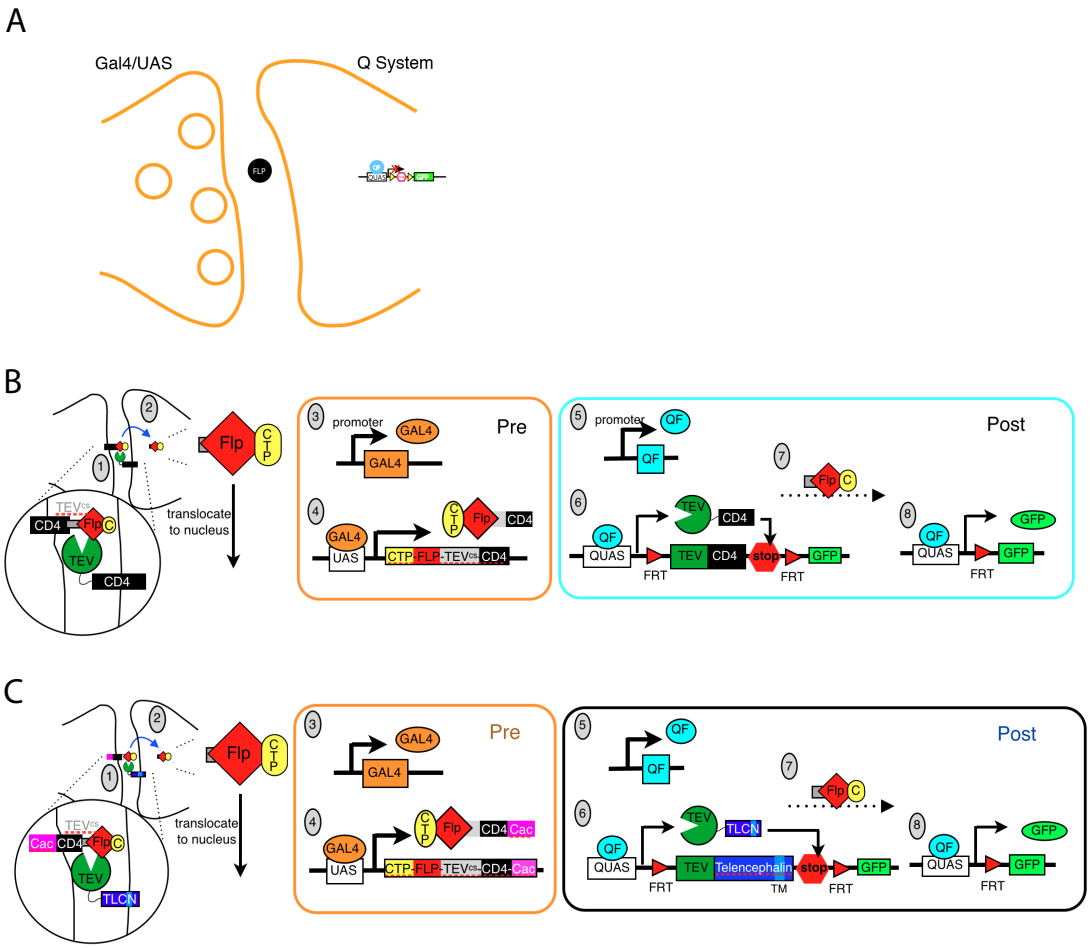
A
Gal4/UAS
Q System
B
translocate
to nucleus
Pre
promoter
GAL4
UAS
Post
QF
QUAS
TEV
CD4
stop
GFP
FRT
C
TLCN
Telencephalin
TM

Figure 3.1 Mechanism of CLAMP (Cell Labeling Across Membrane Partners)

(**A**) CLAMP is based on trans-cellular delivery of a site-specific recombinase (FLPo) from a starter neuron into receiver neurons. The Gal4/*UAS* system is utilized to label the starter neurons whereas receiver neurons utilize the Q system. A Flp-out event is the key to "turn on" Q system reporters. (**B**) Schematic of CLAMP I, in which CD4 was used as the membrane tag to transport pre- and post-synaptic fusion proteins to the cell membrane. (**C**) In synapse specific CLAMP III, CD4-Cacophany was used to target proteins to the pre-synaptic terminal and Telencephalin (TLCN) to target components to the post-synaptic membrane.

Figure 3.2

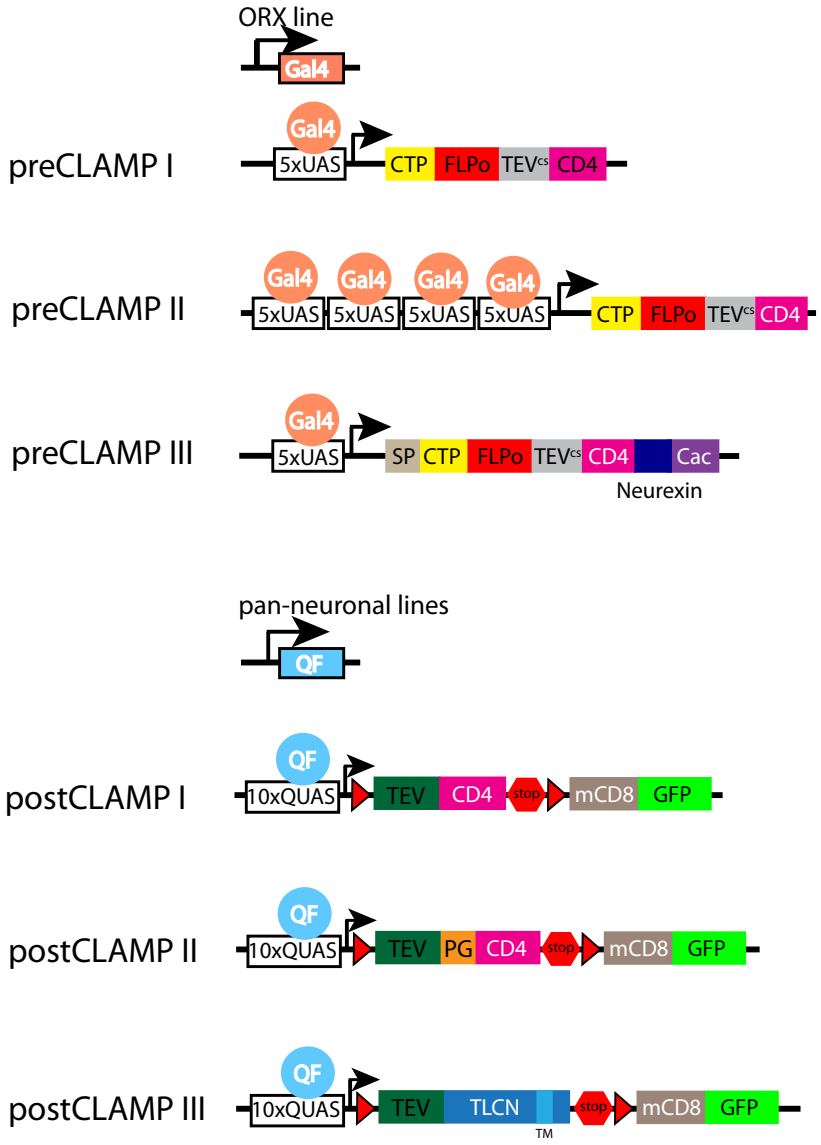
ORX line
Gal4
preCLAMP I
Gal4
5xUAS
CTP
FLPo
TEVcs
CD4
preCLAMP II
Gal4
Gal4
Gal4
Gal4
5xUAS
5xUAS
5xUAS
5xUAS
CTP
FLPo
TEVcs
CD4
preCLAMP III
Gal4
5xUAS
SP
CTP
FLPo
TEVcs
CD4
Cac
Neurexin
pan-neuronal lines
QF
postCLAMP I
QF
10xQUAS
TEV
CD4
stop
mCD8
GFP
postCLAMP II
QF
10xQUAS
TEV
PG
CD4
stop
mCD8
GFP
postCLAMP III
QF
10xQUAS
TEV
TLCN
TM
stop
mCD8
GFP

Figure 3.2 Schematics of different versions of CLAMP

CTP: Cytoplasmic Transduction Peptide; FLPo: codon-optimized site specific (mouse) recombinase FLP; TEV: TEV protease; TEVcs: TEV protease cutting site; CD4: human T-cell protein; SP: signal peptide; Cac: Cacophany; TLCN: Telencephalin/ICAM5

Figure 3.3

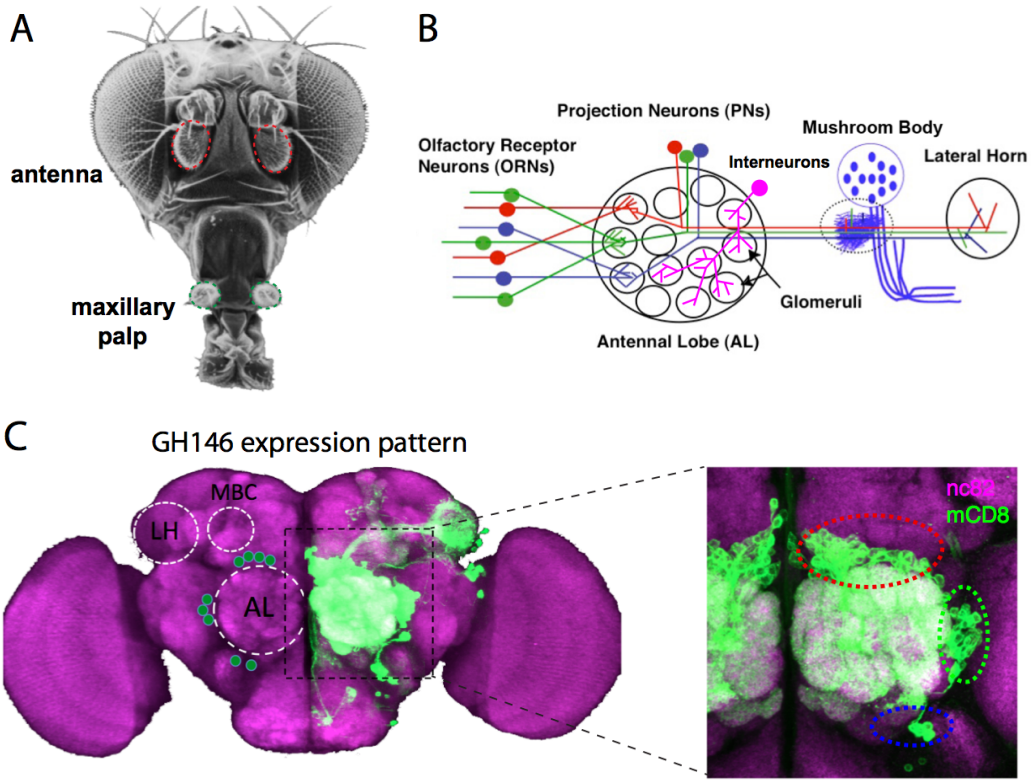
A
antenna
maxillary palp
B
Projection Neurons (PNs)
Olfactory Receptor Neurons (ORNs)
Interneurons
Mushroom Body
Lateral Horn
Glomeruli
Antennal Lobe (AL)
C
GH146 expression pattern
MBC
LH
AL
nc82
mCD8

Figure 3.3 Diagram of Drosophila olfactory organs and circuits

(**A**) Olfactory receptor neurons (ORNs) are housed in a porous cuticular structure call sensilla in the third antennal segments and maxillary palps (B) Odorants bind to olfactory receptors (ORs) on ORNs, which project their axons to discrete foci (called glomeruli) in the antennal lobe (AL), which is the site where olfactory information processing begins. ORNs that express the same olfactory receptors send their axons and converge onto the same glomeruli. Projection neurons (PNs) then relay the odor information from particular glomeruli to higher centers of the brain: the mushroom body and the lateral horn. Local interneurons send interglomerular connections between different glomeruli to modulate information processing in the AL. (**C**) ~60% of olfactory second order neurons (PNs) are labeled by the enhancer trap line *GH146-Gal4* (shown is *GH146-Gal4/ UAS-mCD8GFP*). The cell bodies of PNs are located in three clusters: dorsal (red), lateral (green) and ventral (blue) to the AL.

Figure 3.4

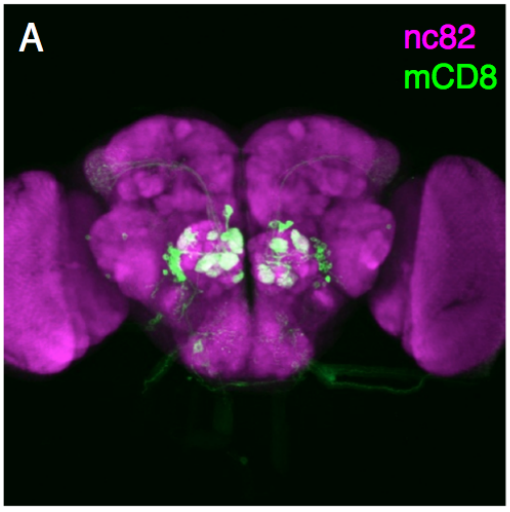

pebbled-Gal4
5xUAS-CTP-FLPo-CD4
GH146-QF
10xQUAS>TEV-CD4-Stop>mCD-GFP

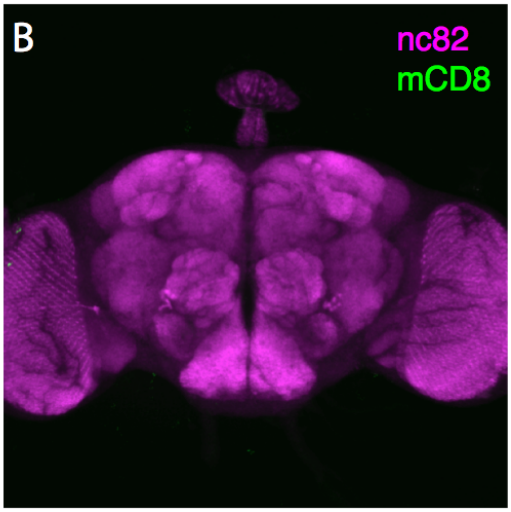

pebbled-Gal4
5xUAS-CTP-FLPo-CD4
GH146-QF
10xQUAS>Stop>mCD-GFP

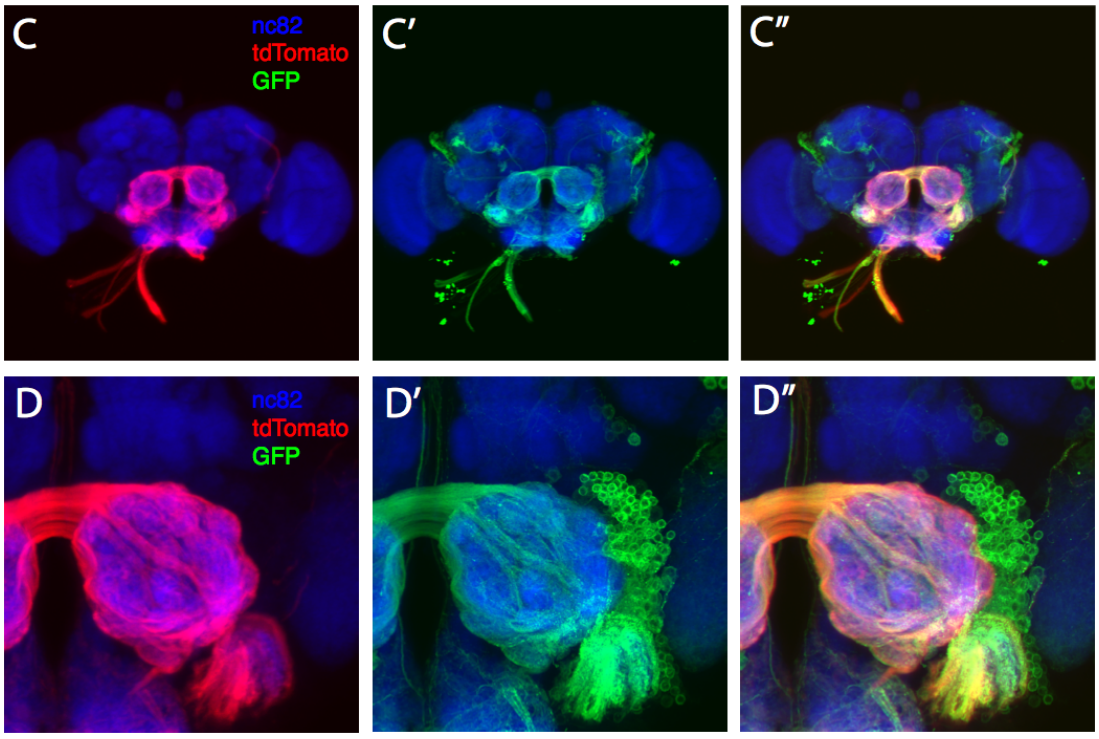

pebbled-Gal4;5xUAS-CTP-FLPo-CD4,10xQUAS>TEV-CD4-Stop>mCD-GFP(2-1M2)
;nsyb-QF2/UAS-IVS-mtdT,QUAS>Stop>TrpA1-2A-mCD8GFP

Figure 3.4 Using the *Drosophila* olfactory system as a proof of principle for CLAMP.

(**A**) Olfactory second order PNs are CLAMP labeled by using a pan-ORN Gal4 to drive pre-synaptic CLAMP components and *GH146-QF* to drive post-synaptic CLAMP components. Genotype: *pebbled-Gal4; GH146QF/5xUAS-CTP-FLPo-TEV^{cs}-CD4, 10xQUAS>TEV-CD4-stop>mCD-GFP*. (**B**) In the absence of TEV protease on the cell membrane, no post-synaptic neurons are labeled. Genotype: *pebbled-Gal4; GH146QF/5xUAS-CTP-FLPo-TEV^{cs}-CD4, 10xQUAS>Stop>mCD-GFP*. (**C**-**D**'') Using *pebbled-Gal4* and *nsyb-QF2* to label all candidate neurons post-synaptic to ORNs, lateral PNs and ventrolateral LNs are successfully labeled. Note that there is self-labeling (mCD8-GFP) for the pebbled+ neurons since both pre and post CLAMP components are simultaneously expressed on these neurons. Genotype: *pebbled-Gal4; 5xUAS-CTP-FLPo-TEV^{cs}-CD4,10xQUAS>TEV-CD4-stop>mCD-GFP; nsyb-QF2/UAS-IVS-mtdT,10xQUAS>Stop>TrpA1-2A-mCD8GFP*.

Figure 3.5

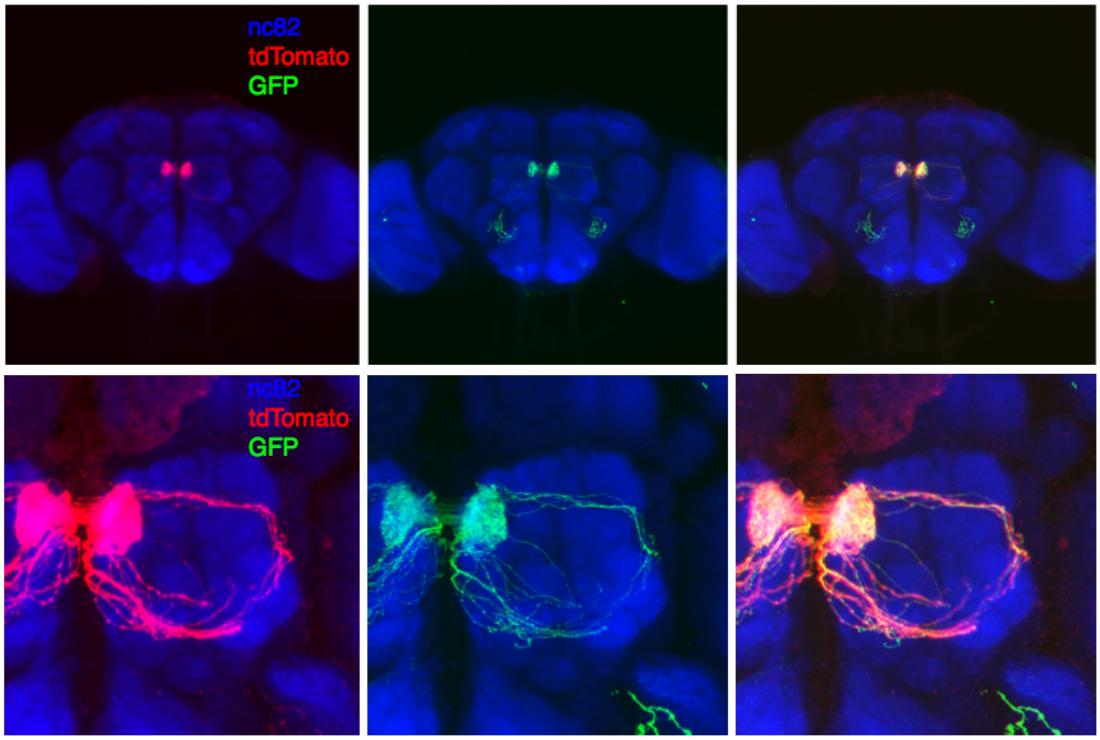

Or42a-Gal4/5xUAS-CTP-FLPo-CD4,10xQUAS>TEV-CD4-Stop>mCD-GFP(2-1M2)

Figure 3.5 In CLAMP I, single classes of labeled ORNs are not sufficient to CLAMP label cognate PNs. Using *Or42b-Gal4* to drive pre-synaptic CLAMP components and *nsyb-QF2* for post-synaptic CLAMP components, self-labeling of ORNs is observed but there was no post-synaptic PN or LN being labeled. Genotype: *Or42a-Gal4/5xUAS-CTP-FLPo-TEV^{cs}-CD4,10xQUAS>TEV-CD4-Stop>mCD-GFP; nsyb-QF2/UAS-IVS-mtdT, 10xQUAS>Stop>TrpA1-2A-mCD8GFP*.

Figure 3.6

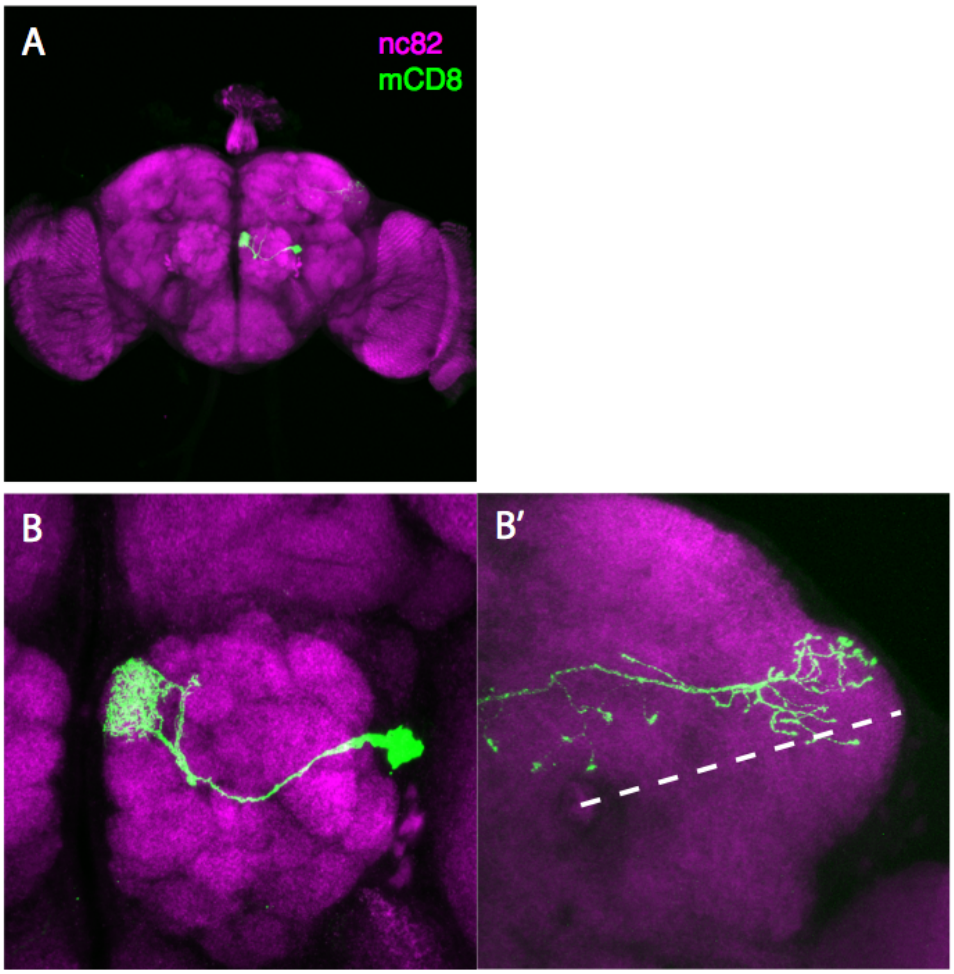

Or42a-Gal4, 20xUAS-CTP-FLPo-CD4,
GH146-QF2, 10xQUAS>TEV-PG-CD4-Stop>mCD-GFP

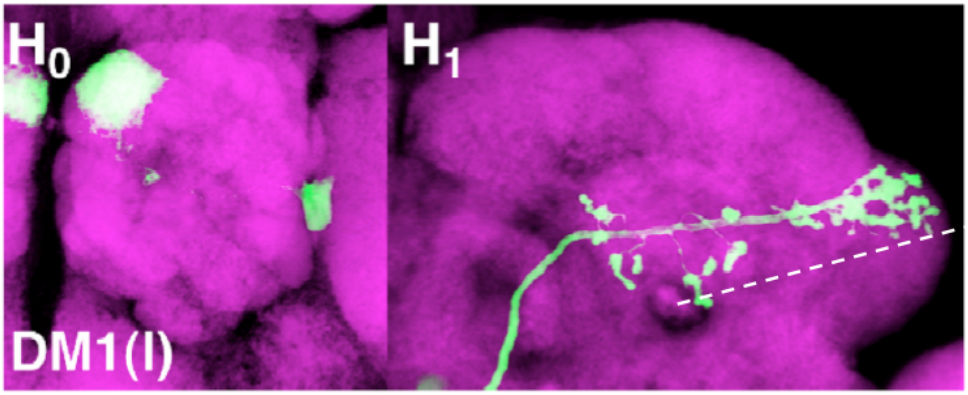

Jefferis and Potter et al, 2007 Cell

Figure 3.6 CLAMP II allows trans-synaptic labeling of cognate post-synaptic neurons starting with single classes of ORNs. (A and B) Increasing the expression level of pre-synaptic CLAMP components and adjusting linker size in post-synaptic fusion protein components allows CLAMP visualization of single ORN to cognate PNs (CLAMP II, see main text for details). Genotype: *Or42b-Gal4/10XQUAS>TEV-PG-CD4>CD8GFP; GH146-QF, 5xQUAS>Stop>CD8GFP/20xUAS-IVS-CTP-FLPo-TEV^{cs}-CD4*. The location of the DM1 PN cell body, dendritic and axonal arborizations of the CLAMP labeled Or42b ORN to DM1 PN is consistent with published MARCM data (Jefferis et al., 2007).

Figure 3.7

Genotype:
Or42b-Gal4/10XQUAS>TEV-PG-CD4>CD8GFP(M10M1); GH146-QF,QUAS>Stop>CD8GFP/20xUAS-CTP-FLP-CD4(2-5M1)

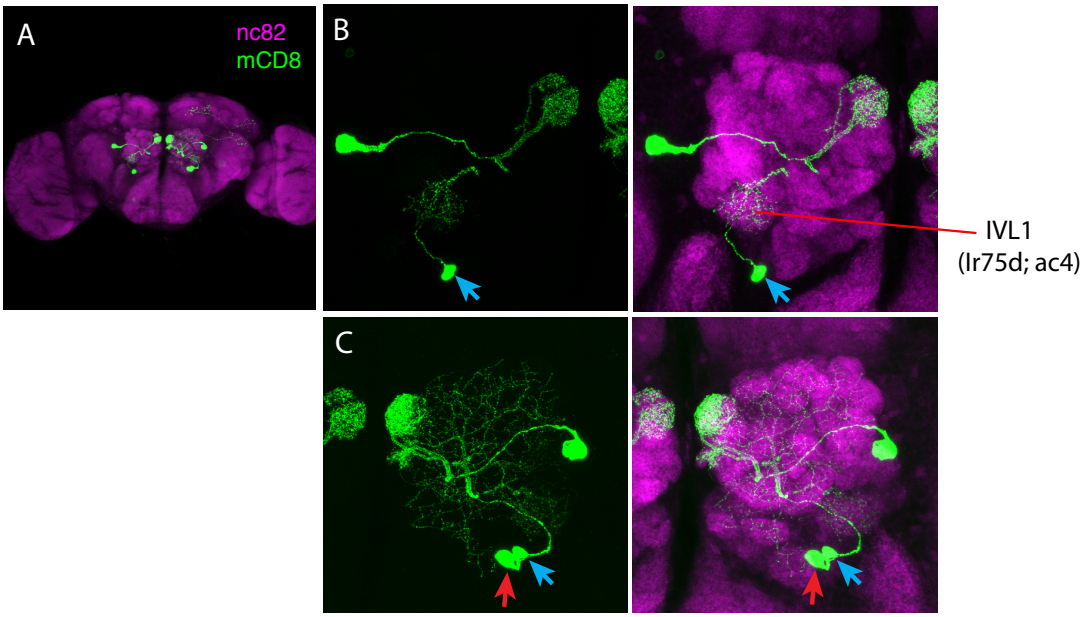

Figure 3.7 Non-specific labeling of CLAMP II

(**A** and **B**) Or42b ORN to DM1 PNs are specifically CLAMP labeled bilaterally. However, non-specific CLAMP labeling of Ir75d IVL1 PN is also observed on both sides of the brain (blue arrow). (**C**) A ventral PN that innervates multiple glomeruli is also often CLAMP labeled (red arrow) (genotype is the same as Figure 3.6).

Figure 3.8

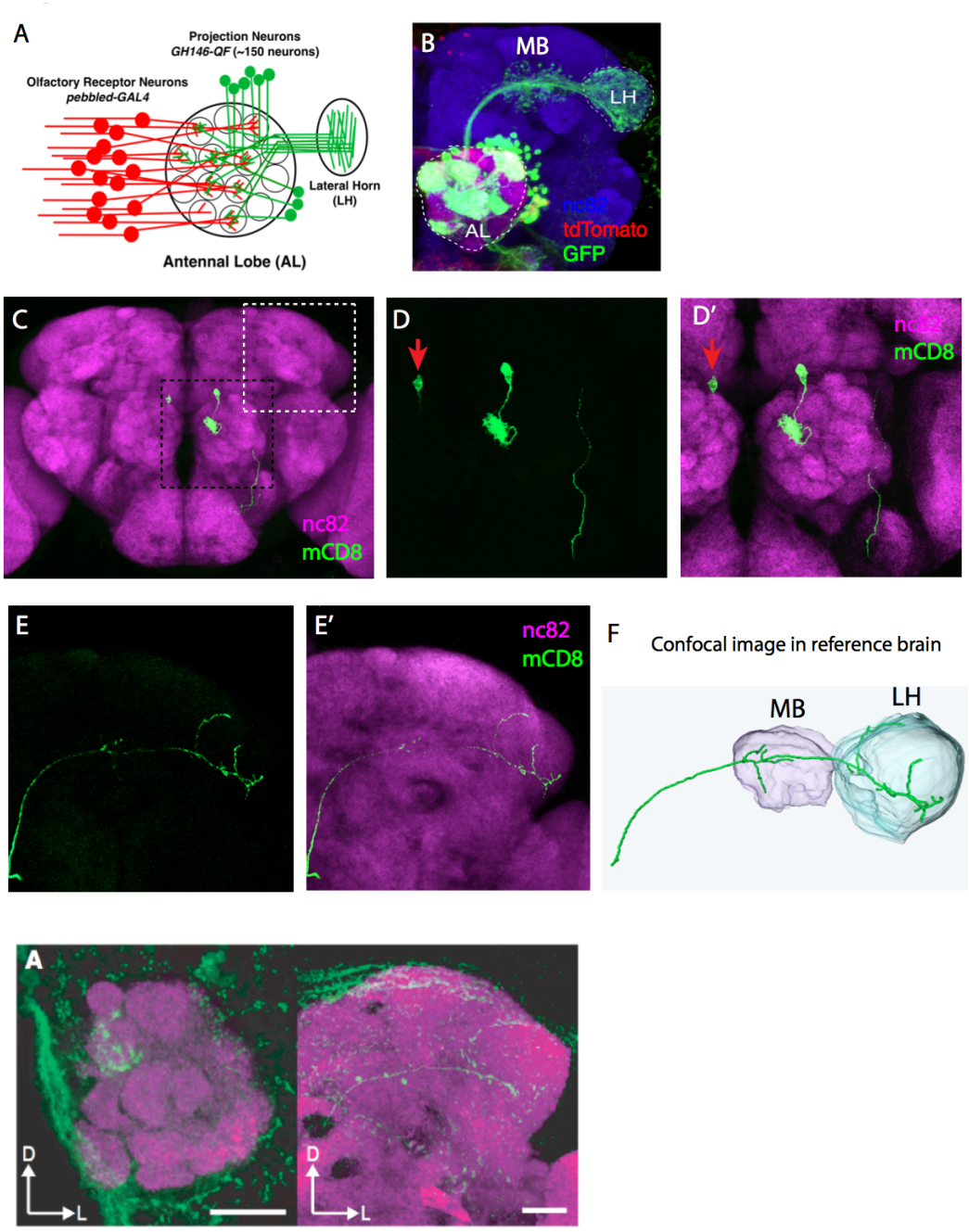

Stensmyr et al., 2012 Cell

Figure 3.8 Synapse-localized CLAMP III is more efficient and specific (**A**) Schematic of *pebbled-Gal4* as the CLAMP starter neuron population and GH146 expressing neurons as the CLAMP receiver population. (**B**) CLAMP III specifically labels PNs synaptically coupled with the ORNs, allowing visualization of the PN's dendrites in the AL and axonal projections to the MB and LH. Genotype: *pebbled-Gal4; 5xUAS-CTP-FLPo-TEV^{cs}-CD4-Neurexin; GH146-QF2/ 10xQUAS>TEV protease-TLCN-stop>mCD8GFP*. (**C**) By using *Or56a-Gal4* coupled with *GH146-QF2*, the DA2 PN in the left antennal lobe is CLAMP labeled. Genotype: *Or56a-Gal4/ 5xUAS-CTP-FLPo-TEV^{cs}-CD4-Neurexin; GH146-QF2/10xQUAS>TEV protease-TLCN-stop>mCD8GFP*. (**D**) Location of DA2 cell body is at dorsal AL (back dashed box in C). Interestingly, the corresponding DA2 PN in the right brain side (red arrow) seems to have begun to turn on mCD8-GFP expression in the cell body. (**E**) DA2 PN axonal projections form a cup shape region in the lateral horn (white dashed box in C), consistent with other repulsive channels, such as CO_2 (Gr21a) and acid (Ir64a). (**F**) The confocal image data is mapped into a reference brain to create a 3-D axonal projection to the MB and LH.

Figure 3.9

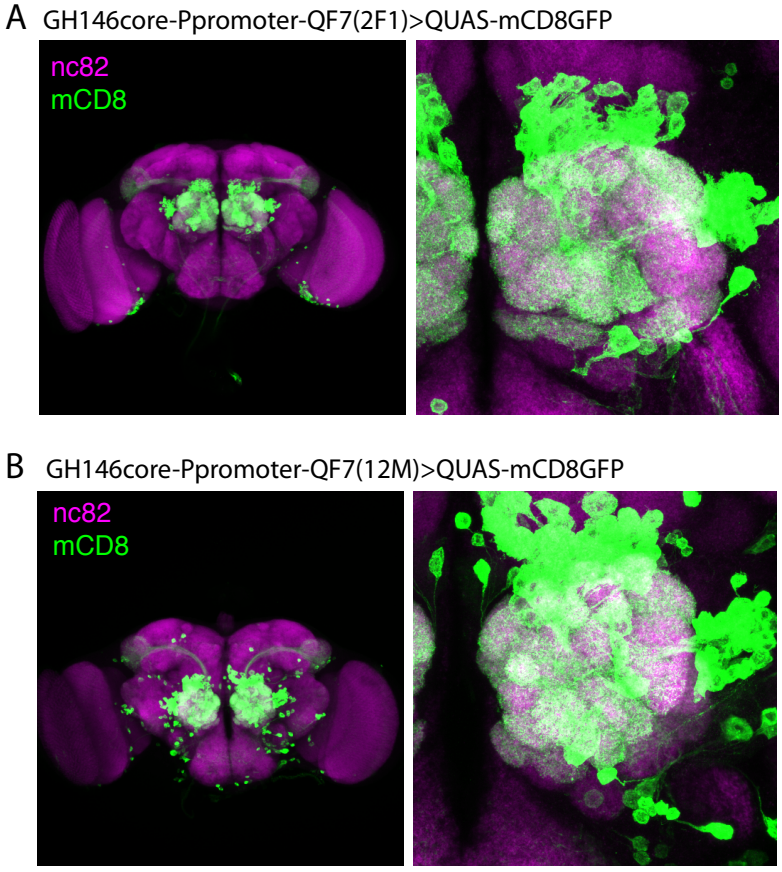
A GH146core-Ppromoter-QF7(2F1)>QUAS-mCD8GFP
nc82
mCD8
B GH146core-Ppromoter-QF7(12M)>QUAS-mCD8GFP
nc82
mCD8

Figure 3.9 Expression pattern analyses of two new *GH146-QF2* lines

(**A**) Line #2F1 specifically labels the PNs in the AL, although there is some neuronal labeling at the base of optic lobes. (**B**) In addition to strong PN labeling, line #12M demonstrates more non-specific labeling in the central part of the brain.

Figure 3.10

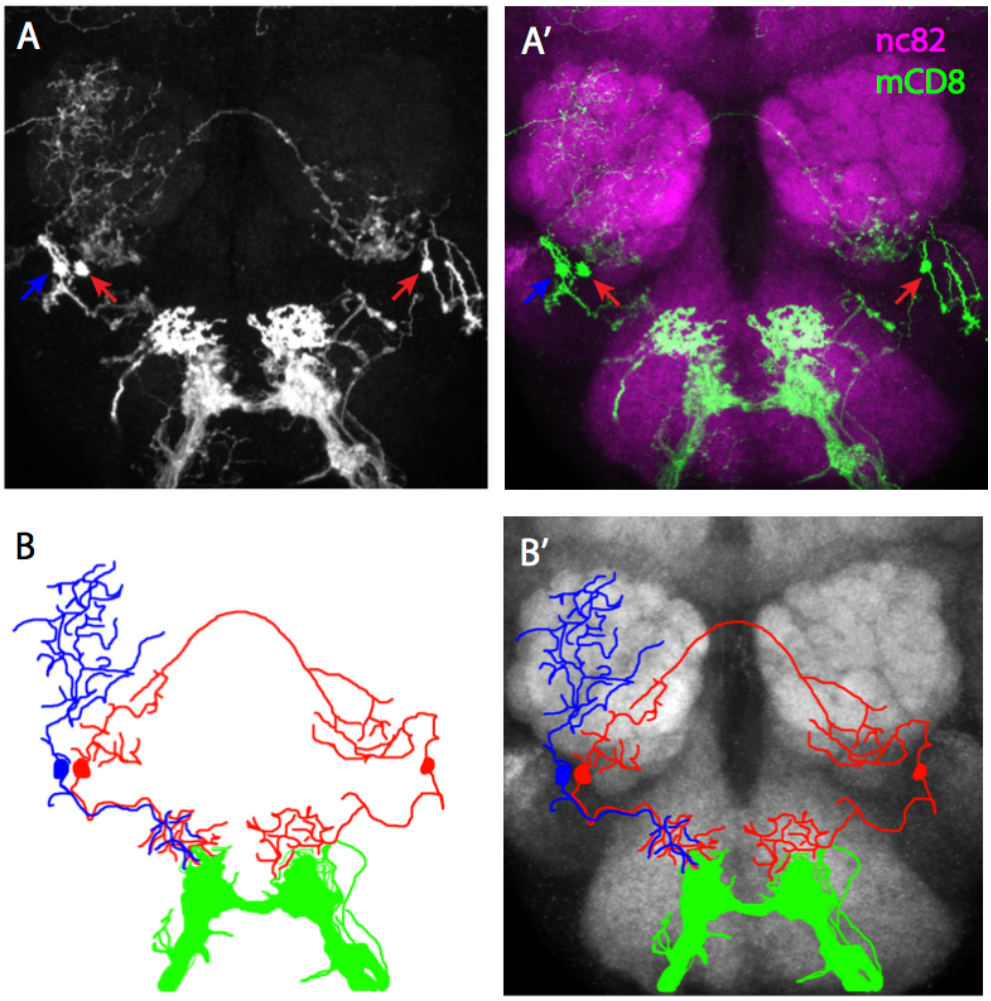

Figure 3.10 Identifying potential gustatory secondary neurons using CLAMP
(**A** and **A**') By using sweet-sensing gustatory sensory neurons as the CLAMP starter (*Gr5a-Gal4*) and pan-neuronal QF (*nsyb-QF*) as the CLAMP receiver line, two neurons located at the right ventral AL are identified (blue and red arrow). A corresponding neuron on the left side of the brain (red arrow) is identified as well. The two neurons (red arrow) send projections to the contralateral sides (through the anterior commissure). The other neuron (blue arrow) on the right side of the brain seems to innervate an ipsilateral AL. (**B** and **B'**) The cartoons of potential secondary gustatory neurons (green: Gr5a+ neuron; blue: ipsilateral secondary neuron; red: contralateral secondary neurons) Genotype: *20xUAS-CTP-FLPo-TEV^{cs}-CD4/10xQUAS>TEV protease-CD4-stop>mCD8GFP; Gr5a-Gal4/nsyb-QF2*.

Figure 3.11

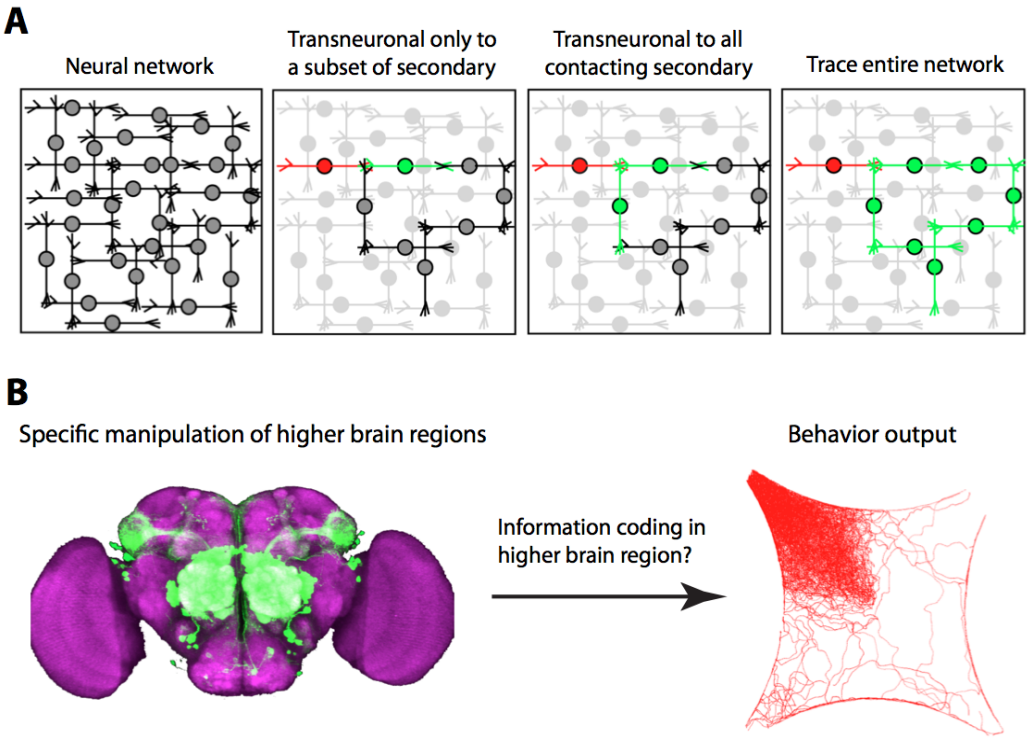
A
Neural network
Transneuronal only to a subset of secondary
Transneuronal to all contacting secondary
Trace entire network
B
Specific manipulation of higher brain regions
Behavior output
Information coding in higher brain region?

Figure 3.11 Summary of trans-synaptic labeling and decoding functional circuitry
(**A**) Schematic of CLAMP applications. By selecting specific or pan-neuronal QF lines to drive post-synaptic CLAMP components, a subset or all cognate post-synaptic neurons can be CLAMP labeled. Labeled neurons might be endowed with the ability to act as starter neurons and label the next order neuron. This will be useful to CLAMP label an entire neural circuit (see main text for details). (**B**) CLAMP can be used to target the manipulation of neuronal circuit activity with behavioral assays. This would enable deciphering the circuitry basis of a variety of behaviors, such as olfactory guided behaviors.

Chapter 4. General discussion

From Food Odors to Pheromones

The numerically simple fly brain provides an ideal model system to study the neural circuitry basis of animal behaviors. In addition, powerful genetic tools in flies allow for delineating the simple and complex behaviors, from basic molecules to electrophysiology, and on to neural circuits. We identified a novel behavior in which male flies actively deposit a pheromone in response to food odors. The pheromone, 9-tricosene, is able to enhance courtship and guide female egg laying decisions. With electrophysiology and bioinformatics, we found that the pheromone activates an evolutionarily divergent olfactory receptor, Or7a. Our study highlights several novel aspects of fly pheromone dection, behavior, and the evolution molecular mechanism that enhance species selection. First, we identify a new pheromone-signaling pathway in *Drosophila* in which pheromone deposition is triggered by an innate attraction behavior. This behavior connects aggregation behavior, complex courtship, and decision-making. This novel phenomenon expands our understanding of complex interactions among different behaviors and, therefore, innate attraction to food odors should no longer be viewed as a "simple" behavior. Rather, it affects or modulates complex behaviors through pheromone signaling. Second, our finding that a basiconic Or7a receptor serves as the main receptor for detecting 9-tricosene changes the concept that pheromones are only detected by ORNs housed in trichoid sensilla in *Drosophila*. This finding is important for future studies linking receptors to pheromone detection. Third, this is the first male

pheromone identified that guides female egg-laying decisions. Given the importance of proper egg-laying site selection, female flies employ complex decision-making processes to judge the best survival opportunities for their progeny. In our study, we find that males use pheromones to influence a decision that was previously considered female-specific. Lastly, our demonstration that Or7a DL5 projects to distinct regions in the lateral horn suggests that this area in fly's olfactory cortex is important for egg-laying decisions. Indeed, recently published ORs circuits important for egg laying (Or19a DC1 and Or71a VC2) are predicted to activate highly projection neurons highly similar to Or7a DL5. Understanding the pattern of axonal arborizations within the "egg-laying decision region," and characterization of the downstream neurons, will reveal how a complex decision is accomplished at the circuit level.

It is interesting that the Or7a receptor is also highly activated by a naturaly abundant chemical, trans-2-hexen-1-al, which is a major volatile released from wounded fruits and plants (Hatanaka and Harada, 1973). Trans-2-hexen-1-al and its precursor cis-3-hexenal are usually detected shortly (seconds to minutes) after tissue injury (Matsui et al., 2000). Since it is well established that *Drosophila* females prefer to lay eggs in rotting fruits, it is possible that trans-2-hexen-1-al could be a marker for fruit tissue damage. This chemical might then also guide egg-laying decisions in female flies by stimulating the same Or7a DL5 circuit as 9-tricosene. Although the Or7a activation pattern is similar for both chemicals, the volatilities of 9-tricosene and trans-2-hexen-1-al are very different: 9-tricosene has very low volatility (vapor pressure=0.000035 mmHg) whereas trans-2-hexen-1-al has very

high volatility (vapor pressure=4.6 mmHg). Thus, 9-tricosene functions as a short-range and long-lasting cue for modulating courtship and oviposition behaviors, whereas trans-2-hexen-1-al could be a long-distance chemical for guiding attraction and oviposition behavior.

We describe here an important process that links odor perception to pheromone signaling and subsequent effects on decision making. However, several questions remain to be solved. For example, how and what olfactory receptor(s) are responsible for generating this pheromone deposition phenotype? Is there a synergistic effect between different olfactory receptor activities? Is there a specific region in the central brain that leads to pheromone deposition? With optogenetic and thermogenetic tools, we will be able to artificially and specifically activate certain odor channels and untangle how these phenotypes are generated. This will facilitate our understanding of an interesting model information integration process. By identifying the olfactory receptors involved in the process, we will be able to decipher how this decision is be interpreted by circuits at higher brain levels.

One of the most challenging and intriguing questions in modern neuroscience is understanding how brains interpret and interact with the environment. Our study provides an example of how complex environment stimuli, pheromone signaling and subsequent behaviors are crtical for species survival. This may serve as a general principle to understand animal behaviors at the circuit level.

Renowned animal behavior biologist Konrad Lorenz said, "… our fellow creatures can tell us the most beautiful stories, and that means true stories, because the truth of nature is always far more beautiful even than what our great poets sing

of it, and they are the only real magicians that exist (Lorenz, 1952)." It is fortunate that we not only we have been able to observe such striking phenotypes but also peek into the deepest molecular and circuit level organization that underlies animal behavior.

Genetically-encoded trans-neuronal labeling

Extensive efforts have been, and are being, devoted to unraveling the ensemble of neural connections in the brain. This is clearly important for understanding how the nervous system works coherently to generate higher brain functions, such as behavior and even cognition. In the second part of my thesis, I developed CLAMP (Cell Labeling Across Membrane Partners), a genetic labeling system that can be used as a general tracer to map out an entire wiring diagram from a defined peripheral starter neuron in an unbiased manner. The idea of CLAMP is based on releasing a cell permeable recombinase at the synaptic cleft in order for it to be transsynaptically transferred into next order neuron where a stop cassette is cleaved out in a reporter transgene. Once the stop cassette is removed, the binary system in the downstream neurons takes over and no longer relies on the trans-synaptic event. Though I have demsontrated that CLAMP successfully fulfilles this function, further development of this approach will greatly increase its efficacy. The modular design of CLAMP requires further optimizations to reach higher efficiency and specificity. To address this issue, we might be able to achieve higher efficiency by increasing the amount of FLP released at synaptic clefts (by making stronger driver (20xUAS), or by providing multiple copies of X-Gal4 and pre-CLAMP). To

increase specificity, we can limit the expression of pre-CLAMP and post-CLAMP at controlled developmental stages by incorporating *tub-Gal80ts* and *tub-QS*, respectively. *Tub-Gal80ts* is expressed ubiquitously and inhibits Gal4 at low temperature (18°C) but not high temperature (29°C). QS binds to and inhibits QF but the inhibition is turned off by quinic acid, which is able to inhibit QS. Thus, by controlling ambient temperature and the supply of quinic acid in the food, we should be able to limit the expression of CLAMP system and thereby increase specificity. It is noteworthy that CLAMP is not merely limited to GFP-labeling the post-synaptic neurons. The expression of effecter genes in downstream neurons depends on removing the stop cassette by the recombinase. There are ample powerful effecters to study functional circuitry, for instance, pro-apoptotic genes (*hid*, *reaper* to induce apoptosis), thermogenetic genes (dTrpA1, TrpM8, to activate neurons at high (29°C) and low (18°C) temperatures, respectively) and optogenetic genes (Cs-Chrimson, to activate neurons with red light (627 nm)). This expands trans-synaptic "labeling" to trans-synaptic "manipulation". By incorporation of a 2A peptide into the constructs, we will be able to co-express multiple proteins under the control of one stop cassette. For instance, by utilizing *QUAS>TEV-TLCN>mCD8GFP-2A-dTrpA1*, we would be able to simultaneously label and activate the downstream neurons with high temperature. This application would be ideal for establishing the link between neural circuitry and behavioral responses. Lastly, in *Drosophila* CLAMP, FLP recombinase was chosen because many existing genetic tools are based on the FLP/FRT system and Cre recombinase can be toxic in flies. However, since both Cre and FLP belong to recombinase families and utilize similar

recombinaitoin mechanisms (Turan et al., 2011), the CLAMP system could be transferred into mammalian systems with Cre recombinase in the future.

The concept of CLAMP is based on the stereotypic structure of the nervous system synapse. Although we used CLAMP to successfully map olfactory and gustatory circuits, CLAMP should be equally applicable in other systems, such as visual and dopaminergic circuits. Furthermore, given the evolutionarily conserved structure of the synapse, the machinery of cell-penetrable recombinase in CLAMP should function in other model systems as well.

Synaptic pruning is important to establish proper connectivity in the nervous system. During development, synapse elimination occurs in the early childhood and before puberty in many mammals (Chechik et al., 1998), and impaired pruning process can result in major neurological diseases, such as autism and schizophrenia (Tang et al., 2014). Since CLAMP is able to label synaptically coupled neurons reliably, CALMP is potentially useful in marking post-synaptic neurons at certain developmental stages (by incorporation of *Tub-Gal80ts* to turn on the transgene at certain time points). Thus, we might be able to ask many interesting questions, such as where do certain molecularly defined neurons for synapses at particular time points? Moreover, in disease states that include impaired pruning, CLAMP might be useful for characterizing altered connectivity by identifying and quantifying aberrantly coupled neurons.

Nearly a century ago, Ramón y Cajal used the Golgi method to reveal the beauty of neuroscience with a detailed and precise analysis of the nervous system. He emphasized the importance of being a “master of technique” by stating that

"…great discoveries are in the hands of the finest and most knowledgeable experts on one or more of the analytical methods (Cajal, 1999)". With that in mind, I hope CLAMP will prove to be a useful and influential technique for scientists aiming to understand how circuits in a brain function together to accomplish incredible feats.

References:

Abuin, L., Bargeton, B., Ulbrich, M.H., Isacoff, E.Y., Kellenberger, S., and Benton, R. (2011). Functional architecture of olfactory ionotropic glutamate receptors. Neuron *69*, 44-60.

Ai, M., Min, S., Grosjean, Y., Leblanc, C., Bell, R., Benton, R., and Suh, G.S. (2010). Acid sensing by the Drosophila olfactory system. Nature *468*, 691-695.

Alekseyenko, O.V., Chan, Y.B., Li, R., and Kravitz, E.A. (2013). Single dopaminergic neurons that modulate aggression in Drosophila. Proceedings of the National Academy of Sciences of the United States of America *110*, 6151-6156.

Allee, W.C. (1931). Animal aggregations, a study in general society. Chiago University Press.

Amrein, H. (2004). Pheromone perception and behavior in Drosophila. Current Opinion in Neurobiology *14*, 435-442.

Awasaki, T., and Kimura, K. (2001). Multiple function of poxn gene in larval PNS development and in adult appendage formation of Drosophila. Development genes and evolution *211*, 20-29.

Azanchi, R., Kaun, K.R., and Heberlein, U. (2013). Competing dopamine neurons drive oviposition choice for ethanol in Drosophila. Proceedings of the National Academy of Sciences of the United States of America *110*, 21153-21158.

Baena-Lopez, L.A., Alexandre, C., Mitchell, A., Pasakarnis, L., and Vincent, J.P. (2013). Accelerated homologous recombination and subsequent genome modification in Drosophila. Development *140*, 4818-4825.

Balice-Gordon, R.J., Chua, C.K., Nelson, V.C., and Lichtman, J.W. (1993). Gradual loss of synaptic cartels precedes axon withdrawal at developing neuromuscular junctions. Neuron *11*, 801-815.

Barnea, G., Strapps, W., Herrada, G., Berman, Y., Ong, J., Kloss, B., Axel, R., and Lee, K.J. (2008). The genetic design of signaling cascades to record receptor activation. Proceedings of the National Academy of Sciences of the United States of America *105*, 64-69.

Bartelt, R.J., Schaner, A.M., and Jackson, L.L. (1985). cis-Vaccenyl acetate as an aggregation pheromone inDrosophila melanogaster. Journal of chemical ecology *11*, 1747-1756.

Beerens, A.M., Al Hadithy, A.F., Rots, M.G., and Haisma, H.J. (2003). Protein transduction domains and their utility in gene therapy. Current gene therapy *3*, 486-494.

Benton, R., Vannice, K.S., Gomez-Diaz, C., and Vosshall, L.B. (2009). Variant ionotropic glutamate receptors as chemosensory receptors in Drosophila. Cell *136*, 149-162.

Benton, R., Vannice, K.S., and Vosshall, L.B. (2007). An essential role for a CD36-related receptor in pheromone detection in Drosophila. Nature *450*, 289-293.

Billeter, J.C., Atallah, J., Krupp, J.J., Millar, J.G., and Levine, J.D. (2009). Specialized cells tag sexual and species identity in Drosophila melanogaster. Nature *461*, 987-991.

Brand, A.H., and Perrimon, N. (1993). Targeted gene expression as a means of altering cell fates and generating dominant phenotypes. Development *118*, 401-415.

Bray, S., and Amrein, H. (2003). A putative Drosophila pheromone receptor expressed in male-specific taste neurons is required for efficient courtship. Neuron *39*, 1019-1029.

Brieger, G., and Butterworth, F.M. (1970). Drosophila melanogaster: identity of male lipid in reproductive system. Science *167*, 1262.

Buchholz, F., Angrand, P.O., and Stewart, A.F. (1998). Improved properties of FLP recombinase evolved by cycling mutagenesis. Nature biotechnology *16*, 657-662.

Buck, L., and Axel, R. (1991). A novel multigene family may encode odorant receptors: a molecular basis for odor recognition. Cell *65*, 175-187.

Budick, S.A., and Dickinson, M.H. (2006). Free-flight responses of Drosophila melanogaster to attractive odors. The Journal of experimental biology *209*, 3001-3017.

Butterworth, F.M. (1969). Lipids of Drosophila: a newly detected lipid in the male. Science *163*, 1356-1357.

Cajal, S.R.y. (1999). Advice for a young investigator. MIT press.

Callaway, E.M. (2008). Transneuronal circuit tracing with neurotropic viruses. Curr Opin Neurobiol *18*, 617-623.

Carlson, D.A., Mayer, M.S., Silhacek, D.L., James, J.D., Beroza, M., and Bierl, B.A. (1971). Sex attractant pheromone of the house fly: isolation, identification and synthesis. Science *174*, 76-78.

Chechik, G., Meilijson, I., and Ruppin, E. (1998). Synaptic pruning in development: a computational account. Neural computation *10*, 1759-1777.

Chou, Y.H., Spletter, M.L., Yaksi, E., Leong, J.C., Wilson, R.I., and Luo, L. (2010). Diversity and wiring variability of olfactory local interneurons in the Drosophila antennal lobe. Nature neuroscience *13*, 439-449.

Clyne, P.J., Warr, C.G., Freeman, M.R., Lessing, D., Kim, J., and Carlson, J.R. (1999). A novel family of divergent seven-transmembrane proteins: candidate odorant receptors in Drosophila. Neuron *22*, 327-338.

Courchamp, F., Clutton-Brock, T., and Grenfell, B. (1999). Inverse density dependence and the Allee effect. Trends in ecology & evolution *14*, 405-410.

Couto, A., Alenius, M., and Dickson, B.J. (2005). Molecular, anatomical, and functional organization of the Drosophila olfactory system. Current biology : CB *15*, 1535-1547.

Datta, S.R., Vasconcelos, M.L., Ruta, V., Luo, S., Wong, A., Demir, E., Flores, J., Balonze, K., Dickson, B.J., and Axel, R. (2008). The Drosophila pheromone cVA activates a sexually dimorphic neural circuit. Nature *452*, 473-477.

Davis, R.L. (2005). Olfactory memory formation in Drosophila: from molecular to systems neuroscience. Annual review of neuroscience *28*, 275-302.

de Belle, J.S., and Heisenberg, M. (1994). Associative odor learning in Drosophila abolished by chemical ablation of mushroom bodies. Science *263*, 692-695.

de Bruyne, M., Clyne, P.J., and Carlson, J.R. (1999). Odor coding in a model olfactory organ: the Drosophila maxillary palp. The Journal of neuroscience : the official journal of the Society for Neuroscience *19*, 4520-4532.

de Bruyne, M., Foster, K., and Carlson, J.R. (2001). Odor coding in the Drosophila antenna. Neuron *30*, 537-552.

Dickerson, R. (1971). The structure of cytochrome c and the rates of molecular evolution. Journal of Molecular Evolution 26-45.

Dobritsa, A.A., van der Goes van Naters, W., Warr, C.G., Steinbrecht, R.A., and Carlson, J.R. (2003). Integrating the molecular and cellular basis of odor coding in the Drosophila antenna. Neuron *37*, 827-841.

Dweck, H.K., Ebrahim, S.A., Kromann, S., Bown, D., Hillbur, Y., Sachse, S., Hansson, B.S., and Stensmyr, M.C. (2013). Olfactory preference for egg laying on citrus substrates in Drosophila. Current biology : CB *23*, 2472-2480.

Ejima, A., Smith, B.P., Lucas, C., van der Goes van Naters, W., Miller, C.J., Carlson, J.R., Levine, J.D., and Griffith, L.C. (2007). Generalization of courtship learning in Drosophila is mediated by cis-vaccenyl acetate. Current biology : CB *17*, 599-605.

Everaerts, C., Farine, J.P., Cobb, M., and Ferveur, J.F. (2010). Drosophila cuticular hydrocarbons revisited: mating status alters cuticular profiles. PloS one *5*, e9607.

Farine, J.P., Ferveur, J.F., and Everaerts, C. (2012). Volatile Drosophila cuticular pheromones are affected by social but not sexual experience. PloS one *7*, e40396.

Feinberg, E.H., Vanhoven, M.K., Bendesky, A., Wang, G., Fetter, R.D., Shen, K., and Bargmann, C.I. (2008). GFP Reconstitution Across Synaptic Partners (GRASP) defines cell contacts and synapses in living nervous systems. Neuron *57*, 353-363.

Ferveur, J.F. (1997). The pheromonal role of cuticular hydrocarbons in Drosophila melanogaster. BioEssays : news and reviews in molecular, cellular and developmental biology *19*, 353-358.

Ferveur, J.F. (2005). Cuticular hydrocarbons: their evolution and roles in Drosophila pheromonal communication. Behavior genetics *35*, 279-295.

Ferveur, J.F., Savarit, F., O'Kane, C.J., Sureau, G., Greenspan, R.J., and Jallon, J.M. (1997). Genetic feminization of pheromones and its behavioral consequences in Drosophila males. Science *276*, 1555-1558.

Ferveur, J.F., and Sureau, G. (1996). Simultaneous influence on male courtship of stimulatory and inhibitory pheromones produced by live sex-mosaic Drosophila melanogaster. Proceedings Biological sciences / The Royal Society *263*, 967-973.

Fischer, J.A., Giniger, E., Maniatis, T., and Ptashne, M. (1988). GAL4 activates transcription in Drosophila. Nature *332*, 853-856.

Fishilevich, E., and Vosshall, L.B. (2005). Genetic and functional subdivision of the Drosophila antennal lobe. Current biology : CB *15*, 1548-1553.

Fitzgerald, T.D., and Edgerly, J.S. (1982). Site of secretion of the trail marker of the eastern tent caterpillar. Journal of chemical ecology *8*, 31-39.

Frankel, A.D., and Pabo, C.O. (1988). Cellular uptake of the tat protein from human immunodeficiency virus. Cell *55*, 1189-1193.

Gao, Q., and Chess, A. (1999). Identification of candidate Drosophila olfactory receptors from genomic DNA sequence. Genomics *60*, 31-39.

Garner, J.A., and LaVail, J.H. (1999). Differential anterograde transport of HSV type 1 viral strains in the murine optic pathway. Journal of neurovirology *5*, 140-150.

Geer, B.W., Heinstra, P.W., and McKechnie, S.W. (1993). The biological basis of ethanol tolerance in Drosophila. Comparative biochemistry and physiology B, Comparative biochemistry *105*, 203-229.

Glover, D.J., Lipps, H.J., and Jans, D.A. (2005). Towards safe, non-viral therapeutic gene expression in humans. Nature reviews Genetics *6*, 299-310.

Goldman, A.L., Van der Goes van Naters, W., Lessing, D., Warr, C.G., and Carlson, J.R. (2005). Coexpression of two functional odor receptors in one neuron. Neuron *45*, 661-666.

Gomez-Diaz, C., Reina, J.H., Cambillau, C., and Benton, R. (2013). Ligands for pheromone-sensing neurons are not conformationally activated odorant binding proteins. PLoS Biol *11*, e1001546.

Gordon, M.D., and Scott, K. (2009). Motor control in a Drosophila taste circuit. Neuron *61*, 373-384.

Green, M., and Loewenstein, P.M. (1988). Autonomous functional domains of chemically synthesized human immunodeficiency virus tat trans-activator protein. Cell *55*, 1179-1188.

Grosjean, Y., Rytz, R., Farine, J.P., Abuin, L., Cortot, J., Jefferis, G.S., and Benton, R. (2011). An olfactory receptor for food-derived odours promotes male courtship in Drosophila. Nature *478*, 236-240.

Guo, S., and Kim, J. (2007). Molecular evolution of Drosophila odorant receptor genes. Molecular biology and evolution *24*, 1198-1207.

Ha, T.S., and Smith, D.P. (2006). A pheromone receptor mediates 11-cis-vaccenyl acetate-induced responses in Drosophila. The Journal of neuroscience : the official journal of the Society for Neuroscience *26*, 8727-8733.

Hadjieconomou, D., Rotkopf, S., Alexandre, C., Bell, D.M., Dickson, B.J., and Salecker, I. (2011). Flybow: genetic multicolor cell labeling for neural circuit analysis in Drosophila melanogaster. Nature methods *8*, 260-266.

Hallem, E.A., and Carlson, J.R. (2006). Coding of odors by a receptor repertoire. Cell *125*, 143-160.

Hampel, S., Chung, P., McKellar, C.E., Hall, D., Looger, L.L., and Simpson, J.H. (2011). Drosophila Brainbow: a recombinase-based fluorescence labeling technique to subdivide neural expression patterns. Nature methods *8*, 253-259.

Harada, E., Haba, D., Aigaki, T., and Matsuo, T. (2008). Behavioral analyses of mutants for two odorant-binding protein genes, Obp57d and Obp57e, in Drosophila melanogaster. Genes & genetic systems *83*, 257-264.

Hatanaka, A., and Harada, T. (1973). Formation of cis-3-hexenal, trans-2-

hexenal and cis-3-hexenol in macerated Thea sinensis leaves. . Phytochemistry *12*, 2341-2346.

Hedlund, K., Bartelt, R.J., Dicke, M., and Vet, L.E. (1996). Aggregation pheromones ofDrosophila immigrans, D. phalerata, andD. subobscura. Journal of chemical ecology *22*, 1835-1844.

Herndon, L.A., and Wolfner, M.F. (1995). A Drosophila seminal fluid protein, Acp26Aa, stimulates egg laying in females for 1 day after mating. Proceedings of the National Academy of Sciences of the United States of America *92*, 10114-10118.

Holldobler, B., and Wilson, E.O. (1978). The multiple recruitment systems of the African weaver ant Oecophylla longinoda (Latreille) (Hymenoptera: Formicidae). Behavioral Ecology and Sociobiology *3*, 19-60.

Hoover, K., Keena, M., Nehme, M., Wang, S., Meng, P., and Zhang, A. (2014). Sex-specific trail pheromone mediates complex mate finding behavior in Anoplophora glabripennis. Journal of chemical ecology *40*, 169-180.

Inagaki, H.K., Ben-Tabou de-Leon, S., Wong, A.M., Jagadish, S., Ishimoto, H., Barnea, G., Kitamoto, T., Axel, R., and Anderson, D.J. (2012). Visualizing neuromodulation in vivo: TANGO-mapping of dopamine signaling reveals appetite control of sugar sensing. Cell *148*, 583-595.

Jaenike, J. (1990). Host specialization by phytofagous insects. Annual Review of Ecology and Systematic, 243-273.

Jagadish, S., Barnea, G., Clandinin, T.R., and Axel, R. (2014). Identifying functional connections of the inner photoreceptors in Drosophila using Tango-Trace. Neuron *83*, 630-644.

Jefferis, G.S., Potter, C.J., Chan, A.M., Marin, E.C., Rohlfing, T., Maurer, C.R., Jr., and Luo, L. (2007). Comprehensive maps of Drosophila higher olfactory centers: spatially segregated fruit and pheromone representation. Cell *128*, 1187-1203.

Jones, W.D., Cayirlioglu, P., Kadow, I.G., and Vosshall, L.B. (2007). Two chemosensory receptors together mediate carbon dioxide detection in Drosophila. Nature *445*, 86-90.

Joseph, R.M., Devineni, A.V., King, I.F., and Heberlein, U. (2009). Oviposition preference for and positional avoidance of acetic acid provide a model for competing behavioral drives in Drosophila. Proceedings of the National Academy of Sciences of the United States of America *106*, 11352-11357.

Karlson, P., and Luscher, M. (1959). Pheromones': a new term for a class of biologically active substances. Nature *183*, 55-56.

Katsov, A.Y., and Clandinin, T.R. (2008). Motion processing streams in Drosophila are behaviorally specialized. Neuron *59*, 322-335

Katz, L.C., and Iarovici, D.M. (1990). Green fluorescent latex microspheres: a new retrograde tracer. Neuroscience *34*, 511-520.

Kido, A., and Ito, K. (2002). Mushroom bodies are not required for courtship behavior by normal and sexually mosaic Drosophila. Journal of neurobiology *52*, 302-311.

Kim, J., Zhao, T., Petralia, R.S., Yu, Y., Peng, H., Myers, E., and Magee, J.C. (2012). mGRASP enables mapping mammalian synaptic connectivity with light microscopy. Nature methods *9*, 96-102.

Kiyokawa, Y., Kikusui, T., Takeuchi, Y., and Mori, Y. (2004). Alarm pheromones with different functions are released from different regions of the body surface of male rats. Chemical senses *29*, 35-40.

Kohl, J., Ostrovsky, A.D., Frechter, S., and Jefferis, G.S. (2013). A bidirectional circuit switch reroutes pheromone signals in male and female brains. Cell *155*, 1610-1623.

Kurtovic, A., Widmer, A., and Dickson, B.J. (2007). A single class of olfactory neurons mediates behavioural responses to a Drosophila sex pheromone. Nature *446*, 542-546.

Kwon, J.Y., Dahanukar, A., Weiss, L.A., and Carlson, J.R. (2007). The molecular basis of CO2 reception in Drosophila. Proceedings of the National Academy of Sciences of the United States of America *104*, 3574-3578.

Kwon, Y., Kim, S.H., Ronderos, D.S., Lee, Y., Akitake, B., Woodward, O.M., Guggino, W.B., Smith, D.P., and Montell, C. (2010). Drosophila TRPA1 channel is required to avoid the naturally occurring insect repellent citronellal. Current biology : CB *20*, 1672-1678.

Lai, S.L., and Lee, T. (2006). Genetic mosaic with dual binary transcriptional systems in Drosophila. Nature neuroscience *9*, 703-709.

Laissue, P.P., and Vosshall, L.B. (2008). The olfactory sensory map in Drosophila. Advances in experimental medicine and biology *628*, 102-114.

Larsson, M.C., Domingos, A.I., Jones, W.D., Chiappe, M.E., Amrein, H., and Vosshall, L.B. (2004). Or83b encodes a broadly expressed odorant receptor essential for Drosophila olfaction. Neuron *43*, 703-714.

Laughlin, J.D., Ha, T.S., Jones, D.N., and Smith, D.P. (2008). Activation of pheromone-sensitive neurons is mediated by conformational activation of pheromone-binding protein. Cell *133*, 1255-1265.

Lee, T., and Luo, L. (1999). Mosaic analysis with a repressible cell marker for studies of gene function in neuronal morphogenesis. Neuron *22*, 451-461.

Livet, J., Weissman, T.A., Kang, H., Draft, R.W., Lu, J., Bennis, R.A., Sanes, J.R., and Lichtman, J.W. (2007). Transgenic strategies for combinatorial expression of fluorescent proteins in the nervous system. Nature *450*, 56-62.

Lorenz, K.Z. (1952). King Solomon's Ring. Harper & Row Publishers, Inc.

Lu, B., LaMora, A., Sun, Y., Welsh, M.J., and Ben-Shahar, Y. (2012). ppk23-Dependent chemosensory functions contribute to courtship behavior in Drosophila melanogaster. PLoS genetics *8*, e1002587.

Lundstrom, J.N., Gordon, A.R., Alden, E.C., Boesveldt, S., and Albrecht, J. (2010). Methods for building an inexpensive computer-controlled olfactometer for temporally-precise experiments. International journal of psychophysiology : official journal of the International Organization of Psychophysiology *78*, 179-189.

Marella, S., Fischler, W., Kong, P., Asgarian, S., Rueckert, E., and Scott, K. (2006). Imaging taste responses in the fly brain reveals a functional map of taste category and behavior. Neuron *49*, 285-295.

Marin, E.C., Jefferis, G.S., Komiyama, T., Zhu, H., and Luo, L. (2002). Representation of the glomerular olfactory map in the Drosophila brain. Cell *109*, 243-255.

Matsui, K., Kurishita, S., Hisamitsu, A., and Kajiwara, T. (2000). A lipid-hydrolysing activity involved in hexenal formation. Biochemical Society transactions *28*, 857-860.

Melcher, C., and Pankratz, M.J. (2005). Candidate gustatory interneurons modulating feeding behavior in the Drosophila brain. PLoS Biol *3*, e305.

Milan, N.F., Kacsoh, B.Z., and Schlenke, T.A. (2012). Alcohol consumption as self-medication against blood-borne parasites in the fruit fly. Current biology : CB *22*, 488-493.

Monsma, S.A., Harada, H.A., and Wolfner, M.F. (1990). Synthesis of two Drosophila male accessory gland proteins and their fate after transfer to the female during mating. Developmental biology *142*, 465-475.

Pauli, A., Althoff, F., Oliveira, R.A., Heidmann, S., Schuldiner, O., Lehner, C.F., Dickson, B.J., and Nasmyth, K. (2008). Cell-type-specific TEV protease cleavage reveals cohesin functions in Drosophila neurons. Developmental cell *14*, 239-251.

Pfeiffer, B.D., Ngo, T.T., Hibbard, K.L., Murphy, C., Jenett, A., Truman, J.W., and Rubin, G.M. (2010). Refinement of tools for targeted gene expression in Drosophila. Genetics *186*, 735-755.

Pool, A.H., Kvello, P., Mann, K., Cheung, S.K., Gordon, M.D., Wang, L., and Scott, K. (2014). Four GABAergic interneurons impose feeding restraint in Drosophila. Neuron *83*, 164-177.

Potter, C.J., Tasic, B., Russler, E.V., Liang, L., and Luo, L. (2010). The Q system: a repressible binary system for transgene expression, lineage tracing, and mosaic analysis. Cell *141*, 536-548.

Quinn, W.G., Harris, W.A., and Benzer, S. (1974). Conditioned behavior in Drosophila melanogaster. Proceedings of the National Academy of Sciences of the United States of America *71*, 708-712.

R'Kha, S., Capy, P., and David, J.R. (1991). Host-plant specialization in the Drosophila melanogaster species complex: a physiological, behavioral, and genetical analysis. Proceedings of the National Academy of Sciences of the United States of America *88*, 1835-1839.

Ramdya, P., and Benton, R. (2010). Evolving olfactory systems on the fly. Trends in genetics : TIG *26*, 307-316.

Raymond, C.S., and Soriano, P. (2007). High-efficiency FLP and PhiC31 site-specific recombination in mammalian cells. PloS one *2*, e162.

Reiner, A., Veenman, C.L., Medina, L., Jiao, Y., Del Mar, N., and Honig, M.G. (2000). Pathway tracing using biotinylated dextran amines. Journal of neuroscience *103*, 23-37.

Riabinina, O., Luginbuhl, D., Marr, E., Liu, S., Wu, M.N., Luo, L., and Potter, C.J. (2015). Improved and expanded Q-system reagents for genetic manipulations. Nature methods.

Ronderos, D.S., Lin, C.C., Potter, C.J., and Smith, D.P. (2014). Farnesol-detecting olfactory neurons in Drosophila. The Journal of neuroscience : the official journal of the Society for Neuroscience *34*, 3959-3968.

Russo, C.A., Takezaki, N., and Nei, M. (1995). Molecular phylogeny and divergence times of drosophilid species. Molecular biology and evolution *12*, 391-404.

Ruta, V., Datta, S.R., Vasconcelos, M.L., Freeland, J., Looger, L.L., and Axel, R. (2010). A dimorphic pheromone circuit in Drosophila from sensory input to descending output. Nature *468*, 686-690.

Schaft, J., Ashery-Padan, R., van der Hoeven, F., Gruss, P., and Stewart, A.F. (2001). Efficient FLP recombination in mouse ES cells and oocytes. Genesis *31*, 6-10.

Schorkopf, D.L., Jarau, S., Francke, W., Twele, R., Zucchi, R., Hrncir, M., Schmidt, V.M., Ayasse, M., and Barth, F.G. (2007). Spitting out information: Trigona bees deposit saliva to signal resource locations. Proceedings Biological sciences / The Royal Society *274*, 895-898.

Schwarze, S.R., Ho, A., Vocero-Akbani, A., and Dowdy, S.F. (1999). In vivo protein transduction: delivery of a biologically active protein into the mouse. Science *285*, 1569-1572.

Schwarze, S.R., Hruska, K.A., and Dowdy, S.F. (2000). Protein transduction: unrestricted delivery into all cells? Trends in cell biology *10*, 290-295.

Scott, D., and Richmond, R.C. (1987). Evidence against an antiaphrodisiac role for cis-vaccenyl acetate in Drosophila melanogaster. Journal of Insect Physiology, 363-369.

Scott, D., and Richmond, R.C. (1988). A genetic analysis of male-predominant pheromones in Drosophila melanogaster. Genetics *119*, 639-646.

Semmelhack, J.L., and Wang, J.W. (2009). Select Drosophila glomeruli mediate innate olfactory attraction and aversion. Nature *459*, 218-223.

Sengupta, P., Chou, J.H., and Bargmann, C.I. (1996). odr-10 encodes a seven transmembrane domain olfactory receptor required for responses to the odorant diacetyl. Cell *84*, 899-909.

Shadlen, M.N., and Movshon, J.A. (1999). Synchrony unbound: a critical evaluation of the temporal binding hypothesis. Neuron *24*, 67-77, 111-125.

Sokolowski, M.B. (2001). Drosophila: genetics meets behaviour. Nature reviews Genetics *2*, 879-890.

Soto, E.M., Betti, M.I., Hurtado, J., and Hasson, E. (2014). Differential responses to artificial selection on oviposition site preferences in Drosophila melanogaster and D. simulans. Insect science.

Stensmyr, M.C., Dweck, H.K., Farhan, A., Ibba, I., Strutz, A., Mukunda, L., Linz, J., Grabe, V., Steck, K., Lavista-Llanos, S., *et al*. (2012). A conserved dedicated olfactory circuit for detecting harmful microbes in Drosophila. Cell *151*, 1345-1357.

Su, C.Y., Menuz, K., Reisert, J., and Carlson, J.R. (2012). Non-synaptic inhibition between grouped neurons in an olfactory circuit. Nature *492*, 66-71.

Suh, G.S., Wong, A.M., Hergarden, A.C., Wang, J.W., Simon, A.F., Benzer, S., Axel, R., and Anderson, D.J. (2004). A single population of olfactory sensory neurons mediates an innate avoidance behaviour in Drosophila. Nature *431*, 854-859.

Takemura, S.Y., Bharioke, A., Lu, Z., Nern, A., Vitaladevuni, S., Rivlin, P.K., Katz, W.T., Olbris, D.J., Plaza, S.M., Winston, P.*, et al.* (2013). A visual motion detection circuit suggested by Drosophila connectomics. Nature *500*, 175-181.

Tang, G., Gudsnuk, K., Kuo, S.H., Cotrina, M.L., Rosoklija, G., Sosunov, A., Sonders, M.S., Kanter, E., Castagna, C., Yamamoto, A.*, et al.* (2014). Loss of mTOR-dependent macroautophagy causes autistic-like synaptic pruning deficits. Neuron *83*, 1131-1143.

Thistle, R., Cameron, P., Ghorayshi, A., Dennison, L., and Scott, K. (2012). Contact chemoreceptors mediate male-male repulsion and male-female attraction during Drosophila courtship. Cell *149*, 1140-1151.

Thom, C., Gilley, D.C., Hooper, J., and Esch, H.E. (2007). The scent of the waggle dance. PLoS Biol *5*, e228.

Turan, S., Galla, M., Ernst, E., Qiao, J., Voelkel, C., Schiedlmeier, B., Zehe, C., and Bode, J. (2011). Recombinase-mediated cassette exchange (RMCE): traditional concepts and current challenges. Journal of molecular biology *407*, 193-221.

Ugolini, G. (2008). Use of rabies virus as a transneuronal tracer of neuronal connections: implications for the understanding of rabies pathogenesis. Developments in biologicals *131*, 493-506.

van der Goes van Naters, W., and Carlson, J.R. (2007). Receptors and neurons for fly odors in Drosophila. Current biology : CB *17*, 606-612.

Varshney, L.R., Chen, B.L., Paniagua, E., Hall, D.H., and Chklovskii, D.B. (2011). Structural properties of the Caenorhabditis elegans neuronal network. PLoS computational biology *7*, e1001066.

Venkatesh, S., and Naresh Singh, R. (1984). Sensilla on the third antennal segment of Drosophila melanogaster meigen (Diptera : Drosophilidae). International journal of insect morphology and embryology *13*, 51-63.

Venken, K.J., Simpson, J.H., and Bellen, H.J. (2011). Genetic manipulation of genes and cells in the nervous system of the fruit fly. Neuron *72*, 202-230.

Vet, L.E.M., Van Lentern, J.C., M., H., and E., M. (1983). An Airflow Olfactometer for Measuring Olfactory Responses of Hymenopterous Parasitoids and Other Small Insects. Physiological Entomology *8*, 97-106.

Vosshall, L.B., Amrein, H., Morozov, P.S., Rzhetsky, A., and Axel, R. (1999). A spatial map of olfactory receptor expression in the Drosophila antenna. Cell *96*, 725-736.

Wang, L., and Anderson, D.J. (2010). Identification of an aggression-promoting pheromone and its receptor neurons in Drosophila. Nature *463*, 227-231.

Wang, L., Han, X., Mehren, J., Hiroi, M., Billeter, J.C., Miyamoto, T., Amrein, H., Levine, J.D., and Anderson, D.J. (2011). Hierarchical chemosensory regulation of male-male social interactions in Drosophila. Nature neuroscience *14*, 757-762.

White, J.G., Southgate, E., Thomson, J.N., and Brenner, S. (1986). The Structure of the Nervous System of the Nematode Caenorhabditis elegans. Philosophical transactions of the Royal Society of London *1165*.

Wilson, E.O. (1970). Chemical communication within animal species. Chemical ecology *9*, 133-155.

Wong, A.M., Wang, J.W., and Axel, R. (2002). Spatial representation of the glomerular map in the Drosophila protocerebrum. Cell *109*, 229-241.

Wu, J.S., and Luo, L. (2006). A protocol for dissecting Drosophila melanogaster brains for live imaging or immunostaining. Nature protocols *1*, 2110-2115.

Wyatt, T.D. (2014). Pheromones and animal behaviour.

Xiao, Y.H., Zhang, J.X., and Li, S.Q. (2010). Male-specific (Z)-9-tricosene stimulates female mating behaviour in the spider Pholcus beijingensis. Proceedings Biological sciences / The Royal Society *277*, 3009-3018.

Xu, P., Atkinson, R., Jones, D.N., and Smith, D.P. (2005). Drosophila OBP LUSH is required for activity of pheromone-sensitive neurons. Neuron *45*, 193-200.

Yamamoto, D., and Koganezawa, M. (2013). Genes and circuits of courtship behaviour in Drosophila males. Nature reviews Neuroscience *14*, 681-692.

Yang, C.H., Belawat, P., Hafen, E., Jan, L.Y., and Jan, Y.N. (2008). Drosophila egg-laying site selection as a system to study simple decision-making processes. Science *319*, 1679-1683.

Yao, C.A., Ignell, R., and Carlson, J.R. (2005). Chemosensory coding by neurons in the coeloconic sensilla of the Drosophila antenna. The Journal of neuroscience : the official journal of the Society for Neuroscience *25*, 8359-8367.

Zuckerkandl, E., and Pauling, L. (1965). Evoultionary divergence and convergence in proteins. In: Bryson V, Vogel HJ (eds) Evolving genes and proteins, 97-166.

Curriculum Vitae

Name	Chun-Chieh Lin
Place of Birth	Tainan, Taiwan
Date of Birth	Oct 02 1981
Email Address	paulcclin@gmail.com

Education

Ph.D.	2015	Solomon H. Snyder Department of Neuroscience, Johns Hopkins School of Medicine, Baltimore, MD
M.D.	2007	Fu Jen Catholic University, Taipei, Taiwan

Publications

Ronderos, DS, **Lin, C-C**, Potter CJ, Smith DP. (2014) Farnesol-detecting olfactory neurons in *Drosophila*. *J Neurosci*. 12;34 (11):3959-68

Gohl, DM, Silies, MA, Gao, XJ, Bhalerao, S, Luongo, FJ, **Lin, C-C**, Potter, CJ, and Clandinin, TR. (2011) A Genetically convertible enhancer trap platform for directed combinatorial dissection of gene expression patterns. *Nat Methods* 8(3):231-237.

Mileykovskaya, E, Ryan, A, Mo, X, **Lin, C-C**, Khalaf, K, Dowhan,W, Garrett, TA. (2009) Phosphatidic acid and N-acylphosphati- dylethanolamine form membrane domains in Escherichia coli mutant lacking cardiolipin and phosphatidylglycerol, *J Biol Chem*., 284(5):2990-3000.

Invited Talks

Lin, C-C, Prigge, K, Preti, G, Potter CJ. Food odors trigger Drosophila males to secrete a pheromone that guides female decisions. *CSH Neurobiology of Drosophila*, October 2013.

Poster Presentations

Lin, C-C, Prigge, K, Preti, G, Potter CJ. Food odors trigger Drosophila males to secrete a pheromone that guides female decisions. *Sensory Transduction Woods Hole, Massachusetts*, September 2014.

Lin, C-C, St. Peter, D, Potter, CJ. Genetic dissection of odor representations encoded by fly projection neurons. *Society for Neuroscience Annual Meeting*, November 2011.

Lin, C-C and Potter, CJ. Olfactory neural networks required for an olfactory aggregation behavior. *CSH Neurobiology of Drosophila*, October 2011.

Lin, C-C and Dowhan W. Analysis of the phospholipid compo- nents at the cell Poles, *University of Texas-Houston Medical School Student Research Abstracts*, 2005, p57

Lin, C-C, Yeh, J-C, Lu, J-F. Differential expression of genes during culture of rat type II pneumocytes, *Fu Jen Catholic University Poster Exhibition of Research Results*, 2003

Honors and Awards:

2013 Feldan award

2012 Nomination for HHMI International Student Research Fellowship, Johns Hopkins University

2009 National Overseas Fellowship, Ministry of Education, Taiwan

2008 National Overseas Fellowship, Ministry of Education, Taiwan

2004 Scholarship for Overseas Summer Research Program, Fu Jen Catholic University

2003 Best Award, Fu Jen Catholic University Poster Exhibition of Research Results

Professional Works &Teaching Experiences

2010-2011 Teaching assistant for NeuroCog I, Department of Neuroscience, Johns Hopkins University

2008-2009 Medical officer, Republic of China Marine Corps 99th Brigade, Kaohusiung, Taiwan

2006-2007 Intern, National Taiwan University Hospital, Taiwan

Liscense & Certifications

2015 Clinical Dementia Rating (CDR) Rater

2015 USMLE Step1

2007 Qualification of Taiwan Medical License Examination